NOTICE

The quality of this microfiche is heavily dependent upon the quality of the original thesis submitted for microfilming. Every effort has been made to ensure the highest quality of reproduction possible.

If pages are missing, contact the university which granted the degree.

Some pages may have indistinct print especially if the original pages were typed with a poor typewriter ribbon or if the university sent us a poor photocopy.

Previously copyrighted materials (journal articles, published tests, etc.) are not filmed.

Reproduction in full or in part of this film is governed by the Canadian Copyright Act, R.S.C. 1970, c. C-30. Please read the authorization forms which accompany this thesis.

THIS DISSERTATION
HAS BEEN MICROFILMED
EXACTLY AS RECEIVED

AVIS

La qualité de cette microfiche dépend grandement de la qualité de la thèse soumise au microfilmage. Nous avons tout fait pour assurer une qualité supérieure de reproduction.

S'il manque des pages, veuillez communiquer avec l'université qui a conféré le grade.

La qualité d'impression de certaines pages peut laisser à désirer, surtout si les pages originales ont été dactylographiées à l'aide d'un ruban usé ou si l'université nous a fait parvenir une photocopie de mauvaise qualité.

Les documents qui font déjà l'objet d'un droit d'auteur (articles de revue, examens publiés, etc.) ne sont pas microfilmés.

La reproduction, même partielle, de ce microfilm est soumise à la Loi canadienne sur le droit d'auteur, SRC 1970, c. C-30. Veuillez prendre connaissance des formules d'autorisation qui accompagnent cette thèse.

LA THÈSE A ÉTÉ
MICROFILMÉE TELLE QUE
NOUS L'AVONS REÇUE

PREFACE

During recent years, much attention has been paid to the potential advantages of immobilized enzymes in industry, analytical chemistry and medicine. Many reactors have been developed but the present report is concerned with only the tubular reactor and the rotating enzyme disc.

Kinetic theories, so far developed, deal with one-substrate enzymes because these show simpler kinetic behaviour than multi-substrate enzymes do. However, fundamental theoretical treatments for multi-substrate enzymes are needed and these may later lead to an efficient exploitation of their catalytic behaviour.

Developing a complete kinetic theory for tubular reactors of two-substrate enzymes poses serious problems, and so far no success has been achieved. To avoid some of these difficulties, we have employed experimental conditions under which the existing Kobayashi and Laidler theory, developed for single-substrate enzymes, applies to two-substrate enzymes.

This thesis reports also a preliminary investigation on the flow kinetics of enzymes immobilized on rotating discs. Experiments are done with immobilized lactate dehydrogenase at an impervious support and at a porous membrane.

Some of our work presented in this thesis has been published and another paper is in course of publication, as follows:

(1) "Flow kinetics of lactate dehydrogenase chemically attached to nylon tubing", N.J. Daka and K.J. Laidler (1978) Canadian Journal of Biochemistry, 56, 774-779.

(2) "Temperature and pH effects on immobilized lactate dehydrogenase kinetics", N.J. Daka and K.J. Laidler (1980) Biochimica et Biophysica Acta, 612, 305-316.

(3) "Immobilized lactate dehydrogenase kinetics at a rotating enzyme disc", N.J. Daka and K.J. Laidler (1980). Submitted to Biotechnology and Bioengineering.

ACKNOWLEDGEMENTS

I am sincerely grateful to Professor K.J. Laidler under whose supervision this research was carried out. I appreciate and acknowledge that without the superiority of his humanity, guidance, encouragement and academic intellectualism a successful realization of this work would have been impossible. The present work is a manifestation of Professor Laidler's failure to remain within the confines of Chemistry alone in his search for truth and human happiness through natural science. Such a virtue and his love for small children, which he has shown through demonstrations at Christmas and other occasions, will forever remain my envy and my inspiration. It has been an honour and pleasure working with a man of Professor Laidler's calibre.

I am gratefully indebted to the University of Zambia, who through their Staff Development Fellowship program have generously financed my stay and my study at the University of Ottawa, in Canada. I wish to express my hearty appreciation of the Staff Development Officer, Miss J.M.F. Calder and her assistant, Ms. S.H. Longwe, for handling my problems and my correspondence with the University of Zambia so efficiently. I am thankful to Professor M. Siamwiza also for introducing me to Professor Laidler and for encouraging me to work towards a Ph. D. degree.

My appreciation to the whole Chemistry Department of the University of Ottawa for their warm friendship and help is beyond expression. I am especially grateful to Professor B.E. Conway for suggesting Rotating-

Disc experiments. I enjoyed his graduate courses as well as those of other professors, such as Dr. M. Back, Dr. J.L. Holmes and Dr. H. Alper. I wish to express my gratitude to Messrs. E. Kristoff and W. Seinsch also for helping me prepare rotating disc cells.

I gratefully acknowledge the drawing of the digrams by Mrs. E. Szabo, the typing of this thesis by Mrs. S. Ryan and the comeradeship of my colleagues in the same laboratory, especially Dr. B.F. Peterman and Mr. M.A. Mazid.

There is an old adage which says "Charity begins at home". With this in mind, I thank my late mother, Taza, and my father, Elefas for all the initial sacrifices and encouragement they made to send me to school. Thanks are also due to my brother, Daniél, and my sisters Lubano, Evaline, Eumice, Mary and Palata for their love and interest in my career.

Finally, I am especially thankful to my wife, Diane, and our baby Jessica (Taza) for their patience, tolerance, understanding and love that they have shown me during the course of this work and also the help and consideration of Mr. and Mrs. A. Blais, my wife's parents, are greatly appreciated.

ABSTRACT

Chapter I

A brief history of immobilized enzymes is given, and areas where immobilization of enzymes is generally found to be useful are discussed. The different factors which may alter the kinetics of enzymes after immobilization are pointed out. The chapter closes with the presentation of some basic properties of lactate dehydrogenase (LDH) and some reasons for choosing this particular enzyme for our research.

Chapter II

Some important features of the Kobayashi and Laidler theory for tubular reactors are outlined and the experimental conditions under which this theory can be used to characterize the behaviour of LDH present at the inner walls of tubes are discussed. Kinetic runs are made with both free and immobilized LDH at 25 °C. The results obtained with the tube system are analyzed in the light of the Kobayashi-Laidler theory. Diffusion-free Michaelis constants for pyruvate and NADH, found with bound LDH, are compared with those from the free-enzyme experiments. Steric effects are implicated in the kinetic behaviour of NADH with the bound enzyme, and the tube system is found to be significantly affected by diffusion factors. The same chapter discusses the procedure for attaching enzymes to nylon supports through glutaraldehyde and benzidine as cross-linking agents. A preliminary calculation of the activation energies for diffusion of NADH and pyruvate is made.

Chapter III

A detailed study of the flow kinetics of LDH-tubular reactors is made at various temperatures, various flow rates and various substrate concentrations. The results are analyzed in terms of the Kobayashi and Laidler theory and show that low flow rates, low substrate concentrations and low temperatures lead to an increase in the extent of diffusion control. A very low activation energy of 0-1 kcal mol^{-1} was obtained at high substrate concentrations. A diffusion-controlled value of 5.0 kcal mol^{-1} estimated by extrapolation to infinitely small substrate concentrations is used to calculate product concentrations at the exit of the tube and dimensionless parameters (ϕ and ρ) at various temperatures. Measurements of the reaction rates at various pH values show that the activity-pH profiles for pyruvate are different from those for NADH, and reasons for the differences are suggested.

Chapter IV

A discussion of the theoretical aspects of rotating enzyme discs is presented. The enzyme LDH is attached to a nylon disc by a method which involves the use of thionyl chloride and 3,3-diaminobenzidine, and shows favourable activity. Analysis of the data obtained with the enzyme disc is made in terms of the theory presented in the same chapter. Consistent results are obtained, which suggests that the theoretical treatment is along the right path. All runs are made at 25 °C with variable NADH and fixed pyruvate.

Chapter V

A porous membrane disc is constructed and used to study the effects of external diffusion on the flow kinetics of entrapped LDH. Internal diffusion is assumed to be negligible, and the theory discussed in Chapter IV is used to treat the data of the kinetic experiments made at 25 °C with variable NADH and fixed pyruvate. The kinetic behaviour is different from that found with the impervious disc of Chapter IV. Reasons for the anomaly are discussed.

Chapter VI

Based on the results of the experiments reported in Chapters II to V, the extent to which diffusional, conformational, partitional and environmental factors influence the kinetics of immobilized LDH is examined. It is concluded that these factors can be better understood from the kinetic point of view if experiments are carried out with multi-substrate enzymes and under situations where substrates are allowed to interact with the fixed enzyme at different but well-controlled flow speeds. A summary of the advantages of immobilizing enzymes is given in this final chapter, and conditions which may help to maximize the predictions of the Kobayashi-Laidler theory and the treatment of the rotating enzyme discs are outlined.

TABLE OF CONTENTS

TABLE OF CONTENTS (cont'd)

TABLE OF CONTENTS (cont'd)

LIST OF FIGURES

LIST OF FIGURES (cont'd)

LIST OF FIGURES (cont'd)

LIST OF FIGURES (cont'd)

LIST OF FIGURES (cont'd)

LIST OF TABLES

LIST OF TABLES (cont'd)

LIST OF SYMBOLS

Symbol	Definition	Unit Used
A, A_s	Surface area	cm^2
[A],[B], etc.	Concentration of substance A, B, etc.	M, mol dm^{-3}
C	Concentration	mol dm^{-3}
D	Diffusion coefficient	$cm^2\ s^{-1}$
DEAE	Diethylaminoethyl	
ε	Molar absorption coefficient	$M^{-1}\ cm^{-1}$
E	An enzyme molecule	
EDTA	Ethylene diaminetetraacetic acid	
E_D	Activation energy for diffusion	kcal mol^{-1}
$E_{S_{ex}}$, E_o	Enzyme saturated with excess substrate	
ψ	Electrostatic potential	
f	Rotation speed of the disc	$rev.s^{-1}$
J_x	Diffusion flux along the x-axis	mol $s^{-1}\ cm^{-2}$
k'_c	True catalytic rate constant for the enzyme process	
K_A,K_B, etc.	Michaelis constants for substrates A, B, etc.	mol dm^{-3}
K_m(app)	Apparent or observed Michaelis constant	M, mol dm^{-3}
K'_m, K_{ms}	Intrinsic Michaelis constant for the immobilized enzyme	M, mol dm^{-3}
K_m^f	Michaelis constant for the free enzyme	mol dm^{-3}
K_m^H	Michaelis constant for the immobilized enzyme affected by partitional, environmental and conformational effects	M, mol dm^{-3}

Symbol	Definition	Unit Used
K-L	Kobayashi and Laidler	
k_L	Mass transfer coefficient	
k	Boltzmann constant	
L	Length of a tube	cm
L-B	Lineweaver-Burk	
LDH	An enzyme lactate dehydrogenase	
NADH	The reduced coenzyme of LDH	
Λ	The Damköhler number	
η	The utilization factor	—
η_1, η_2 etc.	Viscosity of solution 1, 2, etc.	kg m^{-1} s^{-1}
NDS	Nylon disc surface	
$[P]_e$	Product concentration at the exit of the tube	M, mol dm^{-3}
P, P_L	Product species	
ρ	Dimensionless constant of the K-L theory	
ρ_1, ρ_2, etc.	Density of solution 1, 2, etc.	g cm^{-3}
pH, pK_i, pK_m	Negative logarithms of the hydrogen ion concentration, the ionization constant and the Michaelis constant respectively	
ϕ	Dimensionless constant in the K-L theory	
r	Radius of a tube or disc	cm
R	Radial position of a tube	
[S]	Substrate concentration	M, mol dm^{-3}
S, S_L	Substrate species	

Symbol	Definition	Unit Used
T	Absolute temperature	K
t_1, t_2, etc.	Time of flow of solution 1, 2, etc.	s
$V_m(app)$	Apparent (observed) maximum velocity	$M\ s^{-1}$ and $mol\ dm^{-3}\ s^{-1}$
V_m'	Maximum diffusion-free viscosity for the immobilized enzyme	$M\ s^{-1}$, $mol\ dm^{-3}\ s^{-1}$
V_m^f	True maximum velocity for the free enzyme	$M\ s^{-1}$, $mol\ dm^{-3}\ s^{-1}$
V_m^H	Maximum velocity for the immobilized enzyme affected by conformational, partitional and environmental effects	$M\ s^{-1}$, $mol\ dm^{-3}\ s^{-1}$
v_D, v_r, v	Observed or apparent reaction rates	$M\ s^{-1}$, $mol\ dm^{-3}\ s^{-1}$
v_f	Rate of flow of a solution through a tube	$cm\ s^{-1}$
v_x	Hydrodynamic velocity component in the X direction for a rotating disc	$cm\ s^{-1}$
ν	Kinematic viscosity of the solution medium	$cm^2\ s^{-1}$
ω	Angular speed of rotation	$radian\ s^{-1}$
z	Axial position of a tube	cm
Ze	Charge on the substrate or on the enzyme support	

CHAPTER I

GENERAL INTRODUCTION

1.1 Introduction

In recent years, the study of immobilized enzymes has developed significantly because of their many attractive features, some of which will be discussed briefly in this Chapter to provide an introduction and background to the topics of this thesis.

An immobilized enzyme is one whose movement has been restricted to a limited region of space by either adsorption, encapsulation, covalent bonding or a combination of two or more of these classes of methods[1]. Figure 1 gives a summary of the different ways an enzyme can be immobilized. Prior to 1971, various terms such as "solid-supported enzyme", "insolubilized enzyme", "fixed enzyme", "insoluble-enzyme derivative", "trapped enzyme", and "matrix-bound enzyme" were used to distinguish fixed enzymes from their freely moving counterparts. In 1971, the name "immobilized enzyme" was recommended at the First Engineering Conference[2] held at Henmiker (New Hampshire, USA) to include all the above-mentioned terms. Thus, today, the accepted and widely used terminology for description of all supported biological catalysts is "immobilized enzyme".

Historically, the first immobilization of enzymes was made by Grobhofer and Schleith in 1953[3,4]. The second attempt was made in 1955 by Brandenberge[5]. On the whole, the subject received very little

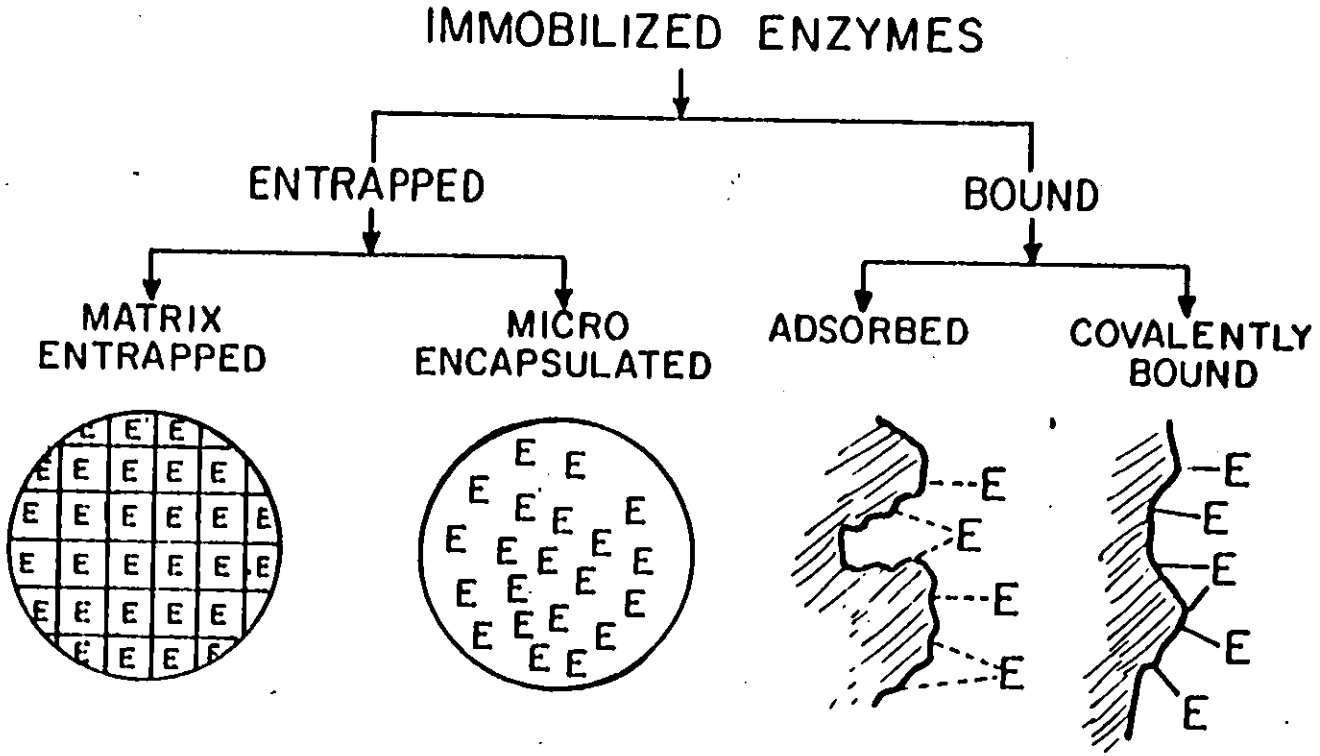

Figure 1. Schematic illustration of different classes of immobilization.

attention in the 1950's. In the 1960's, the interest was initiated by Katchalski and coworkers[6-10]. It rose rapidly and by the end of the 1970's several reviews and books had been written on the subject[11-16]. Techniques for immobilization of enzymes to both organic and inorganic supports have been reviewed recently by Goldstein and Manecke[15] and Chibata[20]. Kinetic aspects have been nicely documented by several workers[1,16,29,71-76].

The advantages of immobilizing enzymes can be found in a number of important areas such as those discussed below.

1.2 Economic Aspects

Most enzyme-catalyzed reaction studies are made with both the enzyme and the substrate in the form of a solution. It has been argued that since the isolation and purification procedures for these highly specific biological catalysts from the cells of living organisms are usually long, tedious and sophisticated, enzymes will always be economically expensive. For example, a new book on Fermentation and Enzyme Technology[21] says that a 1970 survey showed that of more than 1,300 enzymes known at that time only 120 were commercially available. About 50 were available in one-gram lots or less, while 35 were advertized in kilogram quantities and over half the enzymes available in less than one-gram quantities had an effective price of over $2500 per gram. Only a few enzymes from bacteria were produced in tonnage quantities. Wieland[22] also reports that in 1969 the American fermentation industry produced products valued at $2 billion, of which $64 million was

accounted for by enzymes. This gives us a quantitative feeling of how expensive it is to use liquid enzymes. However, such high costs and enzyme expenditure can be reduced significantly through the immobilization technique because then the same enzyme can be used many times over.

1.3 Medical Applications

Despite the basic importance of enzymes in medicine, enzyme therapy for treatment of diseases caused by either enzyme deficiency or accumulation of undesirable substances has lagged far behind the industrial applications; this is because of serious problems encountered by scientists studying possible therapeutic applications of enzymes. For example, when a patient suffers from a disease arising from lack of an enzyme in his body, the correct enzyme may be injected directly into his blood stream or administered orally in the form of a pill to compensate for the deficiency. It has been found that when this is done the enzyme tends to be unstable, losing its activity fast. It has been suggested that perhaps the body sees the administered enzyme as a foreign protein (antigen) and produces antibodies to remove and inactivate it quickly. This may call for repeated administration of the same enzyme. Such a practice has often led to more complicated side effects due to antigen-antibody reactions.[16,19] In some cases, blood clots have developed causing damage to the brain, lungs, kidneys and the heart and ultimately death to the recipient of the soluble enzyme.

Can an immobilized enzyme help in avoiding some of these problems? The answer is yes. When an enzyme is immobilized inside a

semipermeable membrane, for instance, it is prevented from attack by high-molecular-weight substances such as proteolytic enzymes, antibodies and antibody-producing cells, and its activity in the patient's body lasts much longer than that of a free enzyme. This fact has been experimentally confirmed by Chang and Poznansky[23,24] who worked with acatalasemic mice. It was found that the mice that received catalase in solution form required repeated injections of this enzyme for effective removal of sodium perborate (substrate for catalase) which had initially been introduced into their bodies. The animals finally died. On the other hand, no antibody formation, no side effects and no deaths were observed among the mice that had received microcapsules containing the enzyme catalase. In another investigation[25,26], in which asparaginase was administered to mice containing implanted tumor cells, it was observed that after 14 days tumors appeared in animals which had received soluble asparaginase, whilst it took 69 days to see the same effects among those which had received the same enzyme contained in microcapsules. Thus, immobilization improves enzyme stability and can avoid side effects.

An interesting area where immobilized enzymes are finding a bright future in medicine is in the construction and application of "Extracorporeal Shunt" systems. A number of these devices are already in operation. Allison et al[27], for example, have used asparaginase bound to nylon tubes to cure dogs suffering from leukemia. The treatment of diabetic patients using immobilized lactate dehydrogenase with a shunt system has been attempted. Chang[28], using a column packed with urease microcapsules, made an extracorporeal shunt which he called the

"Artificial Kidney" and used it to cure uremic cases. With extracorporeal devices, a patient's blood can be treated outside his body[29]. The blood is allowed to flow out of the sick body, through the shunt system containing the bound enzyme and back into the body. The above-mentioned treatments were carried out this way. Furthermore, with extracorporeal shunts, a doctor has direct contact with the patient's blood and he can easily check the presence or absence of blood clots before any serious damage is done.

Although the therapeutical applications of immobilized enzymes so far are modest, they point the way to future improvements and to the fact that immobilized enzymes in medicine have a great potential over soluble enzymes.

1.4 Commercial Applications

Significant progress with immobilized enzymes has been made in the food processing industry.

1.4.1 Amino Acid Production

The first large-scale use of these bound species was made in Japan by the Tanabe Seiyaku Company[20,30-32] for L-amino acid production. Amino acids are the fundamental building blocks of proteins. There is therefore great need in the world today to enrich foods with amino acids. Chemical techniques for synthesizing amino acids result in racemic mixtures of D and L forms. Since only the L form can be metabolized and used for protein synthesis in living bodies, the mixture must be separated. Although it is usually difficult and inefficient

to separate D and L forms by ordinary physical and chemical methods, enzymes accomplish this purpose very easily. The Japanese company is still in operation. It uses aminoacylase adsorbed on DEAE-Sephadex for the continuous, automatically controlled preparation of L-methiomine, L-pheylalamine, L-tryptophane and L-valine from racemic mixtures of those amino acids. Due to the immobilization technique, production costs have been cut to 60% of that for the conventional batch process using soluble enzymes.

1.4.2 Fructose and Sucrose Production

Up until 1958, commercial corn syrups were produced by acid hydrolysis of corn starch. Higher conversions brought about by the acid, coupled with poor specificity of the method gave products which were low in glucose and bitter in taste. With the introduction of enzymes, it became possible to produce high quality syrups. With the glucoamylase used today, products with glucose content of up to 95% and 70-75% as sweet as sucrose, are easily obtainable. Sweetness is improved by using glucose isomerase which isomerizes glucose to fructose[35].

The enzymic isomerization of glucose to fructose carried out on a commercial scale since 1968 is one of the largest and most important applications of an immobilized enzyme in industry today. The Novo Industri in Denmark and the Clinton Corn Processing Company and the Standard Brands Company in the U.S.A. have operated with glucose isomerase bound to DEAE-cellulose[20]. Various supports have also been tried.

For example, Messing[36] adsorbed the enzyme on alumina. Strandberg and Smiley[37] used diazotized porous glass and Davis[38] entrapped it in polyacrylamide gel.

Immobilization is also being used in the beet sugar industry. The enzyme, α-galactosidase held within pellets of the fungus M.Vinecease yields sucrose from raffinose on a commercial scale[35].

1.4.3 The Milk Industry

Milk, a chief food for babies, contains lactose. Lactose accumulation has been associated with stomach problems experienced by lactase-deficient beings. Patients may receive lactase orally to bring about the hydrolysis of the problem-causing compound to glucose and galactose. However, the administration of the enzyme in soluble form may cause allergic reactions in some people and must be discouraged. The lactase used for treatment usually comes from yeast and bacteria such as Escherichia Coli and Aspergillus. The foreign nature of the enzyme sources can contribute to some allergic problems faced by human bodies. Removing lactose from the milk before it is consumed seems to be the best alternative of avoiding its harmful effects. Today, there are plants in Italy, U.S.A. and Japan, for example, which operate on immobilized lactase and their results are phenomenal[20]. The interest in lactose also stems from the fact that its hydrolysis products are used in many dairyproducts, both as sweeteners and as substitutes for corn syrup solids[35,39]. The industrial application of lactase has used phenol-formaldehyde resins as enzyme supports and glutaraldehyde as a crossing agent[40,41].

1.4.4 Miscellaneous Commercial Uses

The applications of immobilization given above are on very large industrial scale today. There are also many potential large-scale commercial uses of the technique in various stages of research and development and Table 1 gives a summary of some of these applications.

1.5 Analytical Application

Enzymes are very specific for their respective substrates. Their widespread use in analytical procedures for determination of specific chemical substances in solution samples emanates from this powerful property that they have. In recent years, attention has been focussed more on immobilized enzymes than their free counterparts because the former often display enhanced stability[16,57] and repetitive utility, which are economically of value. The latter lack these qualities. Furthermore, the discrete physical form of immobilized enzymes makes it possible to carry out assays with different types of reaction configurations such as the enzyme electrode[58], packed bed[59], stirred tank[59] and open tubular reactors[29].

An enzyme electrode consists of a layer or a membrane of an immobilized enzyme and a sensitive electrode to monitor either pH, gas or ion changes resulting from an enzyme-catalyzed reaction. For example, asparaginase-pH[60], LDH-Pt[61], Catalase-O_2[62] and Urease-CO_2[63] couples, involving an enzyme and an electrode, have been used successfully for detection of asparagine, lactic acid, hydrogen peroxide and urea, respectively, in blood and urine samples of patients.

Table 1. Some potential large-scale uses of immobilized enzymes in industry.

APPLICATION	IMMOBILIZED ENZYME	REFERENCE
a. Production of cheese	Rennin	42
b. Sterilization of milk	Catalase	43,44
c. Isolation and purification of enzyme inhibitors (affinity chromatography)	Trypsin; -chymotrypsin;	45,46,47
	Kallikrein; Trypsinogen	48
	Elastase	49,50
d. Biochemical batteries - fuel cells Electron rich substances (nutrients) get converted to electron poor (metabolites)	Papain Glucose oxidase	51,52
e. Removal of bitterness from orange juice	Naringinase	53
f. Reduction of phenol content in waste water	Polyphenol oxidase	54
g. Removal of polypeptides from beer	Papain	55
h. Production of urocanic acid, a sun screening agent, for cosmetics	L-histidine ammonia-lyase	56
i. Production of 6-aminopenicillanic acid	Penicillin amidase	20
j. Production of L-citrulline for medicine	L-arginine deaminase	39
k. Production of L-Malic acid for treating liver diseases and hyperammonemia	Fumarase	20
l. Production of L-aspartic acid - a food additive	Aspartase	20

Packed beds, fluidized beds, stirred tanks and tubular reactors have been particularly attractive in the use of the Automated Continuous Flow Analyzers[64], such as that developed by the Technicon Instrument Company for clinical and biological research laboratories. For example, automatic determinations of ethanol[65], lactic acid[66] and malic acids[65] have been made very successfully with alcohol dehydrogenase, lactic dehydrogenase and malate dehydrogenase attached to the inner surface of nylon tubes.

1.6 Theoretical Application

In living organisms, enzymes are often immobilized in cells or tissues. It has been found that some enzymes exhibit activity only when they are bound. This is the case with respiratory enzymes and enzymes involved in photosynthesis[66,67]. In short, immobilized enzymes are considered as models for understanding the efficient processes of nature in living bodies.

Research today has also progressed from a study of preparations containing only one immobilized enzyme to systems consisting of different enzymes. This problem has been taken up because in vivo reactions may involve the interaction between many enzymes.

The work of Mosbach and his co-workers[68,69] on the kinetics of matrices each containing three enzymes, is an illustration of the interest expressed in this area. In one case, malate dehydrogenase, citrate synthase and lactate dehydrogenase were attached to one CNBr-activated sephadex. In the other, it was lactase, hexokinase and

glucose-6-phosphate dehydrogenase which were bound to one support. It was concluded that the most efficient catalytic activity is achieved when these enzymes are all bound to the same particle or membrane. Some people have been immobilizing subunits of enzymes in an effort to understand complicated enzyme reaction mechanisms in vivo[70].

Immobilized enzymes also serve as experimental tools for testing and improving a number of theories developed for these systems[57]. Considerable theoretical and experimental work has been done in this regard, but usually the agreement between theory and experiment is best for simple enzymic reactions. There is, however, still great need for theories which can be applied to enzymes exhibiting complicated mechanisms.

Basically, studying the kinetics of immobilized enzymes, which is the central theme of this thesis, is one of the most important aspects of enzymology because kinetic behaviour is the essential feature of an enzyme. The knowledge for better reactor designs and profitable use of labour and other process materials for bound enzymes can be derived from kinetic investigations.

Most immobilized enzymes exhibit altered kinetic behaviour when compared with the corresponding free enzyme for a number of reasons[1,57]. Firstly, immobilization may cause the three-dimensional arrangement (conformation) of the enzyme protein to change. Consequently, the three-dimensional structure of the active sites may also be affected. There is also a possibility that as the conformation changes during immobilization, some active centres of the enzyme would be shielded from

the easy approach of the substrate, so that the reactant, in its effort to reach the active centre, may suffer steric hindrances imparted by the support. Thus, conformation changes may be responsible for the observed difference in kinetic behaviour between the bound and the free enzyme. Secondly, the bound enzymes may function in a different environment. The properties of the support may also help in making the environment of the enzyme different. The resultant surrounding may be charged, neutral, hydrophilic or hydrophobic in character because of immobilization. Thirdly, the substrate may have to distribute itself between the fixed enzyme at the support and the rest of the reaction solution and because of the changed enzyme environment the substrate concentration in the neighbourhood of the enzyme may be different from what it is away from it. This partitioning effect will depend on the relationship between the properties of the substrate and those of the enzyme environment. For example, a relatively non-polar reactant will be more concentrated in the vicinity of a support containing a number of non-polar groups than in an aqueous atmosphere. Conversely, a polar substrate will be attracted more into an aqueous than into a hydrophobic medium. These situations have been discussed by several workers[71,16,59]. Finally, a fourth factor which may be responsible for the altered kinetic behaviour of an enzyme upon immobilization is diffusion. A diffusion layer may be established between the support containing the enzyme and the rest of the solution, so that the rate of transport of the substrate to the enzyme or product from the enzyme through this boundary layer will be rate limiting[29]. Thus, immobilized enzymes have

been used for the investigation of conformational, environmental, partitional and diffusional effects on the heterogeneous enzymic rates. Alternatively, the kinetics of immobilized enzymes can be influenced by one or a combination of two or more of these factors.

The classification of the kinetic parameters (Figure 2) into separate categories are a result of the influence of these factors. Usually, the assessment of the degree of influence imposed by each of the factors on a particular kinetic parameter is not easy. However, generalizations as to which one plays an overwhelming influence can be made from theoretical predictions. This will be illustrated later in the chapters to follow.

1.7 Conclusion

In concluding this Chapter, it should be remembered that enzyme immobilization is a new science, growing and expanding rapidly mainly because of its economic advantages and the chance it allows to develop new important devices such as tubular reactors, extracorporeal shunts, fuel cells[51,52] and microcapsules for use in medicine, industry and research laboratories. Like any other new field, however, it has several unsolved problems, some of which are:

1) So far, no single technique or support material can be used to immobilize over 2,000 enzymes known today with equal efficiency. Under the same experimental conditions, some enzymes may retain their catalytic activity upon immobilization whilst others may lose it completely[20]. This means that favourable techniques for various unstable enzymes

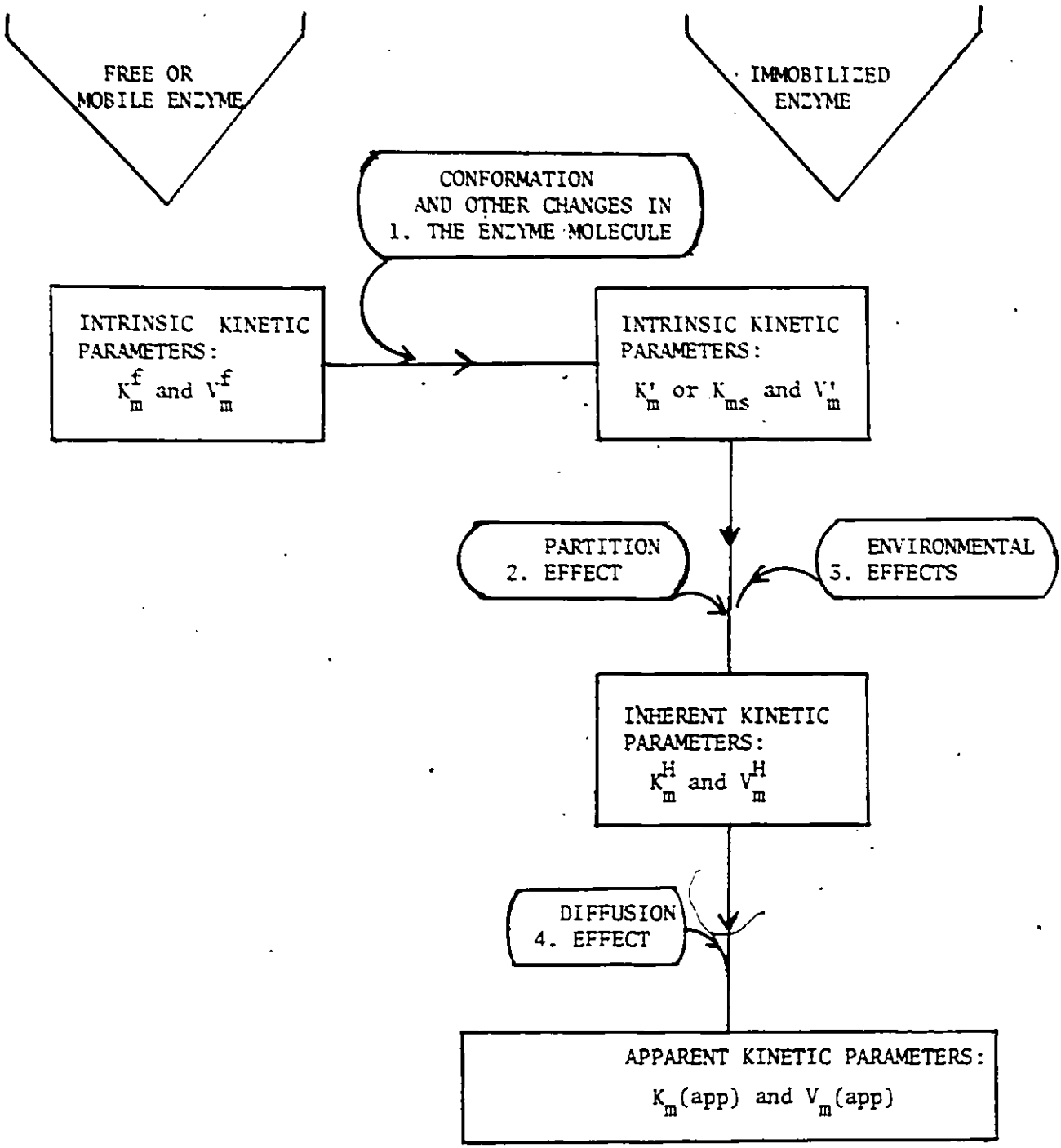

Figure 2. Schematic illustration of: (i) Four major factors that influence the activity of immobilized enzymes; (ii) Different kinetic parameters.

will have to be found through trials and tribulations.

2) Of the six general groups of enzymes (i.e. oxidoreductase, transferases, hydrolyses, lyases, isomerases and ligases or synthatases), only immobilized hydrolases have been used widely[72]. This is mainly due to their relatively simple action and their good catalytic stability after immobilization. There are very few studies and reports on the applications of immobilized enzymes requiring coenzymes. Oxidoreductases, transferases and ligases (synthetases) need coenzymes for their successful action. Coenzymes too are very expensive substances.

3) So far, only a limited number of theories are available for treatment of experimental data. In fact, almost all have been developed to apply to enzymes exhibiting purely simple Michaelis-Menten kinetics[74-78]. This may partially explain why very few detailed kinetic investigations have been carried out with such enzymes as the lactate dehydrogenase (LDH) which have complicated kinetic mechanisms[1].

Today, there is no existing theory for LDH chemically attached to the inner surface of a tube and no work has ever been done with any enzyme present on a rotating disc. These are some of the reasons, plus the fact that LDH has important applications in a number of situations, that attracted our attention to the enzyme and this thesis reports the efforts we have made in our laboratory with LDH.

LDH, a subgroup of oxidoreductases[72], is a tetramer of molecular weight 140,000[79,80]. It consists of two forms; the H_4 predominantly found in the heart cells and M_4 in skeletal muscle. It is found in the cytoplasm and can be liberated into solution when cells are broken with a homogeniser or by osmotic shock. Methods for its isolation include Straub's procedure[81], ion-exchange[82] and affinity chromatography[82-84].

The enzyme LDH catalyzes the following reversible reaction:

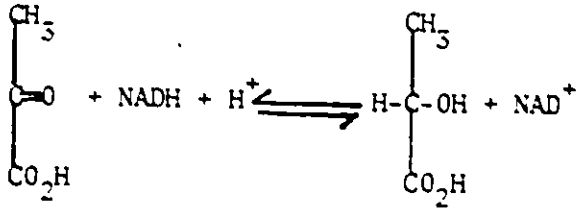

$$K_{eq} = 3.4 \times 10^{11}\ M^{-1}$$

Its catalysis is facilitated by the presence on its active site of Histidine-195 and Arginine-171 and its activity does not require a metal ion as is the case with alcohol dehydrogenase which has a zinc ion[79,80]. Only very high concentrations of lactate can inhibit the forward reaction shown above[80,86,87]. However, the effect is more pronounced with the heart (H_4) than the muscle (M_4) isozymes. For example, Staunbaugh and Post[87] have found that the K_i values for lactate are 26 mM with the heart and 130 mM with the muscle isozymes in free solution. The kinetic equations for LDH in soluble form have been discussed in great detail by Laidler[1].

CHAPTER II

FLOW KINETICS WITH THE ENZYME CHEMICALLY ATTACHED IN A NYLON TUBING

2.1 Introduction

Progress in enzyme-immobilization techniques has made possible the use of enzymes in many forms of reaction configurations such as packed beds, hollow fibres, stirred tanks, fluidized beds and open tubular reactors. Open tubular reactors in which an enzyme is attached to the inner surface of a tube have proven to be particularly effective in fields like clinical medicine[88], food industry[35] and drug technology[89] where they are used as automated analytical flow systems for continuous analysis of specific substrates in liquid samples such as blood serum[90], urine[91] and fermentation fluids[92]. A theoretical treatment of Kobayashi and Laidler[73] has been applied to a number of experimental studies of the flow kinetics of this system[29]. The results of the experiments indicate the treatment to be along the right lines. Up to now, attention has been largely confined to single-substrate-enzyme systems. In this Chapter, a preliminary investigation of the applicability of the theory to the reaction between pyruvate (CH_3COCO_2H) and NADH, catalyzed by LDH, with the enzyme convalently attached to the inner surface of a nylon tube is presented.

2.2 Theoretical

2.2.1 K-L Treatment

Kobayashi and Laidler have presented a detailed theoretical

analysis of the flow kinetics of an enzyme attached to the inner surface of a tube[73,29]. Some important features of the theory will be reviewed here.

The model considered consists of a tube of radius r and length L, with an enzyme chemically attached to the surface of its impermeable inner wall. A solution containing a substrate (reactant) at concentration [S] enters the tube at a constant flow rate of v_f. Reaction takes place at the active surface and the concentration of the product $[P]_e$ is determined at the tube exit. The model identifies three sections of the tube for the velocity and concentration flow patterns as shown in Figure 5: (I) the inlet section, (II) the intermediate section and (III) the fully developed section. In the inlet section, the velocity profile of the fluid entering the tube is flat but due to friction at the wall, it easily becomes parabolic in shape before region II is even reached and remains that way throughout the entire length of the tube. The concentration profile is initially flat too but it changes slowly due to the enzymatic reaction on the wall and becomes fully parabolic only after region II. Thus, in region III, both velocity and concentration profiles are fully developed. Regions I and II are negligibly small compared to the total length of the tube[73] and the parabolic profile is assumed therefore to be developed right from the entrance of the tube.

Assuming that the flow through the tube is laminar, that the tube itself is isothermal and not charged, that the substrate concentration is low and that the enzyme reaction on the wall takes place,

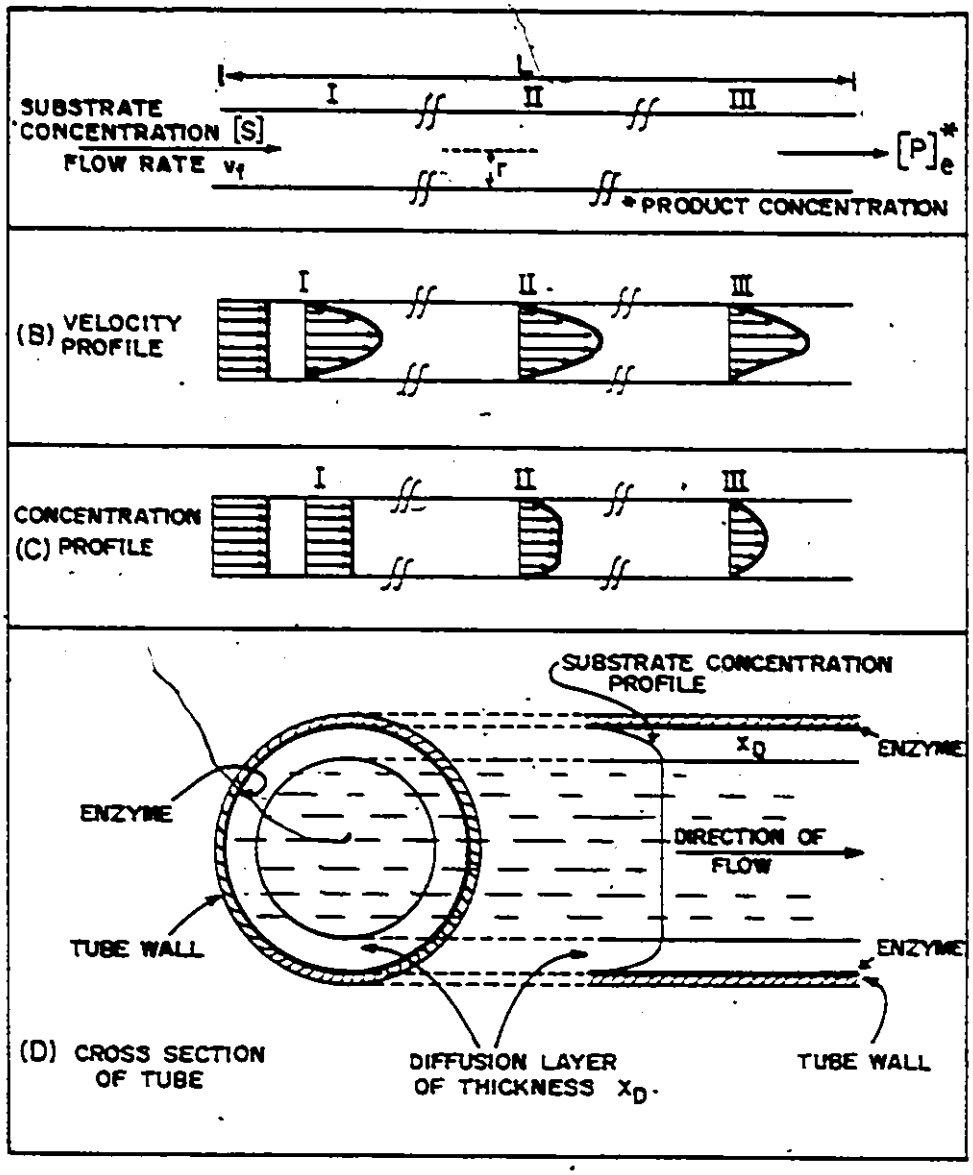

Figure 3. Schematic diagrams showing the important parameters of the tubular model considered in the Kobayashi and Laidler kinetic treatment.

the two workers derived the following mass-balance expression for the substrate:

$$D_s \left(\frac{\partial^2 [S]}{\partial R^2} + \frac{1}{R} \frac{\partial [S]}{\partial R} \right) + D_s \frac{\partial^2 [S]}{\partial z^2} - 2v_f \left(1 - \frac{R^2}{r^2} \right) \frac{\partial [S]}{\partial Z} = 0 \qquad (1)$$

where D is the diffusion coefficient; R a small distance along the radius, r and Z a small length along the tube. Thus, the first and second terms in Eqn. (1) correspond to diffusion in the radial and axial directions respectively and the convective transport flux is described by the third term.

With further analysis of Eqn. (1), which is beyond the scope of this thesis, Kobayashi and Laidler[29,73] found that the concentration of the product at the exit of the tube and the rate with which it is formed can be described by a mass-transfer coefficient, k_L, defined as

$$k_L = \frac{3}{2} \frac{\sqrt[3]{12}}{\Gamma(1/3)} \left(\frac{D^2 v_f}{rL} \right)^{1/3} \qquad (2)$$

for a given flow rate (v_f), diffusion coefficient of substrate (D) and tube length, L. Since the Gamma function of 1/3, $\Gamma(1/3)$ is equal to 2.67, Eqn. (2) reduces to

$$k_L = 1.29 \left(\frac{D^2 v_f}{rL} \right)^{1/3} \qquad (3)$$

The theory assumes that a diffusion layer is established between the inner surface of the tube and the rest of the bulk solution in it (Figure 3d). The quantity k_L therefore defines the rate with which substrate and product species respectively cross this layer to and from

the enzyme at the wall, in a direction normal to the main flow. This rate is given by

$$v_D = k_L A[S] \tag{4}$$

or

$$v_D = 8.06\left(v_f D^2 r^2 L^2\right)^{1/3}[S] \tag{5}$$

because the total area, A, of the interior surface of the tube, is equal to $2\pi rL$. The product concentration at the tube exit is then obtained by dividing the rate (Eqn. (5)) by the volume of the solution that emerges in a unit time, viz. $\pi r^2 v_f$, and is thus expressed as follows

$$[P]_D = 2.56\left(\frac{DL}{r^2 v_f}\right)^{2/3}[S]. \tag{6}$$

The above equations were derived for low flow rates and low substrate concentrations when diffusion and laminar flow conditions are satisfied.

It has been established from a number of studies that the mass-transfer coefficient is related to the thickness of the diffusion layer, X_D, by the following simple equation[71]

$$k_L = \frac{D}{X_D}. \tag{7}$$

In view of Eqn. (3), this simplifies to

$$X_D = 0.78\left(\frac{D\,r\,L}{v_f}\right)^{1/3}. \tag{8}$$

Thus, at high flow rates, there is a reduction in the effective thickness of the diffusion layer. In this case, the Kobayashi and

Laidler treatment gives the rate of enzyme reaction on the wall as

$$v_o = \frac{2\pi r\, L\, k_c'[E]_s[S]v_f^o}{K_m' + [S]} \tag{9}$$

and the product concentration at the tube exit as

$$[P]_o = \frac{2\, L\, k_c'[E]_s[S]}{r\, v_f(K_m'+[S])} \tag{10}$$

where k_c' and K_m' are respectively the inherent rate coefficient and the inherent Michaelis constant (both may be influenced by conformational and environmental effects but not by diffusion) and $[E]_s$ is the enzyme concentration per unit surface area.

According to Kobayashi and Laidler, the mass-transfer coefficient (Eqn. (3)) derived from Eqn. (1) applied to immobilized enzymes obeying the simple Michaelis-Menten kinetics[94] whose mechanism is

$$E + S \rightleftarrows ES \rightarrow E + P \tag{11}$$

where E, S, ES and P stand for the enzyme, the substrate, the enzyme-substrate complex and the product respectively. The theoretical treatment of Sundaran et al[74] and those of a number of other workers[93] show that the rate of reaction of an immobilized enzyme can then be approximated by

$$v = \frac{V_m'[S]}{K_m(app)+[S]} \tag{12}$$

in which V_m' stands for a limiting rate at high substrate concentration

and K_m(app) is an apparent Michaelis constant influenced by conformational, environmental and diffusional effects. The theory for the tubular reactor says that the diffusion-free K_m' of Eqn. (9) is related to the diffusion-controlled K_m(app) by the equation

$$K_m(app) = K_m' + \frac{V_m'}{2k_L} \tag{13}$$

In view of Eqn. (3), this reduces to

$$K_m(app) = K_m' + 0.39\, V_m' \left(\frac{rL}{D\bar{v}_f}\right)^{1/3} \tag{14}$$

so that a plot of K_m(app) against $v_f^{-1/3}$ if linear should yield K_m' as an intercept. This has been confirmed for a number of systems.

2.2.1 (i) Use of Dimensionless Parameters, ϕ and ρ

The treatment of Kobayashi and Laidler also gives a special procedure by which the extent of diffusion control in a particular experiment with the tube system can be assessed through the use of the following two dimensionless variables:

$$\phi = \frac{[P]}{[S]} \left(\frac{v_f r^2}{DL}\right)^{2/3} \tag{15}$$

$$\rho = \frac{K_m(app)}{[S]} \tag{16}$$

The quantities of Eqns. (15) and (16) above are experimentally obtainable. An entry of these ϕ's against their corresponding ρ's into a theoretically made ϕ-ρ indicator diagram will yield experimental points

which will distribute themselves among the regions of the diagram. These regions are defined by means of a utilization factor η. This factor is the ratio of the observed diffusion-free velocity of product formation to the theoretical diffusion-free rate. Figure 4 is an example of the indicator diagram under discussion. It is divided into three regions by two lines corresponding to the utilization factors shown. These regions correspond to small (S), moderate (M) and large (L) diffusion effects. Thus, the degree of diffusion in a particular experiment can be assessed from the location of the experimental points in the ϕ-ε diagram. Appendix A of this thesis explains clearly how to construct the ϕ-ε indicator diagram.

2.2.2 The Kinetics of LDH

It is known from numerous studies that the conversion of the reactants to the products by LDH in free solution passes through a three-membered intermediate complex consisting of NADH, pyruvic acid and the enzyme LDH[79,80]. The reaction occurs by an ordered ternary complex mechanism where NADH binds to the enzyme first and pyruvic acid last[80,81]. If the same is true of the bound LDH, the reversible kinetic mechanism can be represented as follows[1]

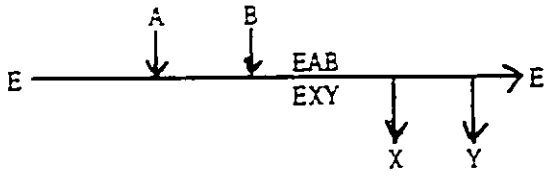

(17)

where A, B, X and Y respectively denote NADH, pyruvic acid, lactic

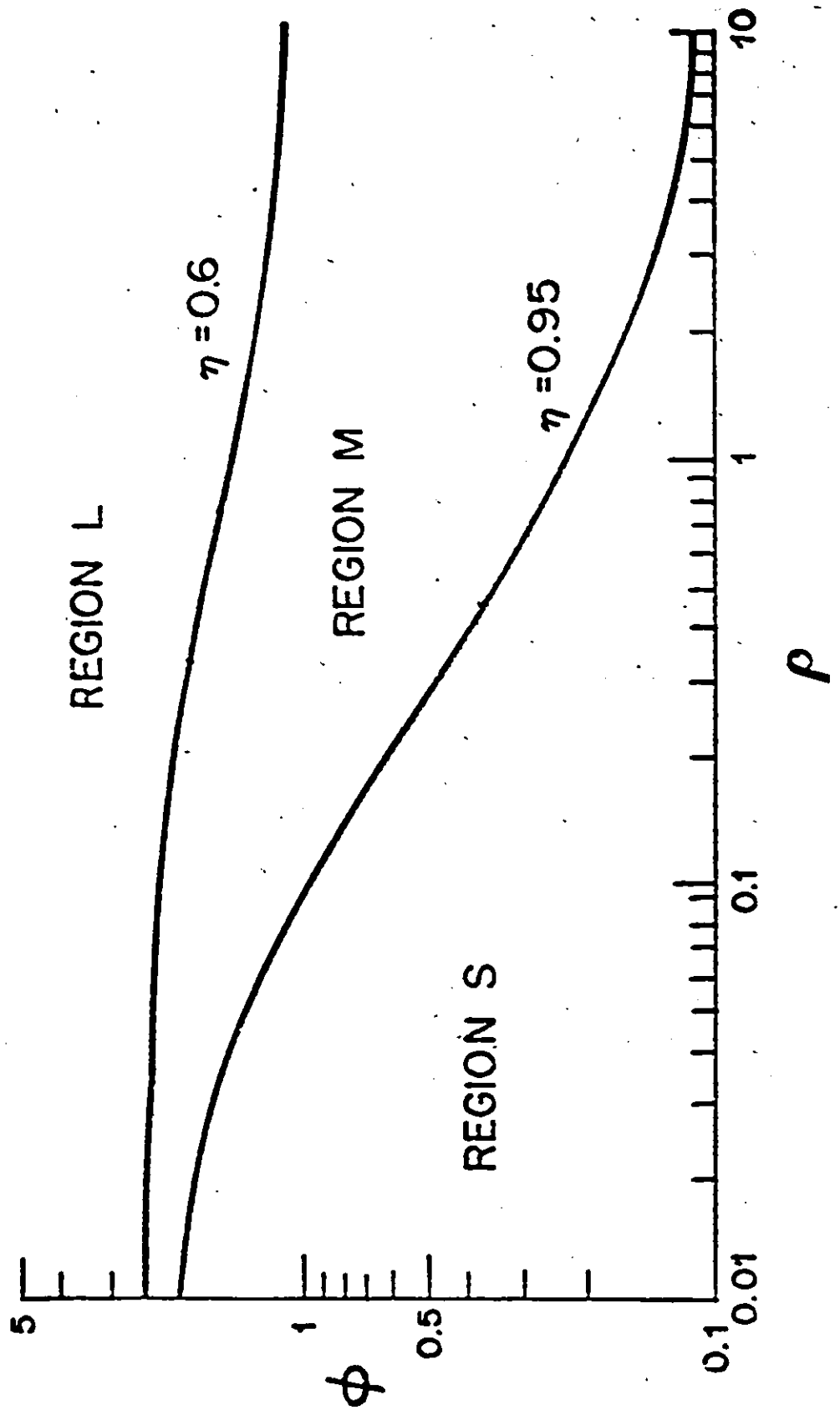

Figure 4. ϕ-ρ indicator diagram showing three regions corresponding to small (S), medium (M) and large (L) diffusional effects.

acid and NAD^+. Here, EAB is a ternary complex for the forward process and EXY for the reverse reaction. The symbol E above stands for either immobilized or free enzyme. In going from left to right, mechanism 17 gives rise to the following complicated rate expression[1]

$$v = \frac{V'_m[A][B]}{K'_A K_B + K_B[A] + K_A[B] + [A][B]} \tag{18}$$

where K'_A, K_A, K_B are the usual Michaelis-Menten constants, and V'_m ($= k'_c[E]$) is the maximum limiting rate. When the attachment of A to E does not affect the ease of attachment of B, $K'_A = K_A$ and Eqn. (18) rearranges[1] to:

$$\frac{1}{v} = \frac{K_A}{V'_m[A]}\left(\frac{K_B}{[B]} + 1\right) + \frac{1}{V'_m}\left(\frac{K_B}{[B]} + 1\right) \tag{19}$$

or

$$\frac{1}{v} = \frac{K_B}{V'_m[B]}\left(\frac{K_A}{[A]} + 1\right) + \frac{1}{V'_m}\left(\frac{K_A}{[A]} + 1\right) \tag{20}$$

so that if the reaction rate, v, varies with the changing concentration of substrate A, in Eqn. (19), for example, a plot of v^{-1} against $[A]^{-1}$ will yield a slope equal to $\frac{K_A}{V'_m}\left(\frac{K_B}{[B]} + 1\right)$ and an intercept expressed as $\frac{1}{V'_m}\left(\frac{K_B}{[B]} + 1\right)$ at constant [B]. The Michaelis-Menten rate constant for A (i.e. K_A) will therefore be obtained from the division of the slope by the intercept. Similarly, K_B can be calculated from the slope and the intercept of a v^{-1}-$[E]^{-1}$ line at constant [A]. Unfortunately, however, the K-L theory was not developed for enzyme reactions involving more than one substrate or for rate expressions as complicated

as Eqn. (18). A theoretical treatment for an enzyme bound to the inner surface of a tube for these complex situations has not yet been presented. Fortunately, for the case of LDH, when NADH is present in high excess for example, it will saturate the enzyme at the surface. The substrate, pyruvic acid, which is in lower concentration will then travel through the diffusion layer and interact with the enzyme-NADH complex to yield the product. Under these conditions, the variation of the rate as a function of the lower substrate concentration is expected to approximate the simple Michaelis-Menten kinetics[94] as explained below.

2.2.2 (i) Explanation

Consider a two-substrate-enzyme system. Let the concentration of one substrate, S_L, be lower than its Michaelis constant and keep the other in excess. The latter substrate, designated S_{ex}, will saturate the enzyme. Thus, we can write

$$[E\ S_{ex}] = [E_o] \tag{21}$$

The reaction rate will be determined by the interaction of $E\ S_{ex}$ with S_L and will obey the following sequence:

$$E\ S_{ex} + S_L \rightleftharpoons E\ S_{ex}\ S_L \rightarrow E\ S_{ex} + P_L \tag{22}$$

This mechanism leads to the following rate expression:

$$v = \frac{k_c'[ES_{ex}][S_L]}{K_m(app)+[S_L]} \tag{23}$$

In view of Equation (21), Equation (23) can be expressed as:

$$v = \frac{k'_c[E_o][S_L]}{K_m(app)+[S_L]} \qquad (24)$$

for an immobilized enzyme. $K_m(app)$ is therefore a diffusion-controlled apparent Michaelis constant for substrate S_L and the diffusion-free limiting rate V'_m is equal to $k'_c[E][S_{ex}]$. It follows from Eqn. (24) therefore that in a two-substrate enzyme system, when one substrate is present in a large excess, the rate equation (18) reduces to an equation identical to (12). Another way of explaining this problem is achieved by rearranging Eqn. (18) into

$$v = \frac{V'_m[A][B]}{(K_A+[A])(K_B+[B])} \qquad (25)$$

When [B] is very large, Eqn. (25) becomes

$$v([B]\to\infty) = \frac{V'_m[A]}{K_A+[A]} \qquad (26)$$

Similarly, at high [A], we get

$$v([A]\to\infty) = \frac{V'_m[B]}{K_B+[B]} \qquad (27)$$

from Eqn. (26). Thus, for the interpretation of experimental data of the flow kinetics of LDH attached to the inner surface of a tube on the basis of the K-L theory, it seems best to concentrate on the two limiting cases; that is, with NADH in excess, the low concentration of pyruvate varied. When pyruvate is in excess, since the mechanism is ordered, the situation may be different. In this case, however, the

NADH will diffuse to the surface and form a complex with the LDH enzyme which will then interact rapidly with the readily-available pyruvate. The rate equations (12, 25, or 28) will again be satisfied.

In principle, using the saturation-constant explanation given above, the K-L theory can be extended to apply also to enzymes that may form quaternary complexes before the release of their products if we let concentrations of two substrates fixed at a large excess and vary the third.

2.3 Experimental

2.3.1 Materials

Nylon tubing of 0.152 cm internal diameter was purchased from Canus Plastics Limited, Ottawa. The enzyme, lactate dehydrogenase (EC 1.1.1.27) type 1, lot 55C-9500 and its two reactants, pyruvic acid lot 31C-1640 and reduced nicrotinamide adenine dinucleotide, lot 57C-73701 were obtained from the Sigma Chemical Company, St. Louis, M.O., U.S.A. The enzyme, an extract from a rabbit muscle, came in crystalline form suspended in 2.1 mol dm^{-3} ammonium sulfate at pH 6.0. Each cm^3 contained 26 mg of enzyme protein and there were 85 units per mg of protein. Before use, the enzyme was dialyzed against 500 cm^3 of 0.1 mol dm^{-3} sodium phosphate buffer, pH 7.5 containing 10^{-3} mol dm^{-3} β-mercaptoethanol. The β-mercaptoethanol, lot 76C-0049, and benzidine (p-diaminodiphenyl) lot 87C-0456, were Sigma products too. EDTA, lot 732338 was bought from the Fisher Scientific Company, N.J., U.S.A. Sodium phosphate salts (monobasic, lot 334185 and dibasic, lot 43780)

used as buffering agents were purchased from the Baker Chemical Company, Philipsburg, U.S.A. Sodium borate, lot 270324, and boric acid, lot 38395, also used as buffering agents respectively, came from Anachemia Chemical Ltd., Montreal, and the British Drug Houses Laboratory Chemical Division, England. Glutaraldehyde, lot D5A, used as a cross-linking agent between the tube and the enzyme, the purpose benzidine was used for, was a product of the Eastman Organic Chemicals Ltd., U.S.A. Dicyclohexylcarbodiimide, a condensing reagent for carboxyl and amino groups, was obtained from the Matheson Coleman and Bell Manufacturing Chemists, Ohio, U.S.A. All chemicals were reagent grade. The water used to make buffer solutions was doubly distilled and cartridges packed with ion exchange resins (products of the Sybron Corporation, U.S.A.) were utilized to de-ionize the water.

2.3.2 Attachment Procedure

The approach used here to attach lactate dehydrogenase to the inner surface of the nylon tubing through chemical bonding was a little different from the methods of Hornby and co-workers[65,95,96], Allison et al[97], Filippusson et al[98] and from those used previously in our laboratory[99-103] in that while these workers used one chemical agent to serve as a bridge between the tube and the enzyme, we used two (i.e. glutaraldehyde and benzidine). This modification was later found to be good because then the enzyme showed stable activity for a long time which was not achievable with the earlier methods.

The procedure we used involves the following steps:

(1) partial hydrolysis of the amide linkages of the inner surface of the nylon tubing to produce carboxyl and amino groups

(2) coupling of the free carboxyl groups to benzidine in the presence of dicyclohexycarbodiimide

(3) reaction of the amino groups on the nylon surface with glutaraldehyde and finally

(4) reaction of the activated nylon surface with the enzyme.

A nylon tubing, 2 m long, was first filled with a mixture of 18.6% (w/w) $CaCl_2$ in water and 18.6% (w/w) water in methanol, and incubated at 40 °C for 30 minutes to etch the interior surface. It was then perfused with water for 20 minutes at a flow rate of 5 cm^3 min^{-1}. The tube and the 4.5 mole dm^{-3} HCl solution were transferred to a water bath kept at 40 °C and then the acid was pumped through this tube at 5 cm^3 min^{-1} for 20 minutes in order to bring about partial hydrolysis. The hydrolysis was stopped by washing the tube with ice-cold distilled water again at 5 cm^3 min^{-1} for 30 minutes.

The presence of liberated amino groups on the inner surface of the tube was confirmed by the red coloration produced on the interior when a small portion of this tube was treated with 0.1 % (w/w) solution of 2,4,6-trinitrobenzene sulphonate saturated with sodium tetraborate. The tube was then perfused for 4 hours at 10 °C with a mixture of 1 % (w/v) benzidine and 1 % (w/v) dicyclohexylcarbodiimide in methylene chloride at 1 cm^3 min^{-1} in order to couple benzidine to surface carboxyl groups. Uncoupled benzidine was removed by successive pumping at

1 cm^3 min^{-1} of 50 cm^3 of methylene chloride, 50 cm^3 of acetone and 50 cm^3 of ice-cold distilled water.

All the remaining steps were carried out with the tube and solutions in crushed ice between 0 and 4 °C.

All amino groups on the nylon surface, that is those generated by partial hydrolysis plus those derived by benzidine attachment, were reacted with 12.5 % (v/v) glutaraldehyde in 0.2 mol dm^{-3} borate buffer, pH 8.5 for 1 hour at a flow rate of 1 cm^3 min^{-1}. Unreacted glutaraldehyde was removed by pumping 50 cm^3 of 0.1 mol dm^{-3} sodium phosphate buffer, pH 7.5 containing 10^{-3} mol dm^{-3} EDTA and 10^{-3} mol dm^{-3} ß-mercaptoethanol at 5 cm^3 min^{-1}. Immediately afterwards, the tube was perfused with the enzyme solution containing 26 mg of enzyme protein in 10 cm^3 of 0.1 mol dm^{-3} sodium phosphate buffer, pH 7.5 at 0.5 cm^3 min^{-1}. Thus, there were 221 enzyme units per cm^3 of solution. To allow complete reaction, the enzyme solution was circulated through the tube for 24 hours at 0.5 cm^3 min^{-1}. Noncovalently bound protein was removed by washing the tube with 1 dm^3 of 0.5 mol dm^{-3} NaCl in 0.1 mol dm^{-3} phosphate buffer, pH 7.0 at a flow rate of 5 cm^3 min^{-1}. When not in use, the tube was filled with the assay buffer and stored at 4 °C.

2.3.3 Kinetic Procedure

(i) Free LDH. Kinetic runs with the free enzyme were carried out in cuvettes with a light-path length of 1 cm , at 25 °C and at atmospheric pressure (1 atm). Changes in absorbance of NADH[104,105] (ε_{340nm} = 6.22 x 10^3 M^{-1} cm^{-1}) as a function of time were automatically

obtained by means of a chart recorder (Unicam AR25 Linear Recorder) connected to the double beam SP1800 U.V. spectrophotometer. The sample chamber of the spectrophotometer was connected to the Mgw Lauda Temperature Control System (Model NB-S15) to fix 25 ± 0.1 °C for all samples. Micropipettes varying in size from 10 to 1000 µL were used to transfer appropriate portions of the stock solutions of the reactants to a reaction vessel where they were diluted up to 3 mL with 0.1 M sodium phosphate buffer, pH 7.5. The concentration of the enzyme protein (2.38 nM) was determined at 280 nm ($\varepsilon = 2.0 \times 10^5$ M^{-1} cm^{-1})[85,86,106] with the U.V. spectrophotometer. Reaction rates were calculated from the initial slopes of the experimental absorbance versus time curves. Each substrate-concentration run was repeated three times and average reaction velocities are reported in Tables 2A and 2B. Equations (19) and (20) were used to obtain Michaelis-Menten constants from the data.

(ii) Immobilized LDH. The arrangement of the apparatus used to obtain experimental data with the tubular reactor is shown schematically in Figure 5.

For initial experiments, a 1-meter piece of the catalytic nylon tube, cut from a 2-meter preparation was used. It was bound into a coil and by means of tygon tubing, one end was connected to a feed solution in a mixing flask and the other to a flow cell (1 cm path length) in the Pye Unicam SP1800 U.V. spectrophotometer.

Substrate concentrations were made in a mixing flask (25 ml) with the assay buffer (0.1 M sodium phosphate buffer, pH 7.5 containing

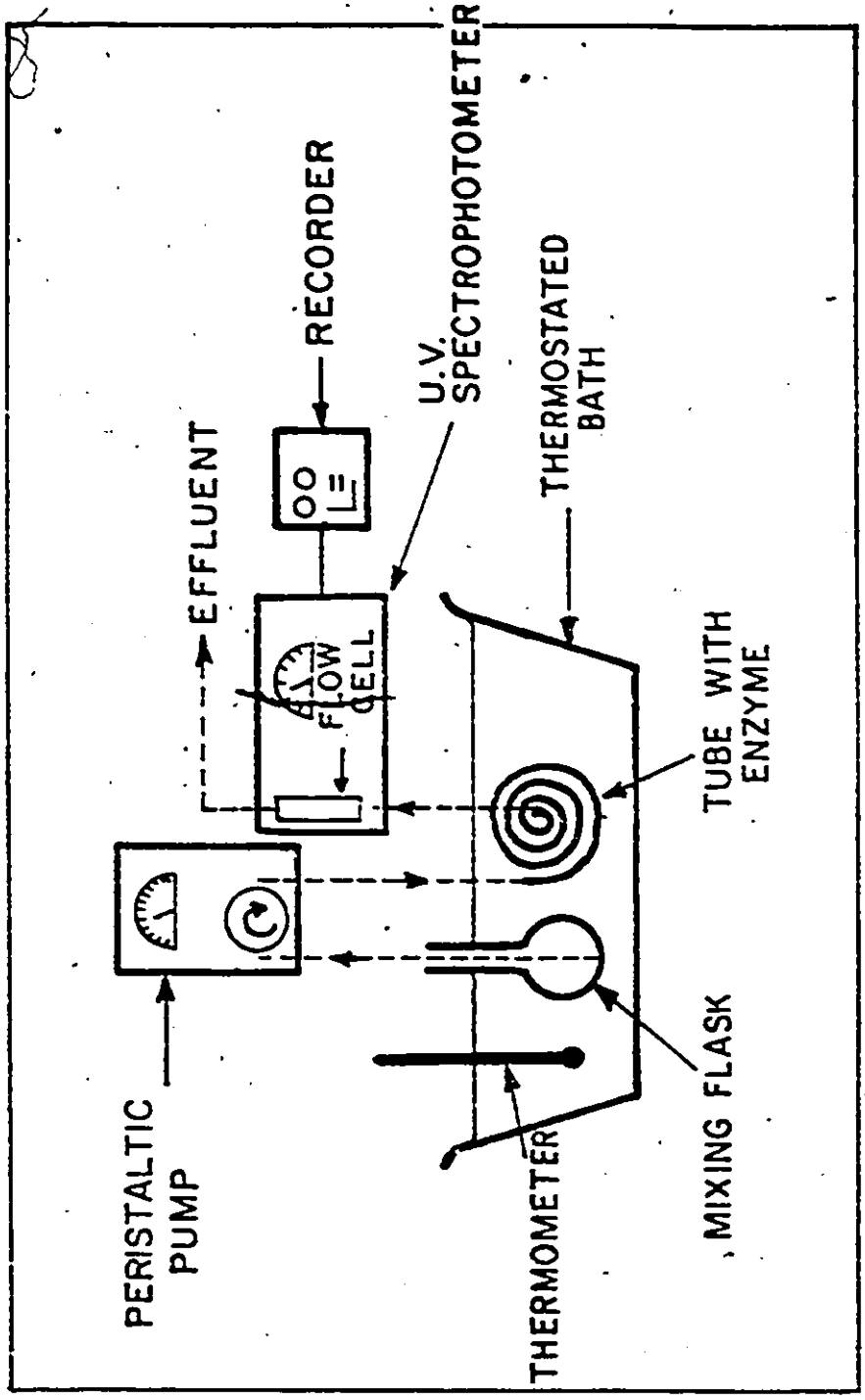

Figure 5. Schematic diagram of the apparatus used for kinetic measurements with LDH immobilized at the inner surface of a nylon tubing.

Table 2. Reaction velocities v_r and kinetic parameters for NADH and pyruvate obtained from the experiments with free LDH.

A. Variable NADH; fixed pyruvate (1.0 mM); fixed enzyme (2.38 nM); temperature = 25 °C								
$[NADH] \cdot 10^6$/M	5.00	10.00	20.00	30.00	50.00	70.00	100.00	150.00
$v \cdot 10^9$/M s^{-1}	2.30	3.42	4.51	5.04	5.57	5.83	6.04	6.22
$K_m^f \cdot 10^6$/M	9.29 ± 2.1 %							
$V_m^f \cdot 10^9$/M s^{-1}	6.80 ± 3 %							

B. Variable pyruvate; fixed NADH (0.30 mM); fixed enzyme (2.38 nM); temperature = 25 °C								
$[Pyruvate] \cdot 10^6$/M	5.00	10.00	20.00	30.00	50.00	70.00	100.00	150.00
$v \cdot 10^9$/M s^{-1}	0.30	0.53	0.85	1.06	1.33	1.49	1.64	1.85
$K_m^f \cdot 10^6$/M	29.98 ± 1.9 %							
$V_m^f \cdot 10^9$/M s^{-1}	2.20 ± 2.7 %							

0.1 mM EDTA and 0.1 mM β-mercaptoethanol). A first series of experiments was made at 25 ± 0.1 °C with the NADH in excess at 2 mM and with the pyruvate concentration varying from 40 to 200 μM. A second series was made at the same temperature; this time, pyruvate was in excess (2 mM) and the concentration of NADH varied (40-200 μM). The LKB Varioperpex II peristaltic pump, Model 2120, was used to pump solutions from the mixing flask through the reactor at flow rates varying from 0.726 to 6.16 cm s^{-1}. The product concentration at the exit of the tube was determined by the decrease in absorbance of NADH at 340 nm. At each flow rate, the reaction rate was calculated by dividing the product concentration by the time it took the solution to flow from one end of the reactor to the other. The time was obtained as a quotient of the length of the reactor and the linear flow velocity of the solution passing through it.

Before each kinetic run was made at any particular flow rate, the whole tube system was washed with a blank buffer solution (a buffer with no NADH and no pyruvic acid) to remove traces of substrate and product species left from a previous experiment. A clean tube was evidenced by a zero absorbance reading, at 340 nm, of the washing solution leaving the tube system. A Mgw Lauda thermostatted bath (Type NB-S15) was used to maintain the temperature of the reaction system at 25 ± 0.1 °C.

Each run with immobilized LDH was repeated four times and the average error of the concentrations of the products (reported in Tables 3A and 3B) at the exit of the tube for indicated flow rates

Table 3. Product concentration $[P]_e$ in μM obtained at the exit of a 100 cm tube for various substrate concentrations (mM) at various flow rates, v_f (cm s^{-1}); temperature = 25 °C; r = 0.076 cm. Average percentage error in $[P]_e$ = ±0.36%.

A. Variable NADH and fixed pyruvate

	v_f	0.726	1.32	2.50	3.63	4.84	6.16
[Pyruvate]	[NADH]	$[P]_e$	$[P]_e$	$[P]_e$	$[P]_e$	$[P]_e$	$[P]_e$
2.00	0.20	137.74	88.09	53.33	41.74	35.62	31.82
2.00	0.16	116.73	72.15	44.94	36.25	30.84	27.05
2.00	0.14	107.61	65.88	40.82	33.60	27.92	24.97
2.00	0.12	94.34	57.83	36.36	29.62	25.83	22.54
2.00	0.10	80.18	50.51	32.00	26.24	22.96	19.55
2.00	0.08	65.59	42.09	26.67	21.52	18.61	16.39
2.00	0.06	51.59	32.51	20.51	16.90	14.55	12.98
2.00	0.05	41.57	27.20	16.91	14.00	12.10	10.70
2.00	0.04	32.02	20.40	12.60	10.71	9.20	8.40

B. Variable pyruvate and fixed NADH

	v_f	0.726	1.320	2.50	3.63	4.84	6.16
[NADH]	[Pyruvate]	$[P]_e$	$[P]_e$	$[P]_e$	$[P]_e$	$[P]_e$	$[P]_e$
2.00	0.25	156.37	94.70	57.14	48.31	39.73	34.53
2.00	0.20	127.54	84.18	54.05	42.43	36.89	32.46
2.00	0.15	119.85	72.78	44.44	34.46	30.84	27.98
2.00	0.10	81.12	52.25	34.48	25.97	22.96	20.54
2.00	0.08	65.00	43.29	28.37	23.03	19.68	17.37
2.00	0.06	50.09	33.94	22.47	18.35	15.89	13.99
2.00	0.05	43.59	29.71	18.18	16.10	13.86	12.02
2.00	0.04	36.25	23.31	16.00	12.55	10.99	9.84

was ±0.36 %. Such a small error can be attributed to the high precision of the spectrophotometric technique for product detection and the consistent flow rates produced by the LKB peristaltic pump.

2.3.4 The Diffusion Coefficient of NADH

Since the application of some equations presented by the K-L theory required the knowledge of the diffusion coefficient of the substrate, experiments were done to measure the value of D, for NADH. The apparatus set up for the purpose was as shown schematically in Figure 6. The formula used to calculate this D was the same as that used by Bunting[57] in his determination of the diffusion coefficient of nitrophenol in polyacrylamide gel having a known length X and a cross-sectional area A, in a solution volume, V:

$$\text{Diffusion rate} = \frac{AD}{XV}(S_o - S) \qquad (28)$$

where, in the case of the present work, A was the cross-sectional area of the diffusion barrier (sintered-glass disc) separating a solute containing solution O, from a pure solvent, P and X was the thickness of this barrier. V was the volume of the solution in the inner vessel. The initial and the time-dependent concentrations of the diffusant were respectively represented by S_o and S.

Throughout the experiments, A, X and V were fixed, the ratio (A/XV) of Eqn. (28) was therefore called the "cell constant" and was evaluated by calibration with a known value of the diffusion coefficient of p-aminobenzoic acid (8.43×10^{-6} cm^2 s^{-1})[107]. With the known value

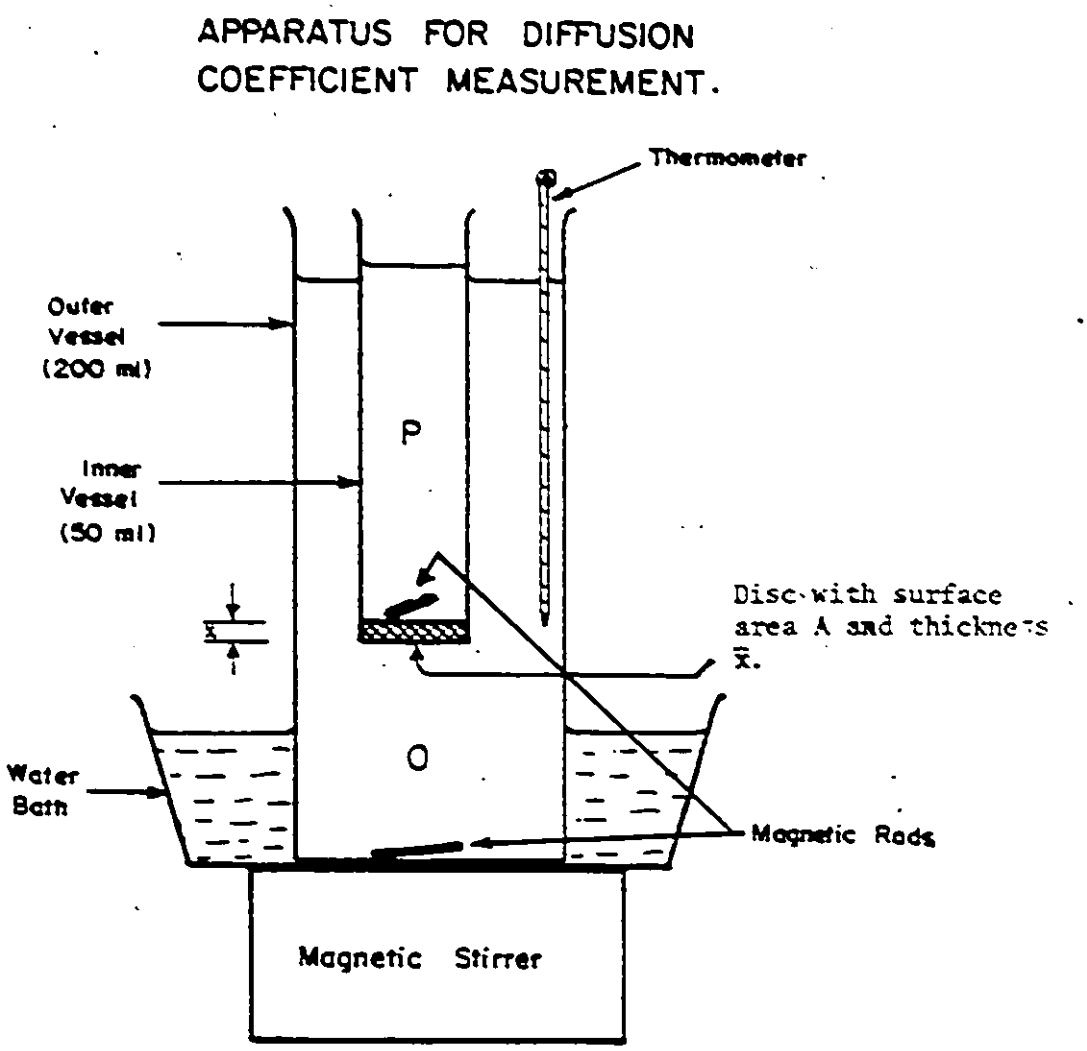

Figure 6. Schematic diagram of the apparatus used for measurements of diffusion coefficients.

of the "cell constant", it was then easy to calculate D for NADH from the variation of the diffusion rate with (S_o-S) as predicted by Eqn. (2.8). The initial concentration of the diffusant in O, for each set of the experiments, was 0.2 mM and the SP1800 U.V. spectrophotometer was used to measure the amount of material entering P from O at 310 nm for p-aminobenzoic acid and 340 nm for NADH. Samples 3 mls in volume were taken from the inner vessel at hourly intervals for analysis and were carefully poured back into P after.

The value of D obtained from this work was 3.89×10^{-6} cm^2 s^{-1} ± 5 % which was in good agreement with the prediction of the nomogram of Othmer and Thakar[108]. Diffusion coefficients of solids in liquids can be measured by many methods[109] such as:

(1) the high absorption techniques

(2) refractive index methods

(3) conductivity methods

(4) the "time-lag" approach[110]

(5) the interference methods developed by Kegeles and Gosting[111], Longsworth[112] and Coulson et al[113], and

(6) the Wilke-Chang calculation method using the molal volume increments listed by Sherwood, Pigford and Wilke[114].

2.4 Analysis and Discussion

Since a complete theoretical treatment of the flow kinetics for a two-substrate-enzyme system has not yet been developed (as already pointed out) and presents considerable difficulty, experiments with

immobilized LDH were carried out with one of the two substrates in excess while the concentration of the other was varied, so that under these conditions, the Kobayashi-Laidler case would then apply and the following methods were used to analyze our experimental data.

2.4.1 Lineweaver-Burk Plots

Plots of $1/v$ against $1/[S]$ based on Eqn. (12) or (25) were made with the aid of the SR-51-II Texas Instruments Calculator to get $K_m(app)$ and V'_m values shown in Table 4, for various flow rates. Figure 7 is an example of a typical Lineweaver-Burk Plot.

Since the extent of diffusion control varies with the substrate concentration, L-B plots may show curvature being convex to the $1/[S]$ axis[29]. Such a curvature shows that the reaction is neither completely diffusion-free nor completely diffusion-controlled. A linear behaviour, however, may mean that the system remains in one region throughout the range of the experiments. Figure 7 clearly shows that the data lay mainly in one region because the curvature is not very pronounced. The results show also that the Michaelis-Menten kinetics is obeyed even with immobilized LDH.

2.4.2 Dependence of Product Concentration and Reaction Velocity on Flow Rate

Since the theory predicts the product concentration at the exit of the tube by Eqn. (6) for a diffusion-controlled case and by Eqn. (10) if the reaction is free from diffusion effects, then a plot of log [P] against log v_f will provide information about the degree of diffusion

Table 4. Apparent kinetic parameters for NADH and pyruvate obtained with the 100 cm tube at various flow rates, v_f (cm s^{-1}) with an average error of ±5 % in both K_m(app) and V_m(app); temperature = 25 °C.

v_f	K_m(NADH).10^4/M	V_m(NADH).10^6/M s^{-1}	K_m(pyr).10^4/M	V_m(pyr).10^6/M s^{-1}
0.726	5.42	3.70	4.66	3.17
1.32	4.71	3.85	3.76	3.23
2.50	4.17	4.17	3.05	3.39
3.63	3.55	4.26	2.64	3.64
4.84	3.32	4.55	2.55	4.08
6.16	3.15	5.00	2.57	4.55

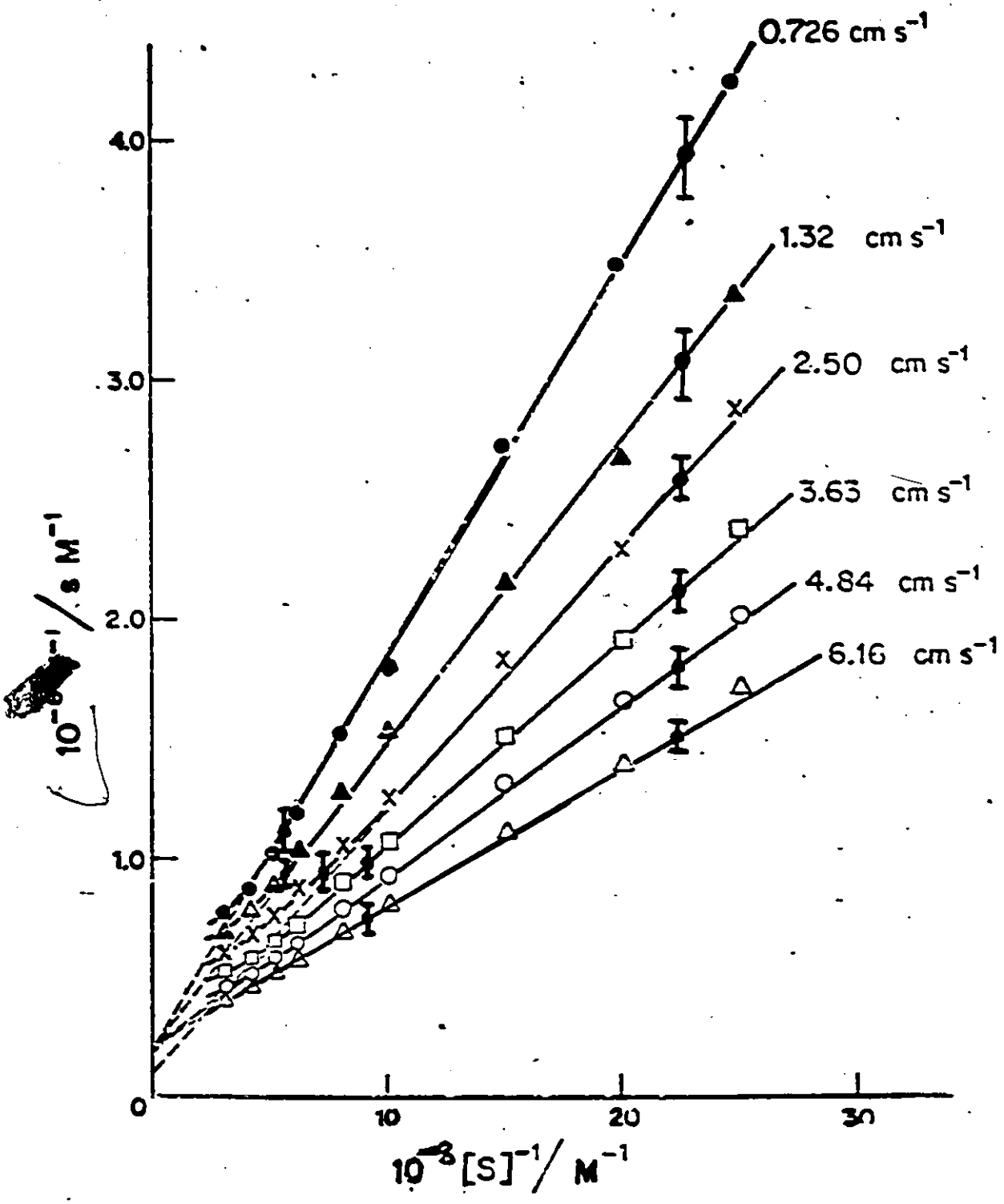

Figure 7. Lineweaver-Burk plots with the pyruvate concentration in excess at 2.0 mM. The flow rates are shown. The K_m(app) values are obtained from the linear portions of the curves; the dashed lines are extrapolations of these linear portions. Temperature = 25 °C, pH = 7.5.

control in a particular experiment. When Eqn. (6) applies, the slope will be -0.67 and if Eqn. (10) is obeyed, the slope of -1.0 will be obtained. From Figure 8, it seems most likely that our experiments were predominantly affected by diffusion, since all of the slopes, particularly those corresponding to the lower substrate concentrations, are closer to -0.67 than to -1.0. The results were therefore more consistent with Eqn. (6) than with Eqn. (10). With regard to defining a sharp boundary between diffusion and diffusion-free regions, these double-logarithmic plots appear to be superior to the Lineweaver-Burk plots. The support for the conclusion that diffusion played an important role in our experiments also came from the results of the double-logarithmic plots of reaction rate against flow rate as shown in Figure 9, which was constructed on the basis of Eqns. (5) and (9). Experimental points obeying Eqn. (5) would produce lines parallel to the standard "diffusion line" of slope +0.33. A slope of zero predicted by Eqn. (9) implies the absence of diffusion.

2.4.3 Dimensionless Parameters

Table 5 and Figure 10 show that all our experiments at all flow rates were heavily influenced by diffusion since all experimental ϕ-ρ points lay in the region marked "L" for large diffusion control.

The most attractive feature of the dimensionless variable approach is in its power to distinguish experiments which are affected by various degrees of diffusion through the use of the utilization factor. While the Lineweaver-Burk approximation and the double-logarithmic

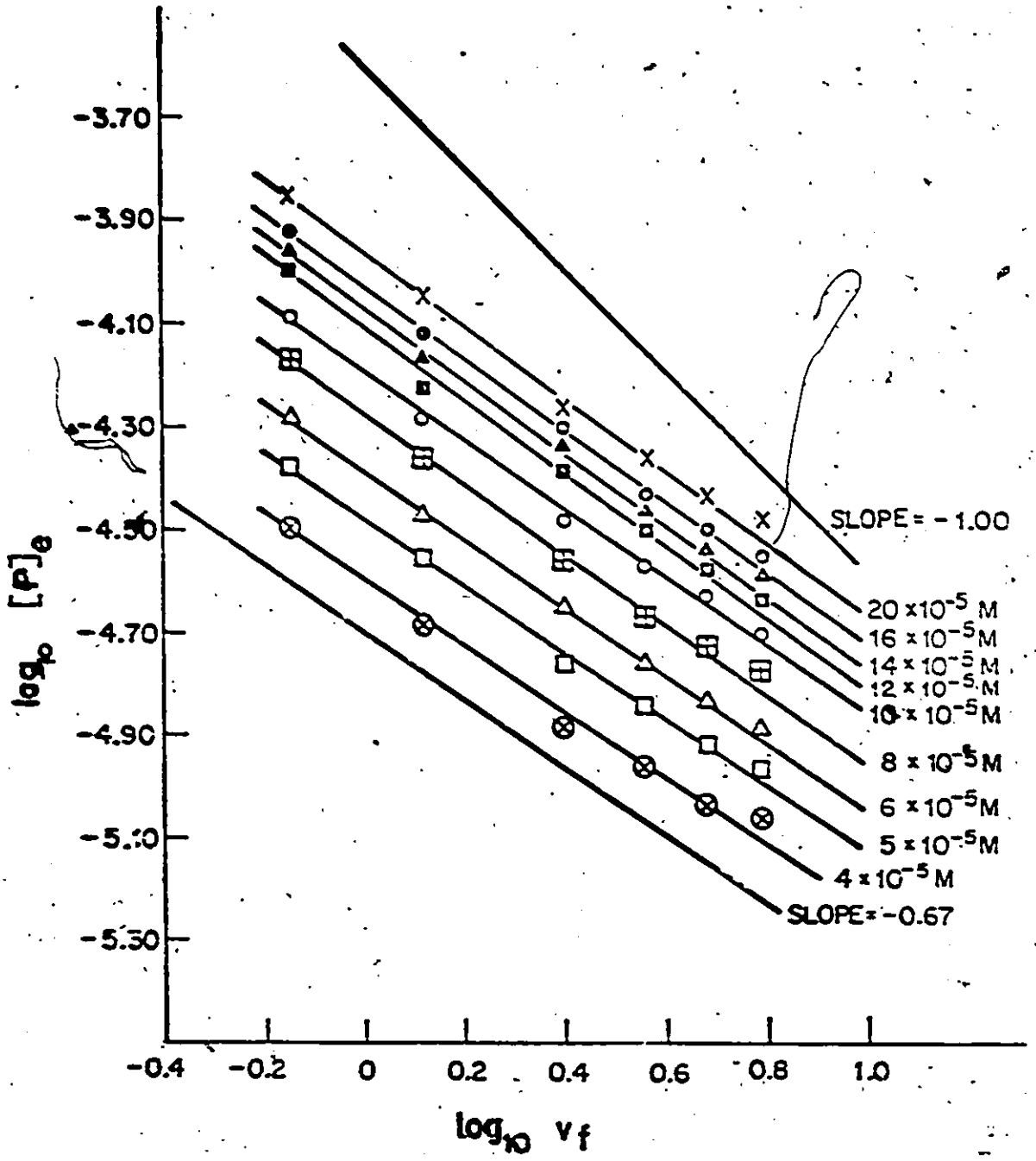

Figure 8. Double logarithmic plots of the concentration of product at the tube exit against flow rate. The concentrations of NADH are shown; the concentration of pyruvate was held in excess at 2.0 mM. Temperature = 25 °C; pH = 7.5.

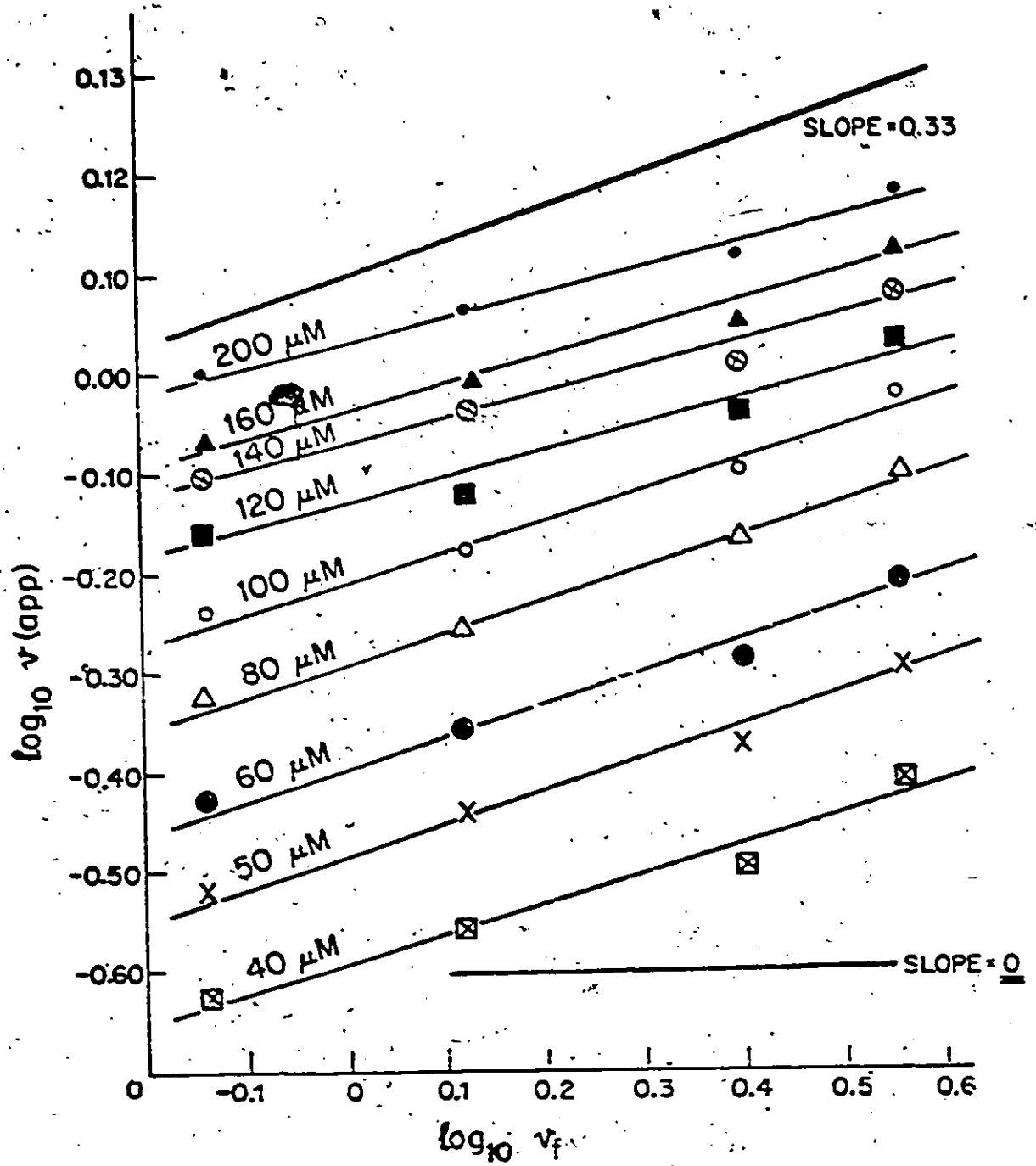

Figure 9. Double logarithmic plots of apparent reaction rates v_r(app) against flow rate v_f. The concentrations of NADH are shown; the concentration of pyruvate was held in excess at 2.0 mM. Temperature = 25 °C; pH = 7.5.

Table 5. Dimensionless parameters obtained for various substrate concentrations (mM) at various flow rates (cm s^{-1}); temperature = 25 °C; L = 100 cm; r = .0.076 cm.

A. Variable NADH and fixed pyruvate

	v_f	0.726		1.32		2.50		3.63		4.84		6.16	
[Pyruvate]	[NADH]	ϕ	ρ	ϕ	ρ	ϕ	ρ	ϕ	ρ	ϕ	ρ	ϕ	ρ
2.00	10.20	3.24	2.71	3.09	2.36	2.86	2.08	2.87	1.77	3.04	1.66	3.15	1.58
2.00	0.16	3.43	3.39	3.16	2.94	2.99	2.60	3.12	2.22	3.22	2.07	3.32	1.97
2.00	0.14	3.62	3.87	3.30	3.37	3.13	2.98	3.29	2.53	3.34	2.37	3.48	2.25
2.00	0.12	3.70	4.52	3.39	3.93	3.25	3.47	3.39	2.95	3.59	2.77	3.67	2.63
2.00	0.10	3.77	5.42	3.54	4.71	3.43	4.17	3.61	3.55	3.84	3.22	3.81	3.15
2.00	0.06	3.86	6.78	3.69	5.89	3.59	5.21	3.71	4.43	3.94	5.14	4.03	3.94
2.00	0.06	4.00	9.03	3.87	7.85	3.68	6.95	3.86	5.91	4.00	5.33	4.21	5.25

B. Variable pyruvate and fixed NADH

	v_f	0.726		1.32		2.50		3.63		4.84		6.16	
[NADH]	[Pyruvate]	ϕ	ρ	ϕ	ρ	ϕ	ρ	ϕ	ρ	ϕ	ρ	ϕ	ρ
2.00	0.25	2.94	1.86	2.73	1.51	2.60	1.22	2.66	1.06	2.76	1.02	2.83	1.03
2.00	0.20	3.24	2.33	3.12	1.88	2.90	1.53	2.91	1.32	3.14	1.28	3.15	1.28
2.00	0.15	3.76	3.10	3.40	2.51	3.21	2.03	3.16	1.76	3.43	1.70	3.67	1.71
2.00	0.10	3.82	4.66	3.50	3.85	3.42	3.05	3.30	2.64	3.84	2.55	4.03	2.57
2.00	0.08	3.84	5.82	3.77	4.70	3.69	3.81	3.96	3.31	4.09	3.19	4.22	3.21
2.00	0.06	3.86	7.76	3.92	6.27	4.02	5.08	4.21	4.41	4.42	4.25	4.58	4.28

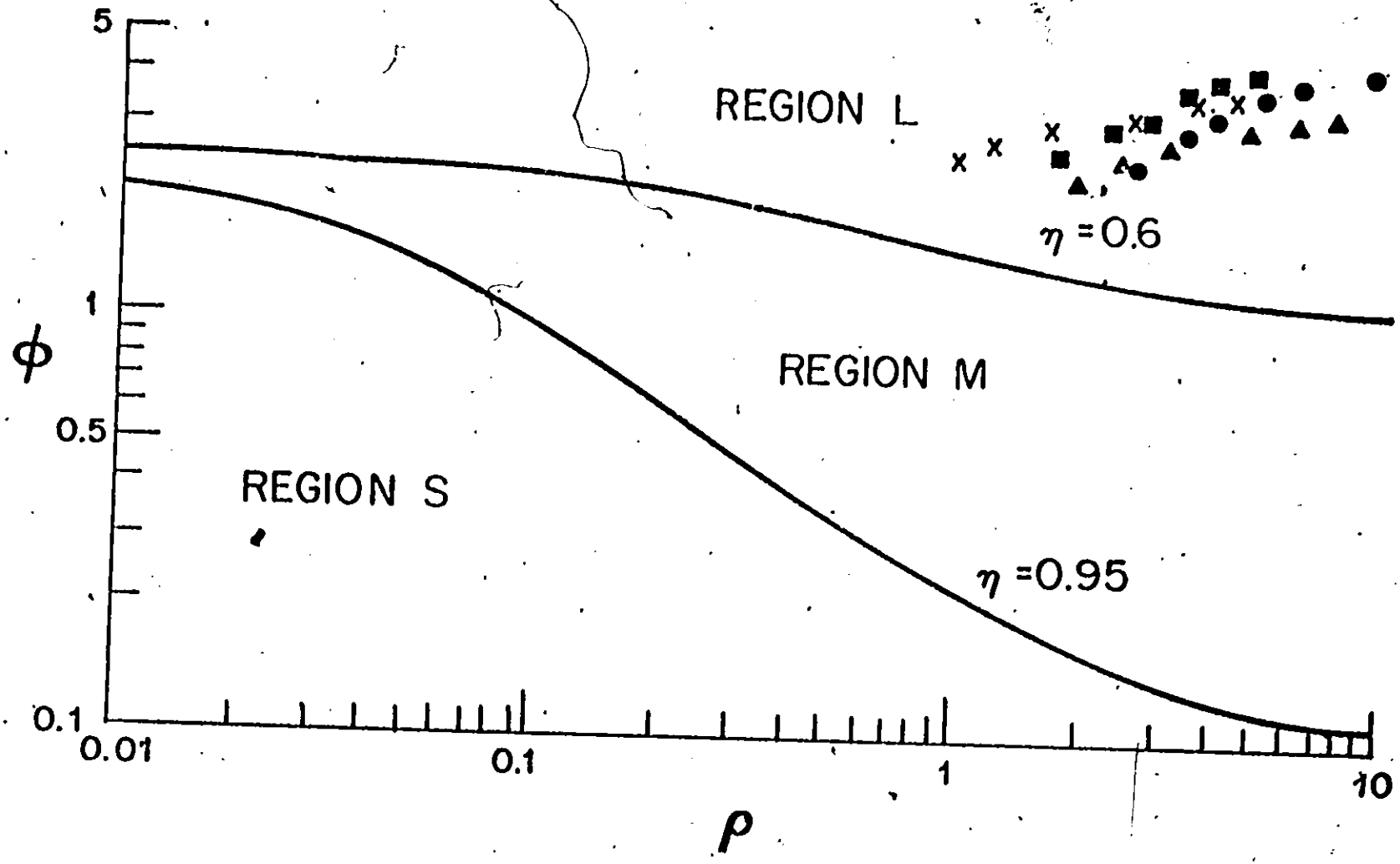

Figure 10. Plots of the kinetic parameters ϕ and ρ for low and high flow rates. All of these experimental points lie in Region 3, indicating substantial diffusion control.

■ variable [NADH]; v_f = 6.16 cm s^{-1}; ● variable [NADH]; v_f = 0.726 cm s^{-1}

✕ variable [CH_3CO_2H]; v_f = 6.16 cm s^{-1}; ▲ variable [CH_3CO_2H]; v_f = 0.726 cm s^{-1}

plots may fail to give a clear quantitative picture of the intermediate kinetics (i.e. mixed situations of free and diffusion-controlled cases) the ϕ-ρ analysis gives an easy answer.

2.4.4 Dependence of K_m(app) on Flow Rate

It was confirmed by methods 2.4.1 thru 2.4.3 above that diffusion controlled the flow kinetics of the enzyme lactate dehydrogenase attached to the inner surface of a nylon tube. The K_m(app) thus obtained in the experiments were definitely diffusion-controlled Michaelis-Menten constants. The K-L theory predicts that such constants obtained at various flow rates can be used to estimate the diffusion-free K_m' values by extrapolation to $(1/v_f)^{1/3} = 0$ (Figure 11), as required by Eqn. (14). The values of K_m' can then be compared with those of K_m^f (see Figure 2 of Chapter 1) to check whether or not immobilization changed the conformation of the LDH. Comparison of the K_m' values for NADH and pyruvate with corresponding K_m^f quantities from this work as well as from other published sources was made (see Table 6). From this work, K_m' and K_m^f for pyruvate were similar, implying that the enzyme did not undergo much change in its conformation as a result of immobilization. However, the NADH K_m' and K_m^f values differed by a factor of almost 10 which would mean that the enzyme's conformation did change upon attachment to the surface. We believe that the enzyme did not change its conformation and that the difference between the two K_m values for NADH could be due to the fact that NADH, being a larger molecule than pyruvate, suffered greater steric hinderances than the smaller pyruvate when LDH was immobilized.

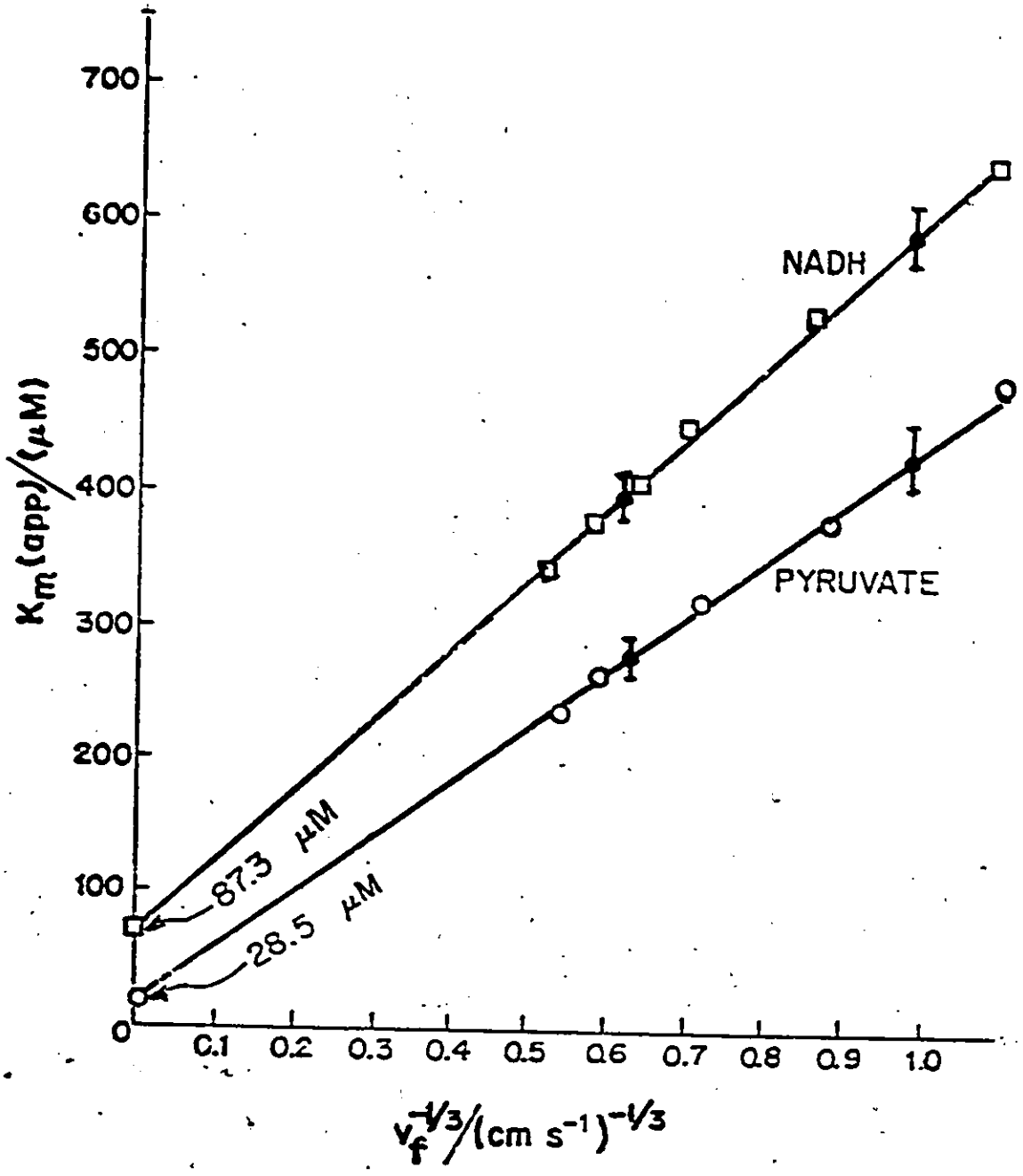

Figure 11. Variation of the apparent Michaelis constants with flow rate. The upper curve is for variable [NADH] with [pyruvate] in excess; the lower for [NADH] in excess with [pyruvate] varied. Temperature = 25 °C and pH = 7.5.

Table 6. Comparison of the values of K_m obtained with the free and bound LDH.

System	Flow Rate	K_m (NADH)	K_m (pyr)	Reference
		µM	µM	
LDH-nylon	0.726	542	466	Present work
LDH-nylon	1.32	471	376	"
LDH-nylon	2.50	417	305	"
LDH-nylon	3.65	355	264	"
LDH-nylon	4.84	332	255	"
LDH-nylon	6.16	315	257	"
LDH-nylon	∞	87.3*	28.5*	"
LDH-cellulose	-	2200	-	115
Free LDH	-	9.3	30	Present work
Free LDH	-	28	250	115
Free LDH	-	7.8	48	116
Free LDH	-	2.8	37	117
Free LDH	-	2.6	17	118
Free LDH	-	10.0	52	119
Free LDH	-	3.5	15	120
Free LDH	-	16	80	121
Free LDH	-	2.5	65	122

* Extrapolated values (see Figure 11)

In the free-enzyme state, the reaction between the LDH and the NADH seemed to occur to a greater extent than with the pyruvate as evidenced by the small values of K_m^f (NADH) and large quantities of K_m^f (Pyruvate). This behaviour changed when the enzyme was immobilized. With regard to this discussion, the Kobayashi-Laidler theory gives us the power to investigate the influence of immobilization on the enzyme's conformation through the application of Eqn. (14).

2.4.5 Temperature Dependence

The theoretical treatment[73] led to the conclusion that the rate is given by (Eqn. (5))

$$v = 8.06\left(v_f\ D^2\ r^2\ L^2\right)^{1/3}[S] \qquad (5)$$

when there is full diffusion control. Only D in the above equation is temperature dependent, and since the rate is proportional to $D^{2/3}$, an Arrhenius plot of log $v^{3/2}$ against 1/T will give the activation energy for the diffusion process. Preliminary temperature-dependence experiments were carried out from 2.0 to 40.0 °C. In one case, the NADH was in excess at 0.3 mM, with [$CH_3COCOOH$] equal to 0.03 mM; in the other, pyruvate was in excess at 0.30 mM and [NADH] equal to 0.03 mM. Figure 12 shows Arrhenius plots of log $v^{3/2}$ against 1/T. As has been discussed, these activation energies relate to diffusion; the values are as follows:

E_D (NADH) = 2.93 kcal mol^{-1} ± 1.03%

E_D (Pyruvate) = 5.72 kcal mol^{-1} ± 1.02%

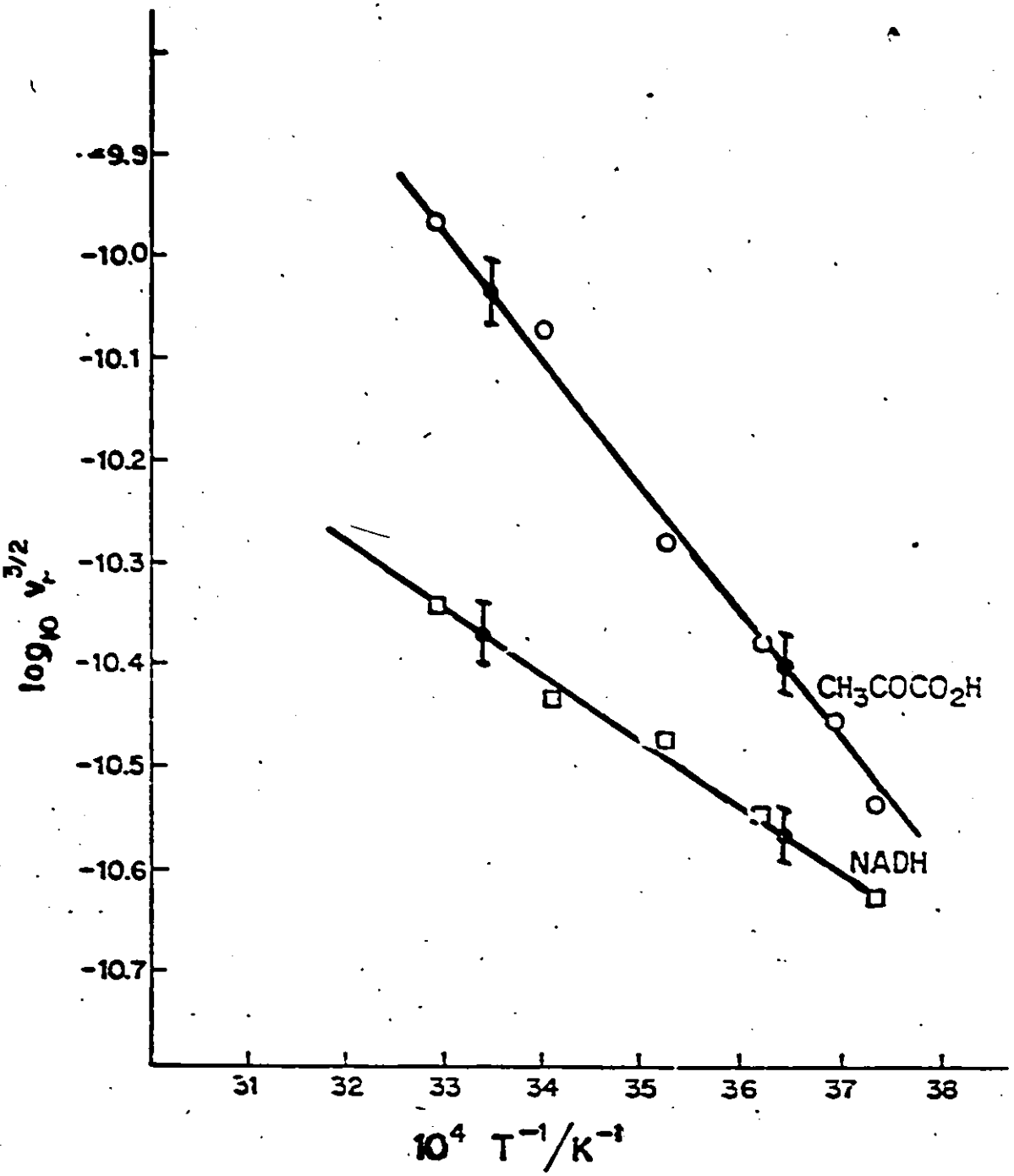

Figure 12. Arrhenius plots of $\log_{10} v_f^{3/2}$ against 1/T. The upper curve is for NADH in excess, with [pyruvate] varied; the lower for pyruvate in excess, with [NADH] varied at pH = 7.0.

2.5 Concluding Remarks

2.5.1 The Immobilization Technique

The summary of the technique employed to attach LDH to the inner surface of a nylon tube is given in Figure 13. Enzyme molecules were convalently joined to the support through two types of cross-linking agents (i.e. glutaraldehyde and benzidine). Some measurements were made to test the stability of the immobilized enzyme layer. Experiments carried out with a given tube on three occasions, with pyruvate in excess at 2 mM, NADH at 0.2 mM and a flow rate of 0.726 cm s^{-1} led to the following product concentrations: 118.3, 119.0, 118.2 μM whose average was 118.5 μM. Forty days later, after storage at 4 °C, the values were 117.2, 117.5 and 118.0 μM, averaging to 117.6 μM, so that the activity was then 99 % of the original value. Three months later, the average of 112.3 or 95 % of the initial activity was obtained from the following readings: 112.5, 112.7, 110.9, 112.4 and 112.7. These results showed that the loss of activity, due to enzyme inactivation, was relatively small over a period of months.

Attempts to attach LDH to nylon tubing by techniques previously employed[95-103], that is, methods using only one cross-linking agent (glutaraldehyde) as well as the modification which required the use of N,N-dimethyl-1,3-propanediane[65] were not very successful, the enzyme losing its activity rapidly with the result that consistent kinetic data could not be obtained. LDH has four polypeptide chains and is less stable than many other enzymes. The usual techniques of Bunting

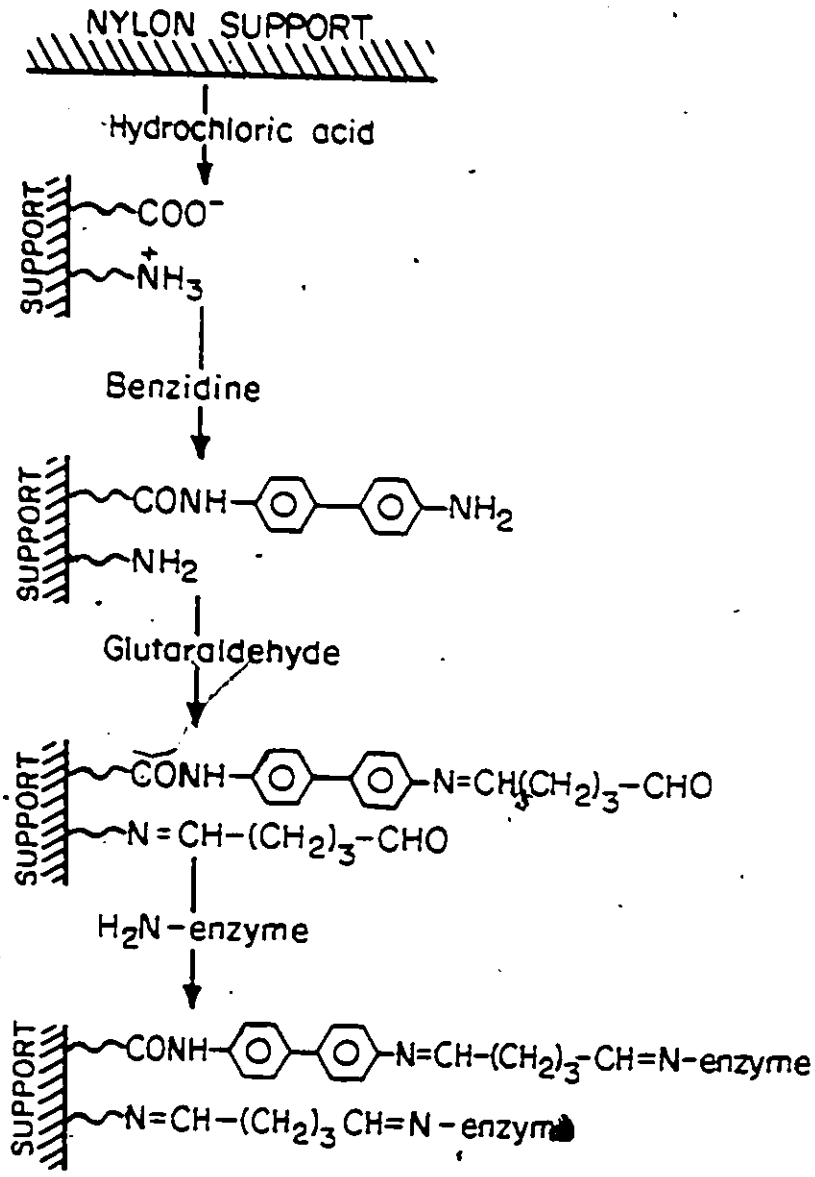

Figure 13. Summary of the immobilization technique which employs both benzidine and glutaraldehyde for cross-linking enzymes to nylon supports.

and Laidler[99] and of Sundaram and Hornby[95] leave a residual negative charge on the surface (Figure 14) and it appears that this is not favourable to dehydrogenase activity. Conversely, the attachment technique of Hornby et al[65] which uses N,N-dimethyl-1,3-propanediane, to remove carboxyl groups from the nylon surface leaves positive charges.

The success of the attachment technique we employed (Figure 13) is probably due to the following reasons:

(i) it led to a neutral surface

(ii) it utilized both carboxyl and amino groups to attach LDH, thus producing a tube with more enzyme attached to its surface than would be the case with the other mentioned methods

(iii) it produced a configuration in which the enzyme was far removed from the surface it was attached to, thus minimizing possible interactions (steric hinderances) between the enzyme and the support which would help in inactivating the immobilized enzyme.

2.5.2 Kinetics

The various tests that were applied showed conclusively that the reactions were largely diffusion controlled, especially at lower substrate concentrations and flow rates. This was indicated partially by the curvature of the Lineweaver-Burk plots (Figure 7), the ϕ-ρ plots (Figure 10) and the double-logarithmic plots (Figures 8 and 9).

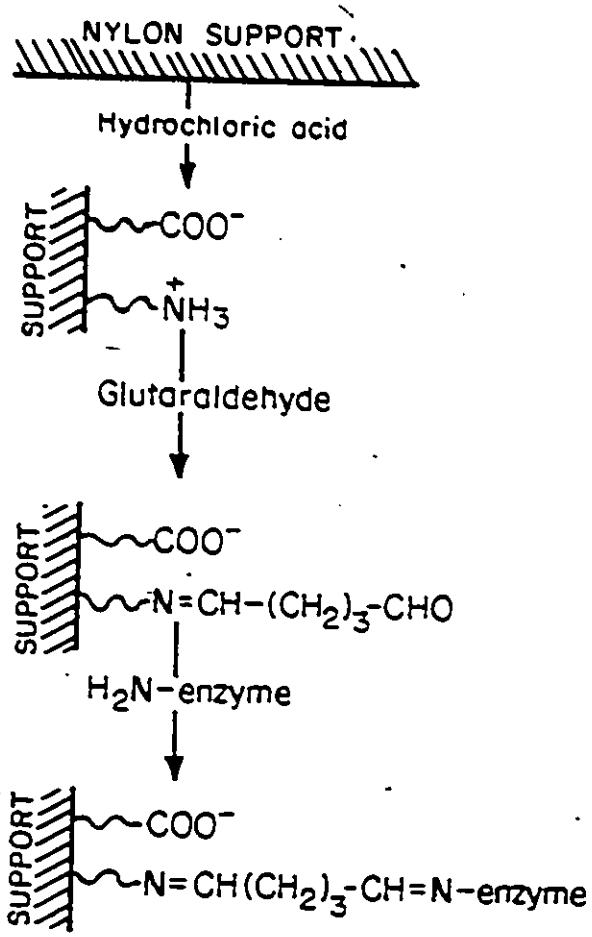

Figure 14. Summary of the immobilization technique which employs only glutaraldehyde as a cross-linking agent between an enzyme and a nylon support.

If the reactions were completely diffusion controlled, the product formed in a particular experiment is given according to the Kobayashi-Laidler treatment by Eqn. (6). This equation allows absolute calculations of the amounts of product formed to be made in terms of D, L, r and v_f at various substrate concentrations. Table 7 was made to show a comparison of observed and calculated values, with D equal to 4×10^{-6} cm^2 s^{-1}, L equal to 100 cm, r = 0.076 cm and P_o = 0. In view of the fact that these are absolute calculations from a purely theoretical equation, the agreement is very satisfactory. There are uncertainties in the values of r, P_o and D aside from the approximations made in carrying out the experiments and in developing the theory. The theoretical equation obviously accounts for the trends in a very satisfactory way.

The variation of K_m(app) with flow rate v_f (Figure11) were similar to those noted in previous investigations with asparaginase[99], acetylcholinesterase[100,103] and β-galactosidase[102]. The apparent Michaelis constants for flow systems when there is diffusion control are very much larger, sometimes by orders of magnitude, than those for the free enzyme. According to the theory[73], the K_m(app) values extrapolated to infinite flow rate are the K_m' values for the surface-attached enzyme in the absence of diffusion control. The values are not expected to be exactly the same as for the free enzyme, as already discussed in Chapter 1, since the surface attachment brings about some change in properties, but one might expect them to be somewhat similar. This work's extrapolated K_m' values are much closer to the values of K_m^f for the free enzyme than are the unextrapolated K_m(app) values.

Table 7. Calculated and observed values of the concentration of product at the tube exit at selected flow rates and selected substrate concentrations.
T = 25 °C; D = 4 x 10^{-6} cm^2 s^{-1}; L = 100 cm; r = 0.076 cm

v_f/cm s^{-1}	[NADH]/mM	[Pyruvate]/mM	Concentration of Product/μM	
			Calculated	Observed
0.726	0.04	2.00	21.8	32.00
6.16	0.04	2.00	5.3	8.40
0.726	0.10	2.00	54.6	80.20
6.16	0.10	2.00	13.1	19.50
0.726	0.20	2.00	109.0	138.00
3.63	0.20	2.00	37.3	41.74
6.16	0.20	2.00	26.3	31.82
0.726	2.00	0.04	21.8	36.25
6.16	2.00	0.04	5.3	9.84
2.50	2.00	0.10	24.1	34.50
1.32	2.00	0.25	91.6	94.70
4.84	2.00	0.25	38.6	39.73

It has long been known that diffusion coefficients and viscosity coefficients obey the Arrhenius law[122]. The activation energies for diffusion are smaller than those for ordinary chemical reactions and vary in a complex manner with the size and structure of the solvent and solute molecules. The values tend to be low for systems with weak intramolecular forces for example, 3.5 kcal for the diffusion of tetrabromethane in tetrachloroethane[123] and higher when there is hydrogen bonding, for example, 5.3 kcal for water in water[124]. The values obtained in the present work are on the whole comparable with other values, although the value of 2.93 kcal for NADH is lower than might have been expected.

CHAPTER III

TEMPERATURE AND pH EFFECTS ON IMMOBILIZED LACTATE DEHYDROGENASE KINETICS

3.1 Introduction

The previous Chapter showed that the application of the Kobayashi-Laidler theory to the flow kinetics of lactate dehydrogenase attached to the inner surface of a nylon tube was satisfactory provided suitable experimental conditions were established. The treatment led to the conclusion that the system was heavily affected by diffusion. Since one of the aims of carrying out kinetic investigations is to find conditions under which the efficiency of a given process can be improved, this Chapter explores the effect of temperature and pH on the same nylon-LDH system, as one of the means of trying to find those suitable conditions; it is obvious that temperature and pH may have some controlling effect on the four principal factors[1,29] that have been proposed as responsible agents for the kinetics of immobilized enzymes. These factors have been discussed in Chapter I of this thesis. Thus, a temperature or a change of pH may:

(1) induce a kinetically more favourable conformation of the immobilized enzyme

(2) bring about improved partitioning of the substrate between the enzyme and the rest of the bulk solution

(3) make the microenvironment, where the substrate and the enzyme interact, support the reaction and

(4) reduce diffusional effects to some degree.

The theory of Kobayashi and Laidler was used to analyze most of the data.

3.2 Experimental Section

3.2.1 Materials and Methods

All chemicals used here and the procedure for covalent attachment of the enzyme were the same as those already described in Chapter II of this thesis.

3.2.2 Rate Measurements

(i) Temperature Dependence

Rates were measured at five temperatures, 10, 20, 30, 40 and 50 °C and at flow rates ranging from 0.36 cm s^{-1} to 1.50 cm s^{-1} with tubes 50 cm in length and 0.076 cm internal radius. The extent of the reaction was followed by the decrease in absorbance of NADH at 340 nm using the apparatus arranged as shown in Figure 5 of the previous Chapter. In one series of experiments, the concentration of pyruvic acid was held at a high value (3.00 mM) and the concentration of NADH was varied. In the second series, the concentration of NADH was held at 2.00 mM and that of pyruvic acid varied. The average concentrations of the products at the exit of the tube at each temperature and flow rate for both series of the experiments are shown in Tables 8A and 8B.

Table 8A. Product concentrations (μM) obtained at the exit of the tube at various NADH concentrations (mM), various flow rates (cm s^{-1}) and various temperatures; L = 50 cm; r = 0.076 cm; with pyruvate = 3.0 mM. Average percentage error in $[P]_e$ = ±0.4%.

		$[P]_e$ at Indicated Temperatures				
v_f	[NADH]	10 °C	20 °C	30 °C	40 °C	50 °C
	50	20.85	26.41	31.28	36.84	41.70
	60	27.80	31.28	34.75	41.01	48.65
	80	34.75	40.31	45.18	51.43	59.77
0.36	100	44.48	50.04	55.60	62.55	83.40
	150	63.94	86.18	93.96	100.78	111.20
	200	90.35	99.52	108.42	118.15	126.49
	300	114.68	128.58	137.61	142.48	145.95
	400	139.00	144.56	148.73	150.12	152.91
	500	151.51	152.90	148.75	152.90	153.00
	600	151.52	152.92	148.76	152.91	152.92
	700	151.52	152.93	148.76	152.90	152.98
	50	16.66	19.09	20.82	24.30	29.84
	60	19.99	21.86	24.29	27.76	30.19
0.72	80	23.60	28.45	31.92	36.44	41.64
	100	27.76	32.97	38.17	42.96	50.38
	150	39.91	46.50	52.05	57.26	62.46
	200	48.58	55.52	62.46	65.93	69.40
	300	65.24	69.40	72.18	74.61	75.65
	400	71.14	74.60	75.65	76.31	76.33
	500	76.34	76.34	76.33	76.32	76.34
	600	76.33	76.36	76.35	76.34	76.35
	700	76.35	76.35	76.34	76.34	76.34
	50	11.58	14.55	17.35	19.68	21.99
	60	13.89	17.36	19.58	22.22	25.93
	80	18.52	20.84	24.31	27.78	31.95
	100	22.46	25.47	27.78	31.25	35.19
1.08	150	28.94	32.41	35.88	39.36	41.67
	200	35.19	37.50	41.67	43.99	46.30
	300	45.14	46.76	48.61	49.77	49.77
	400	50.47	50.47	50.90	50.46	50.46
	500	50.93	50.93	50.92	50.91	50.93
	600	50.98	50.95	50.95	50.93	51.00
	700	51.00	50.94	50.94	50.94	51.33
	50	8.33	10.49	12.72	14.99	16.65
	60	9.99	12.48	15.32	17.35	19.98
	80	13.32	15.82	18.32	20.31	23.64
	100	16.65	19.15	20.81	23.32	26.97
1.50	150	22.44	24.31	26.97	29.14	31.97
	200	26.64	29.14	31.46	33.63	34.97
	300	33.30	34.97	35.80	36.29	36.35
	400	35.80	36.60	36.30	36.43	36.63
	500	36.30	36.65	36.66	36.56	36.63
	600	36.63	36.64	36.95	36.59	36.64
	700	36.70	36.93	37.00	36.64	36.64

Table 8B. Same as in Table 8A, but now NADH is fixed at 2.0 mM and pyruvate is varied.

		$[P]_e$ at Indicated Temperatures				
v_f	[Pyruvate]	10 °C	20 °C	30 °C	40 °C	50 °C
0.36	50	28.48	33.36	36.14	43.09	50.00
	60	32.67	38.23	41.70	48.65	59.08
	80	41.70	49.35	56.30	62.55	72.98
	100	52.13	57.69	65.33	76.45	86.88
	150	68.11	79.93	86.88	99.39	109.81
	200	86.88	97.30	107.03	120.93	129.97
	300	116.76	130.66	139.00	145.95	152.90
	400	139.00	149.45	152.90	156.38	159.85
	500	152.90	156.38	157.07	157.76	159.85
	600	158.46	160.00	159.16	159.85	159.85
	700	160.00	159.16	159.16	159.85	159.85
0.72	50	17.35	19.09	21.86	24.29	26.40
	60	18.04	21.17	23.94	26.37	31.23
	80	22.56	25.68	29.15	34.01	39.56
	100	27.76	31.23	34.70	38.86	43.38
	150	38.17	41.64	46.15	51.01	56.21
	200	46.85	51.36	55.52	60.73	64.20
	300	63.50	65.93	69.40	72.87	79.80
	400	72.18	75.56	76.34	78.08	79.84
	500	77.03	78.08	78.42	79.12	80.00
	600	79.81	79.81	79.81	80.50	79.81
	700	79.81	80.00	79.83	79.86	79.80
1.08	50	10.65	12.50	14.35	16.67	21.76
	60	13.43	15.51	17.36	21.76	26.34
	80	15.97	18.06	20.84	26.39	30.10
	100	19.45	21.76	24.77	30.10	34.73
	150	26.58	30.97	33.80	38.20	41.67
	200	35.19	37.97	40.74	44.45	46.76
	300	46.07	48.38	49.54	50.93	52.09
	400	50.93	52.09	49.54	52.78	53.25
	500	53.25	53.24	52.32	53.71	53.28
	600	53.26	53.48	53.25	53.24	53.22
	700	53.25	53.50	53.35	53.71	53.25
1.50	50	8.49	10.32	11.99	12.00	15.65
	60	10.50	12.49	15.65	15.65	18.95
	80	12.99	15.82	18.98	18.98	21.64
	100	15.98	18.28	21.15	21.65	24.98
	150	20.65	23.31	25.81	27.47	29.97
	200	25.81	27.64	30.14	31.98	33.63
	300	33.13	34.13	34.97	36.63	37.46
	400	36.63	37.30	37.63	37.96	38.30
	500	38.46	38.30	38.26	38.62	38.32
	600	38.50	38.32	38.30	38.30	38.33
	700	38.52	38.33	38.33	38.30	38.30

(ii) pH Effect

The effect of pH on the catalysis of immobilized LDH was measured with a nylon tube (L = 50 cm, r = 0.076 cm) coated with LDH. The temperature and the flow rate were respectively fixed at 35 °C and 1.0 cm s^{-1}. Aided by a pH meter, phosphate buffer solutions (0.1 M) were made using various NaH_2PO_4-K_2HPO_4 and Na_2HPO_4-K_3PO_4 mixtures[125] to which EDTA (0.1 mM) and -mercaptoethanol (0.1 mM) were added. These additives were used to improve the stability of the immobilized enzyme. The rates measured within the pH range 6 to 10 for various substrate concentrations will be discussed later in this Chapter.

3.3 Data Analysis and Discussion

3.3.1 Temperature Effect

(i) Lineweaver-Burk Plots

Under the conditions of the experiments, the variation of the rate with substrate concentration was expected to be of the Michaelis-Menten form. The validity of this case was confirmed by Lineweaver-Burk plots of 1/v against the inverse of the concentration of the varied substrate, made for both series of the experiments at different temperatures and flow rates. Figure 15 shows such a test, for pyruvic acid in excess at 3.00 mM and the concentration of NADH varying between 0.05 mM and 0.70 mM. For all flow rates covered, there was good linearity at the lower substrate concentrations, where substantial diffusion control was expected, but there were deviations from linearity at NADH

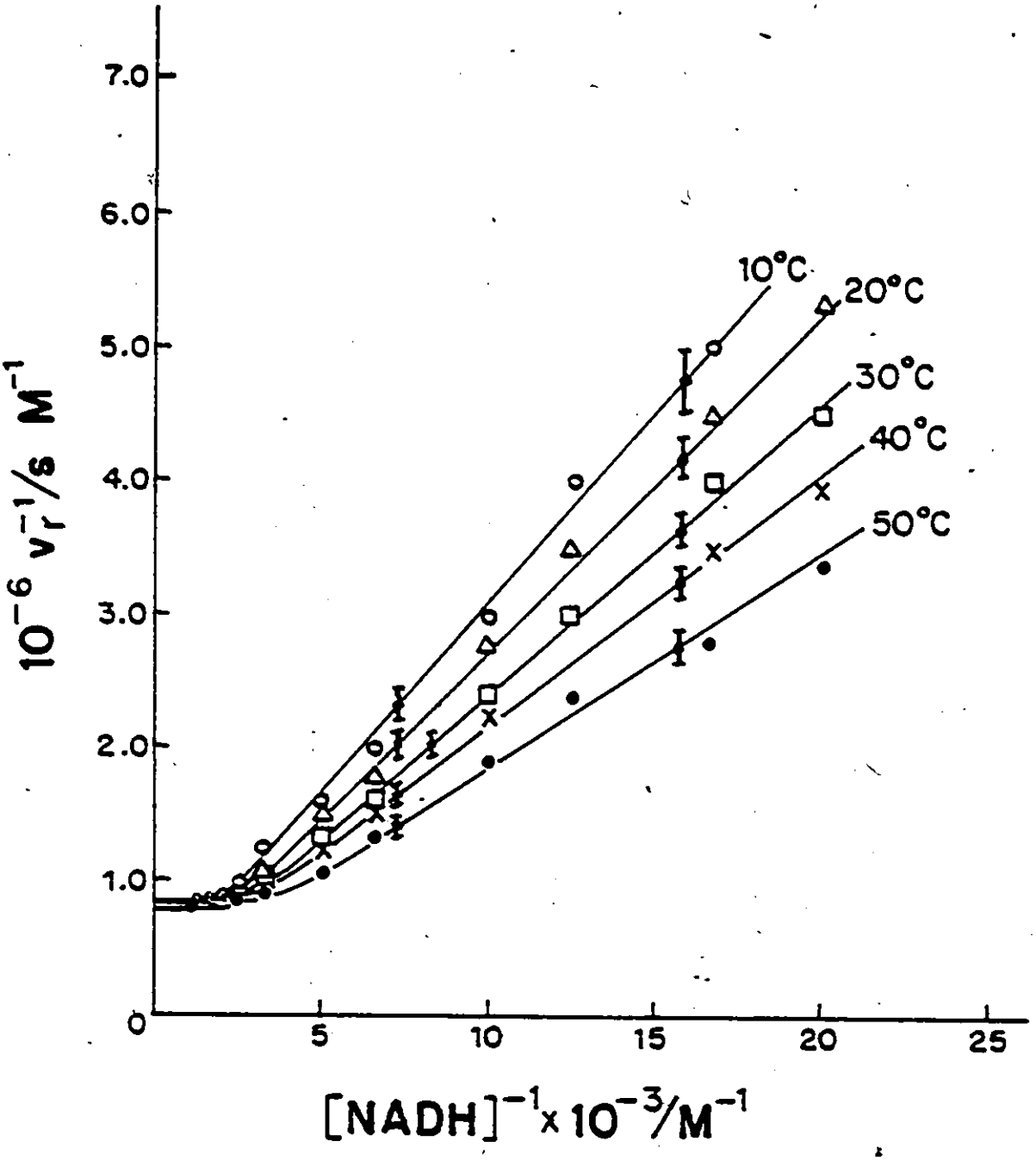

Figure 15. Typical Lineweaver-Burk plots. These curves are for pyruvic acid in excess at 3.00 mM and with the NADH concentration varied from 0.05 mM to 0.70 mM. The nylon tube was 50 cm long with an internal radius of 0.076 cm; pH = 7.5, v_f = 0.36 cm s^{-1}.

concentrations above 0.2 mM. This type of curvature of the Lineweaver-Burk plots is typical of systems of the kind where there is a change in the degree of diffusion control[29,99] and was also found in all measurements made with NADH in excess. The K_m(app) values obtained from the linear portions of these plots are shown in Table 9. It was clear that an increase in temperature led to an increase in the reaction rate.

(ii) Dependence of K_m(app) on Flow Rate

The dependence of the diffusion controlled K_m(app) on flow rate is predicted by Eqn. (14) (given in Chapter II) of the Kobayashi and Laidler theory. The diffusion-free K_m' values were obtained as intercepts of the K_m(app)-$v_f^{-1/3}$ lines. Plots of this type were as shown in Figure 16 for pyruvic acid in excess. Similar plots were made for NADH in excess and Table 10 lists all of these K_m' values. If conformational and environmental factors were unimportant, the K_m' values thus obtained would be close to the Michaelis constants (K_m^f) for the enzyme in free solution[100]. For example, values for the latter at 25 °C are:

$$K_m^f(\text{NADH}) = 0.009 \text{ mM} \pm 2.1\%$$

$$K_m^f(\text{pyruvate}) = 0.030 \text{ mM} \pm 1.9\%$$

The latter value is similar to the corresponding K_m' value, but the former is significantly smaller, indicating that attachment to the surface brought about some change in the enzyme's behaviour towards NADH.

Table 9. Values of K_m(app) in mM obtained from Lineweaver-Burk plots. Average percentage error = ±5%.

A. Variable [NADH], and [$CH_3COCOOH$] fixed at 3 mM					
v_f/cm s^{-1}	10 °C	20 °C	30 °C	40 °C	50 °C
0.36	0.55	0.40	0.32	0.25	0.18
0.72	0.46	0.34	0.26	0.21	0.15
1.08	0.42	0.30	0.24	0.19	0.13
1.50	0.40	0.28	0.23	0.17	0.12

B. Variable [CH_3COCO_2H], [NADH] fixed at 2 mM					
v_f/cm s^{-1}	10 °C	20 °C	30 °C	40 °C	50 °C
0.36	0.60	0.44	0.38	0.31	0.25
0.72	0.51	0.38	0.31	0.24	0.19
1.08	0.45	0.34	0.28	0.20	0.16
1.50	0.42	0.30	0.25	0.18	0.14

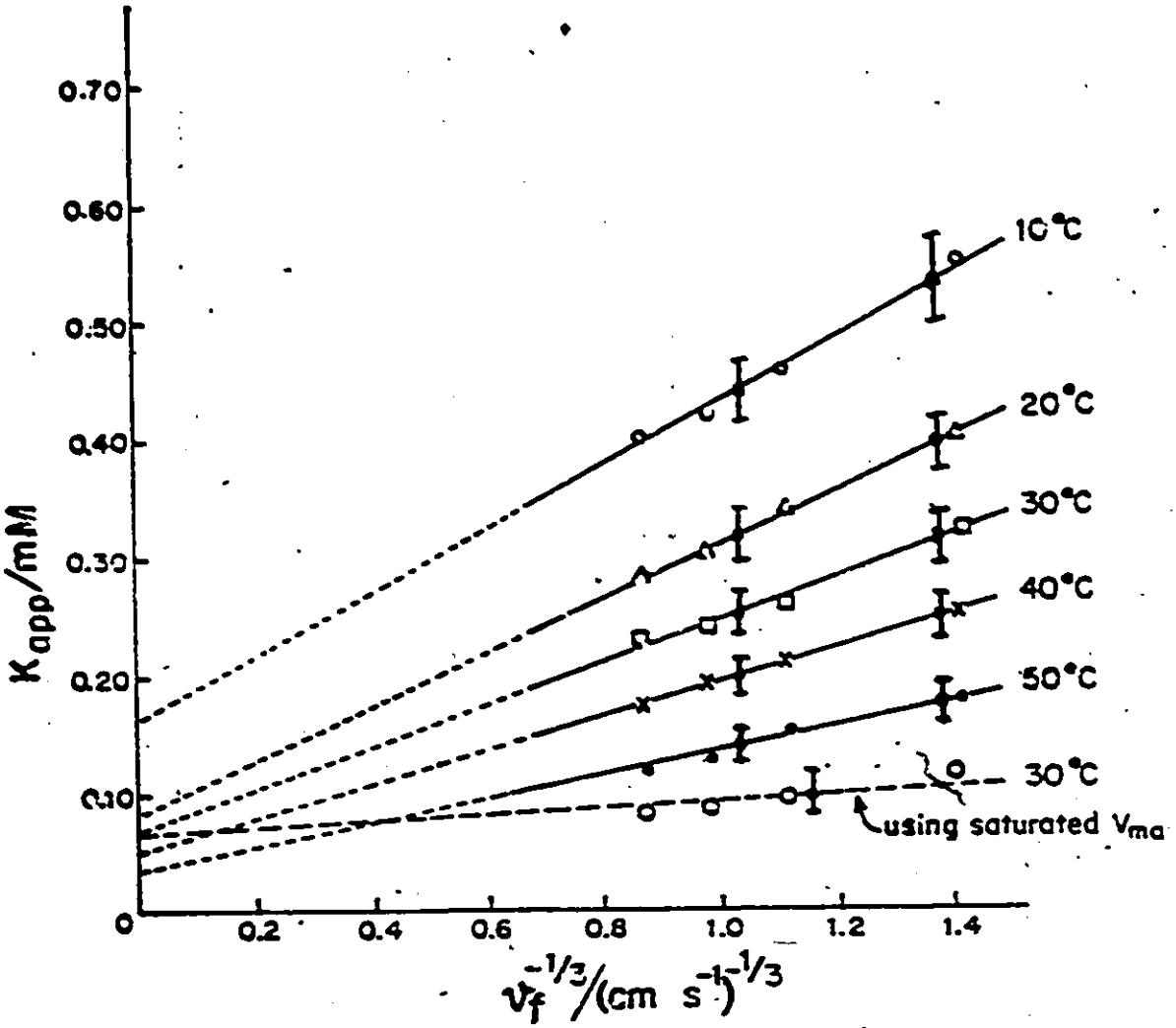

Figure 16. Variation of the apparent Michaelis constant K_m(app) with flow rate. Pyruvic acid in excess at 3.0 mM; pH = 7.5.

Table 10. Values of K'_m obtained from plots of $K_m(app)$ against $v_f^{-1/3}$. Average percentage error = 4.8%.

T (°C)	K'_m[NADH]/mM	K'_m[Pyruvate]/mM
10.0	0.160	0.075
20.0	0.080	0.045
30.0	0.070	0.026
40.0	0.049	0.015
50.0	0.035	0.005

(iii) Arrhenius Plots

Equation (5) of the Kobayashi-Laidler theory provides a good basis for calculating the activation energies of diffusion especially for experiments done at low substrate concentrations and low flow rates. In this equation, only the diffusion coefficient D is temperature dependent, its variation being given to a good approximation by an equation of the Arrhenius form[105]. If there is considerable diffusion control, plots of log v_r against 1/T (v_r being the reaction rate) should be linear and the slopes will be equal to $2\ E_D/3(2.303R)$. The value of the gas constant, R, used to calculate activation energies for diffusion, E_D, was 1.987 cal mol^{-1} K^{-1}. Calculated E_D values for all flow rates were as shown in Table 11. Figure 17, a case for variable [NADH] and fixed [pyruvate] is typical of the Arrhenius plots obtained. Similar plots were obtained at different flow rates and also with variable [pyruvate]. There was a tendency for the activation energies to decrease with increasing substrate concentration, presumably because there was a decreasing degree of diffusion control at higher substrate concentration. A plot of the activation energies against substrate concentration led to an extrapolated value, at [S]= 0, of 5.0 ± 0.2 kcal mol^{-1}, which was taken to be E_D, the activation energy for the diffusion process.

If the activation energies obtained directly from Figure 17, without correction by the factor of 3/2, are plotted against 1/[S], the limiting value of the activation energy is found to be very small, between 0 and 1 kcal mol^{-1}. This small activation energy corresponds to minimum diffusion control, and is therefore taken to be the value for the pure chemical process occurring at the surface.

Table 11. Activation energies for diffusion (kcal mol^{-1}) obtained from the Arrhenius plots of the logarithms, rates of product formation against reciprocals of absolute temperature; L = 50 cm; r = 0.076 cm; average error = ±1.2 %.

v_f/cm s^{-1}	[S]/mM	(A) Variable [NADH] Fixed [CH_3COCO_2H]	(B) Variable [CH_3COCO_2H] Fixed [NADH]
		E_D	E_D
0.36	0.06	4.10	5.08
	0.08	3.95	3.49
	0.10	3.54	2.85
	0.15	2.85	2.28
	0.20	2.85	2.05
	0.30	1.80	1.50
	0.40	0.92	1.00
0.72	0.06	3.43	4.48
	0.08	3.68	3.45
	0.10	3.10	3.42
	0.15	2.53	2.74
	0.20	2.28	1.95
	0.30	1.05	1.84
	0.40	0.68	1.70
1.08	0.06	3.27	4.39
	0.08	2.90	4.10
	0.10	2.85	3.66
	0.15	2.70	2.85
	0.20	1.92	2.26
	0.30	0.88	2.07
	0.40	0.90	1.47
1.50	0.06	3.78	4.75
	0.08	3.42	4.56
	0.10	3.02	3.60
	0.15	2.49	2.84
	0.20	1.95	2.24
	0.30	1.14	1.95
	0.40	0.94	1.00

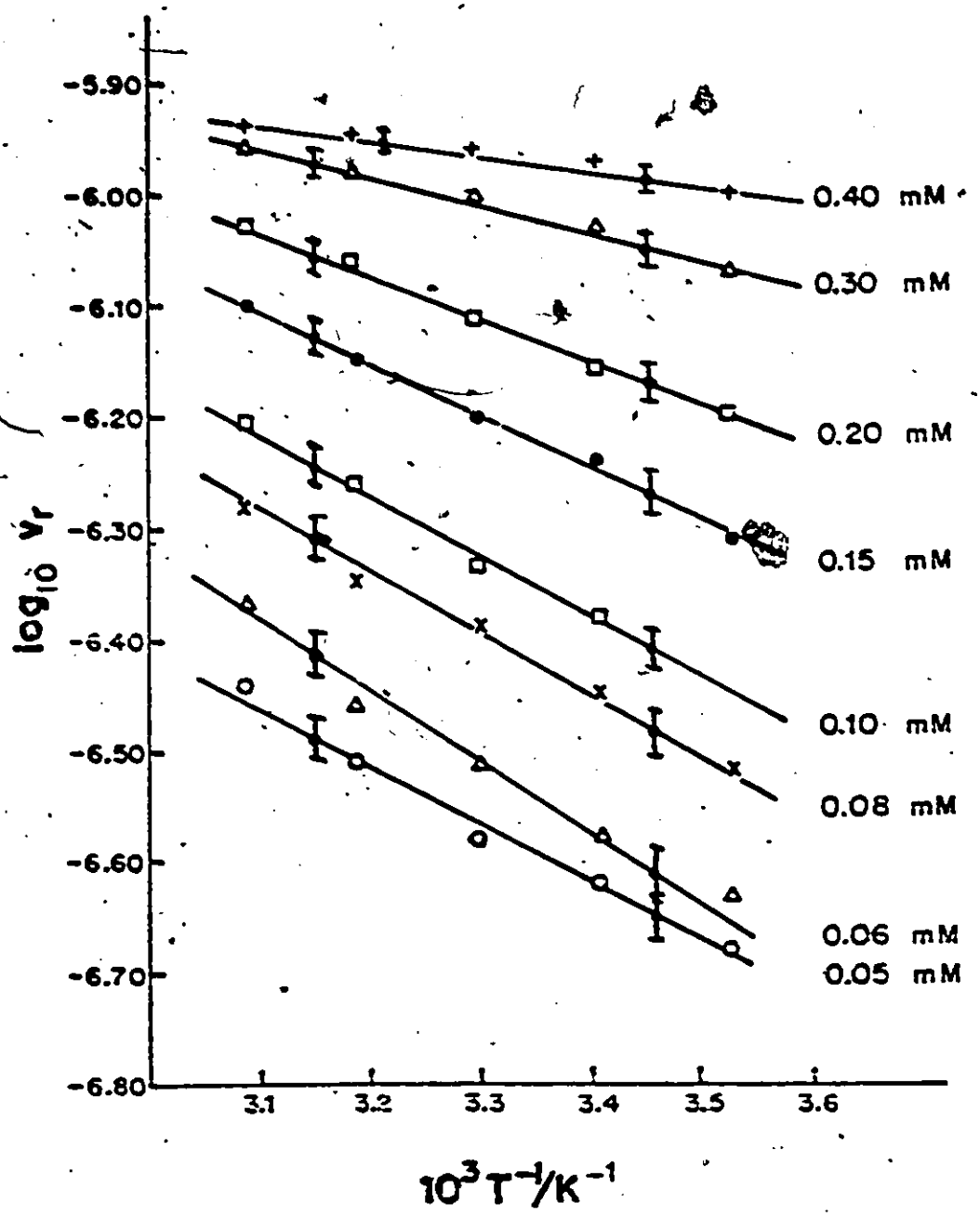

Figure 17. Arrhenius plots of rate of product formation with v_f = 0.36 cm s^{-1} and [pyruvate] fixed at 3.0 mM; the concentrations of NADH are shown. pH = 7.5.

(iv) Dependence of Product Concentration on Flow Rate

Equations (6) and (10) given in the previous Chapter lead to the theoretical product concentrations at the exit of the tube for the extreme cases of no diffusion control and complete diffusion control. In the former case, plots of log $[P]_e$ against log v_f will have slopes of -1.0 and in the latter case slopes will be -0.67. Such plots are shown in Figure 18 for a variety of temperatures and two substrate concentrations (0.05 and 0.30 mM). A diagram for variable [NADH] is shown in Figure 18A and Figure 18B is for variable pyruvate.

At the higher substrate concentrations (0.30 mM in this case) all slopes were very close to -1.0, indicating little diffusion control, while at the lower substrate concentrations the rates were closer to -0.67, indicating considerable diffusion control. These plots showed also that there was less diffusion control at the higher temperatures.

The K-L theory gives the theoretical product concentration at the tube exit for full diffusion control (Eqn. (6)) and it was of interest to compare the predictions of Eqn. (6) with the results obtained under conditions leading to substantial diffusion control, i.e., low substrate concentrations and low flow rates. Table 12 gives the results of some calculations. Diffusion coefficients at different temperatures were calculated with the aid of the value of D_o obtained at 25 °C using $D = 4 \times 10^{-6}$ cm^2 s^{-1} and $E_D = 5.0$ kcal mol^{-1} in the following relation[103]:

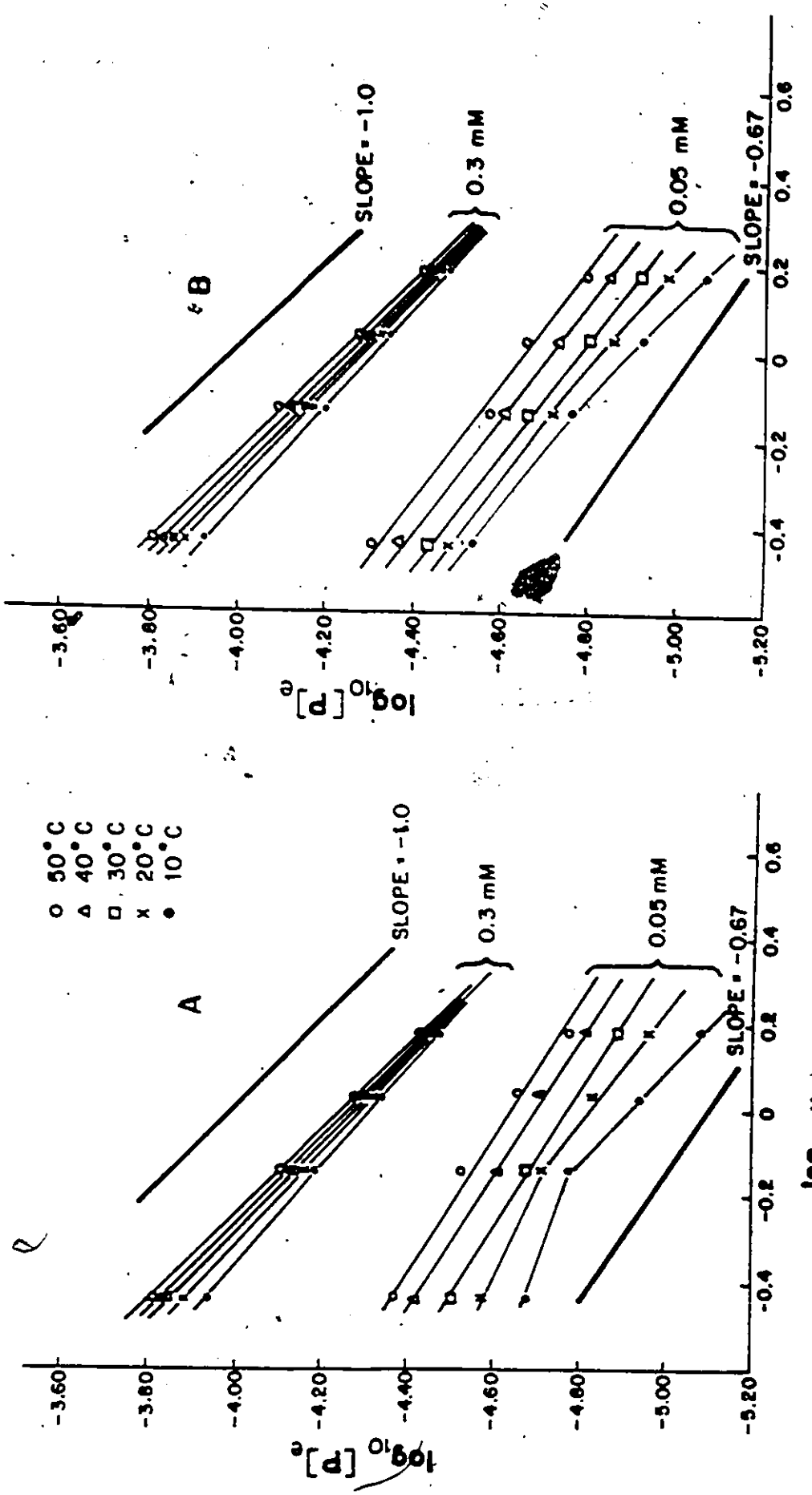

Figure 18. Double-logarithmic plots of the product concentration at the tube exit, against flow rate. A, Pyruvic acid in excess at 3.0 mM; B, NADH in excess at 2.0 mM. In both cases, pH = 7.5.

Table 12. Selected theoretical $[P]_e$ values at the tube exit compared with experimental values.
r = 0.076 cm; L = 50 cm; D(25 °C) = 4 x 10-6 $cm^2\ s^{-1}$;
E_D = 5 kcal mol^{-1}

v_f/cm s^{-1}	[S]/mM	T (°C)	[P]calc/μM	[P]exp/μM
0.36	0.05	10.0	20.0	29.0*
0.36	0.05	20.0	24.5	33.4*
0.36	0.05	30.0	29.6	36.1*
0.36	0.05	40.0	35.2	43.1*
0.36	0.05	50.0	41.5	50.0*
0.72	0.08	10.0	20.1	22.6*
0.72	0.05	50.0	26.2	26.4*
0.36	0.05	10.0	20.0	20.9
0.36	0.05	30.0	29.6	31.3
0.72	0.08	10.0	20.1	23.6
0.72	0.08	50.0	41.8	41.6

* With [NADH] fixed at 2 mM and [$CH_3COCOOH$] varied. The unstarred experimental values are for [$CH_3COCOOH$] fixed at 3 mM and [NADH] varied.

$$D = D_o \exp(-E_D/RT) \qquad (29)$$

where D_o is independent of temperature. Considering that this (Table 12) was an absolute calculation, and that the reactions were not fully diffusion-controlled, the agreement was quite satisfactory.

(v) Dimensionless Parameters

In Chapter II of this thesis, the ϕ-ρ indicator diagram was divided into three regions: Region S , in which $\eta > 0.95$ corresponded to essentially diffusion-free kinetics; Region M, in which $0.95 > \eta > 0.6$, an intermediate region, and Region L, with $\eta < 0.6$ where there was substantial diffusion control. For the present purposes, it was more expedient to divide the plots into a larger number of regions (Appendix A) the boundaries between them corresponding to η = 0.10, 0.40, 0.60, 0.70, 0.80, 0.90 and 0.95.

Figures 19A and 19B show plots of ϕ against ρ. In calculating experimental ϕ values at different temperatures, the diffusion coefficient D was taken to be 4.0×10^{-6} cm^2 s^{-1} at 25 °C and to have an activation energy of 5.0 kcal mol^{-1} estimated in Section 3.3.1.(iii). Equation (29) was used in these calculations. Results from experiments done with fixed pyruvate and variable NADH concentration appear in Figure 19A. Figure 19B reports results for the case of fixed NADH and varied pyruvate concentration. To avoid crowding the diagrams with points and confusing the whole picture, only a small selection of values was used in the plots, i.e., two temperatures (10 and 50 °C), two flow rates (0.36 and

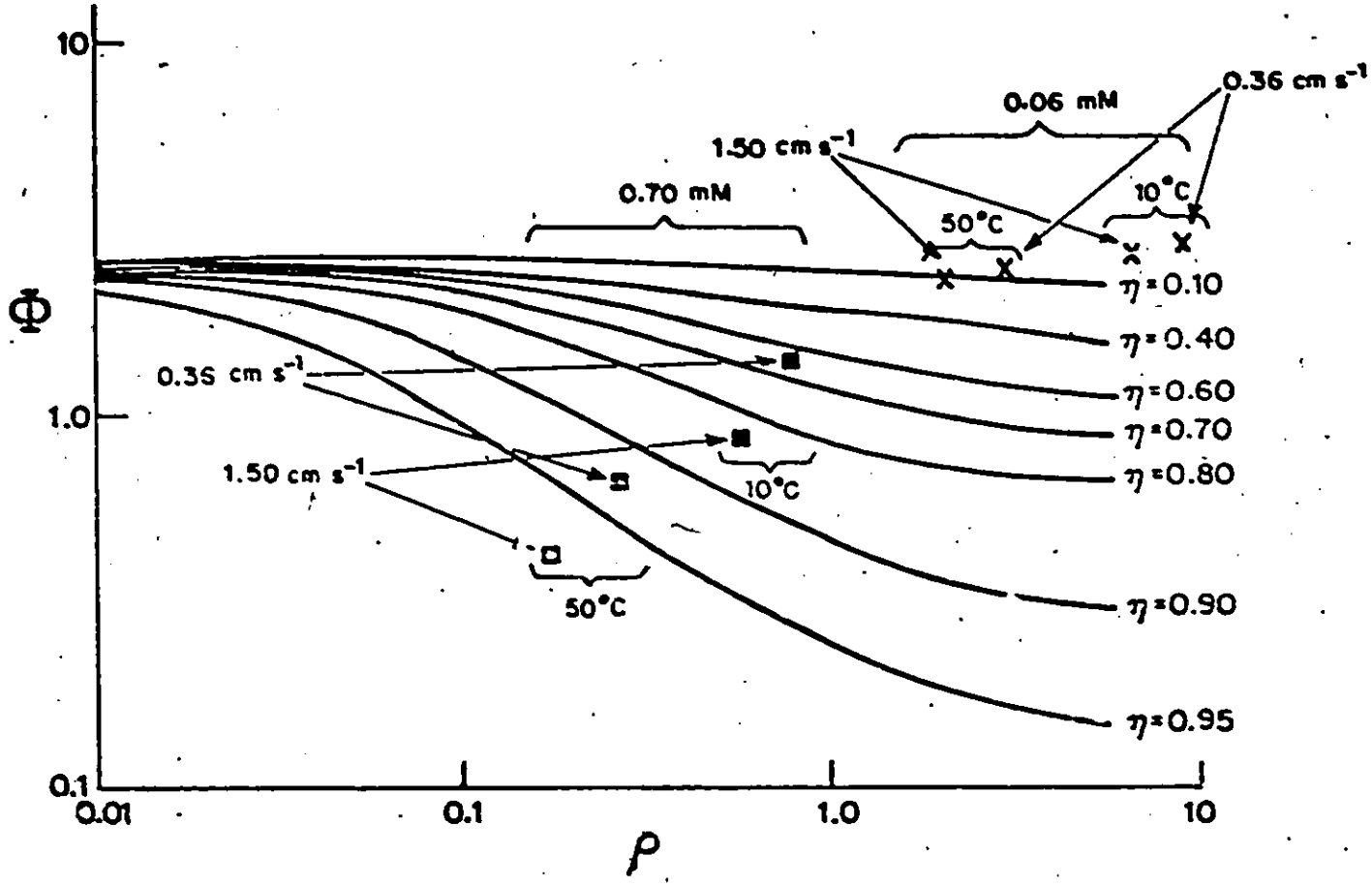

Figure 19A. Double-logarithmic plots of the parameters ϕ and ρ for pyruvate concentration fixed at 3.0 mM and for two NADH concentrations (0.06 mM and 0.70 mM), two flow rates (0.36 and 1.50 cm s^{-1}) and two temperatures (10 °C and 50 °C); pH = 7.5.

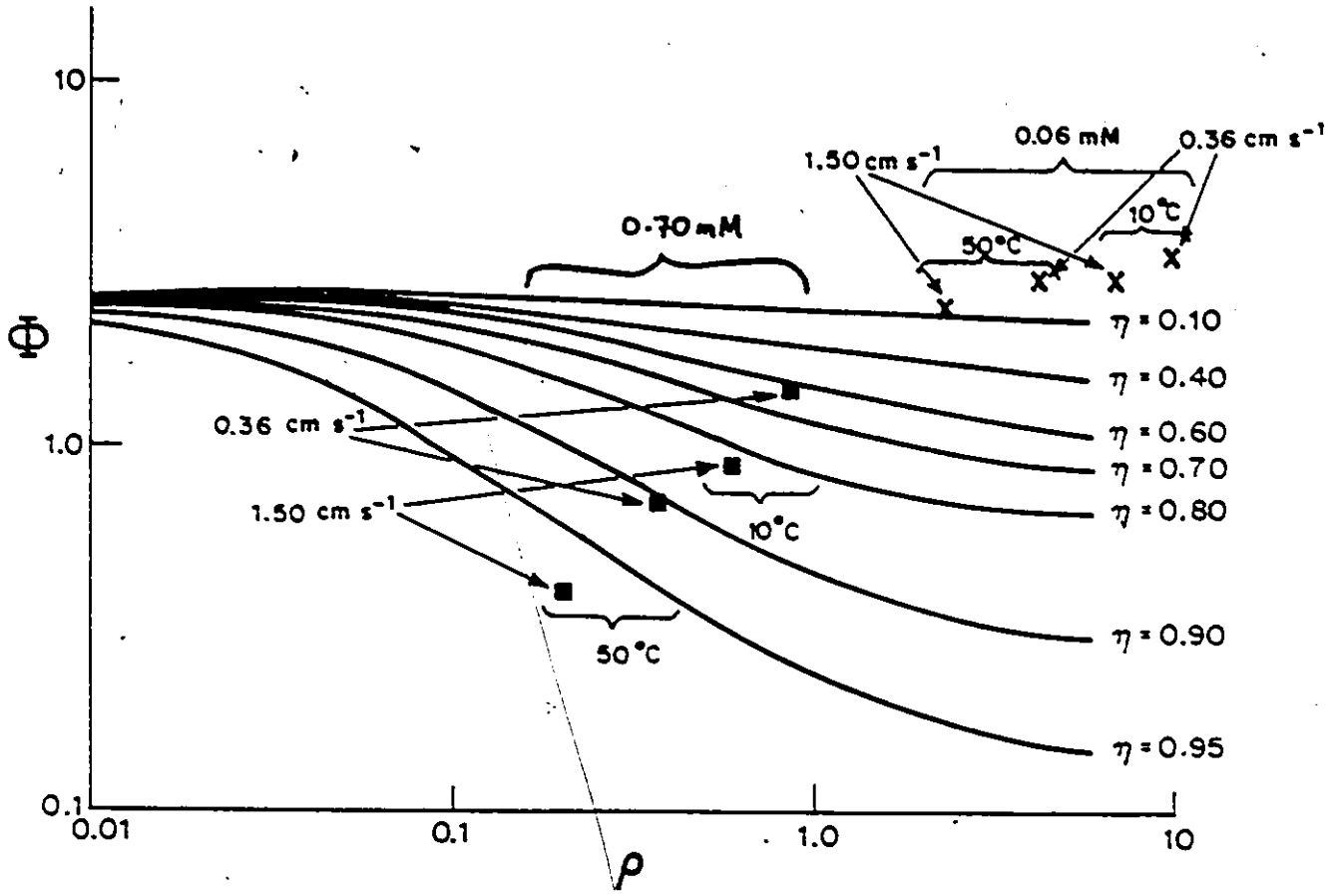

Figure 19B. Similar plots to those in Figure 19A for [NADH] fixed at 2.00 mM, and at two $CH_3COCOOH$ concentrations, two temperatures, and two flow rates. pH = 7.5.

1.50 cm s^{-1}) and two substrate concentrations (0.06 and 0.70 mM). The other ϕ and ρ values listed in Tables 13A and 13B also showed consistent results and they all led to the same general conclusions which may be summarized as follows:

(a) At low substrate concentrations, large diffusion effects come into play. This is manifested by the fact that all experimental ϕ-ρ points lie in the regions described by small utilization factors (η). These experiments, for low substrate concentrations, are so significantly affected by diffusion that temperature and flow rate have little effect.

(b) At high substrate concentration, the diffusion control is less.

(c) At the higher substrate concentrations, the degree of diffusion control is decreased by increasing the flow rate. For example, in Figure 19A, a point at 10 °C and 0.70 mM substrate which lies between η = 0.60 and η = 0.70 when the flow rate is 0.36 cm s^{-1}, gets shifted to the region between η = 0.90 and η = 0.80 upon increasing the flow to 1.50 cm s^{-1}. The latter region which has larger η values corresponds to low diffusion effects. Thus, high flow rates decrease diffusion effects of certain substrate concentrations. This finding is predicted by the Kobayashi-Laidler theory and the same behaviour was found in all systems previously investigated by Laidler and coworkers[99-103].

Table 13A. ϕ and ρ values for various pyruvate concentrations, various temperatures and various flow rates. L = 50 cm; r = 0.076 cm; D (25 °C) = 4.0×10^{-6} cm^2 s^{-1}; E_D = 5.0 kcal mol^{-1}.

[Pyruvate].10^6/M	10 °C		20 °C		30 °C		40 °C		50 °C	
	ϕ	ρ	ϕ	ρ	ϕ	ρ	ϕ	ρ	ϕ	ρ
v_f = 0.36 cm s^{-1}										
50	2.97	11.0	2.77	8.80	2.72	6.40	2.68	5.00	2.57	3.60
60	2.95	9.17	2.73	7.33	2.51	5.33	2.49	4.17	2.50	3.00
80	2.88	6.88	2.64	5.50	2.45	4.00	2.34	3.12	2.30	2.25
100	2.85	5.50	2.62	4.40	2.41	3.20	2.28	2.50	2.57	1.80
150	2.73	3.67	3.01	2.93	2.72	2.13	2.45	1.67	2.28	1.20
200	2.60	2.75	2.61	2.20	2.35	1.60	2.15	1.25	1.95	0.90
300	2.45	1.83	2.24	1.47	1.99	1.07	1.73	0.83	1.50	0.60
400	2.25	1.38	1.89	1.10	1.61	0.80	1.37	0.63	1.18	0.45
500	1.94	1.10	1.60	0.88	1.29	0.64	1.11	0.50	0.94	0.36
600	1.62	0.92	1.34	0.73	1.08	0.53	0.93	0.42	0.78	0.30
700	1.39	0.79	1.14	0.63	0.92	0.46	0.80	0.36	0.67	0.26
v_f = 0.72 cm s^{-1}										
50	3.39	9.20	3.17	6.80	2.87	5.20	2.80	4.20	2.92	3.00
60	3.24	7.67	3.03	5.67	2.79	4.33	2.67	3.50	2.46	2.50
80	3.00	5.75	2.96	4.25	2.75	3.25	2.63	2.63	2.55	1.88
100	2.82	4.60	2.74	3.40	2.63	2.60	2.48	2.10	2.46	1.50
150	2.71	3.07	2.58	2.27	2.39	1.73	2.20	1.40	2.04	1.00
200	2.47	2.30	2.31	1.70	2.15	1.30	1.90	1.05	1.70	0.75
300	2.21	1.53	1.92	1.13	1.66	0.87	1.43	0.70	1.23	0.50
400	1.81	1.15	1.55	0.85	1.30	0.65	1.10	0.53	0.93	0.38
500	1.55	0.92	1.27	0.68	1.05	0.52	0.88	0.42	0.75	0.30
600	1.29	0.77	1.06	0.57	0.88	0.43	0.73	0.35	0.62	0.25
700	1.11	0.66	0.91	0.49	0.75	0.37	0.63	0.30	0.53	0.21
v_f = 1.08 cm s^{-1}										
50	3.09	8.40	3.13	6.00	3.14	4.80	2.98	3.80	2.82	2.60
60	3.09	7.00	3.15	5.00	2.95	4.00	2.80	3.17	2.77	2.17
80	3.09	5.25	2.84	3.75	2.74	3.00	2.63	2.38	2.56	1.63
100	3.00	4.20	2.78	3.00	2.51	2.40	2.37	1.90	2.25	1.30
150	2.57	2.80	2.36	2.00	2.16	1.60	1.99	1.27	1.78	0.87
200	2.35	2.10	2.04	1.50	1.88	1.20	1.67	0.95	1.48	0.65
300	2.01	1.40	1.70	1.00	1.46	0.80	1.26	0.63	1.06	0.43
400	1.68	1.05	1.38	0.75	1.15	0.60	0.95	0.48	0.81	0.33
500	1.36	0.84	1.11	0.60	0.92	0.48	0.77	0.38	0.65	0.25
600	1.13	0.70	0.93	0.50	0.77	0.40	0.64	0.32	0.54	0.22
700	0.97	0.60	0.79	0.43	0.66	0.34	0.55	0.27	0.47	0.19
v_f = 1.50 cm s^{-1}										
50	2.77	8.00	2.84	5.60	2.82	4.60	2.82	3.40	2.66	2.40
60	2.76	6.67	2.82	4.67	2.87	3.83	2.72	2.83	2.66	2.00
80	2.76	5.00	2.68	3.50	2.57	2.88	2.39	2.13	2.36	1.50
100	2.76	4.00	2.60	2.80	2.34	2.30	2.20	1.70	2.15	1.20
150	2.48	2.67	2.20	1.87	2.02	1.53	1.83	1.13	1.70	0.80
200	2.21	2.00	1.98	1.40	1.77	1.15	1.58	0.85	1.40	0.60
300	1.84	1.33	1.58	0.93	1.34	0.77	0.14	0.57	0.97	0.40
400	1.49	1.00	1.24	0.70	1.02	0.58	0.86	0.43	0.73	0.30
500	1.21	0.80	0.99	0.56	0.82	0.46	0.67	0.34	0.58	0.24
600	1.01	0.67	0.83	0.47	0.69	0.38	0.57	0.28	0.49	0.20
700	0.87	0.57	0.72	0.40	0.59	0.33	0.49	0.24	0.42	0.17

Table 13B. ϕ and ρ values similar to Table 13A, except that now variable NADH concentrations are considered.

[NADH] $.10^6$/M	10 °C		20 °C		30 °C		40 °C		50 °C	
	ϕ	ρ	ϕ	ρ	ϕ	ρ	ϕ	ρ	ϕ	ρ
	v_f = 0.36 cm s^{-1}									
50	3.72	12.00	3.50	8.80	3.14	7.60	3.14	6.20	3.08	5.00
60	3.49	10.00	3.34	7.33	3.02	6.33	2.95	5.17	3.03	4.17
80	3.34	7.50	3.23	5.50	3.05	4.75	2.85	3.88	2.81	3.13
100	3.34	6.00	3.02	4.40	2.84	3.80	2.78	3.10	2.68	2.50
150	2.91	4.00	2.79	2.93	2.51	2.53	2.41	2.07	2.25	1.67
200	2.78	3.00	2.55	2.20	2.32	1.90	2.20	1.55	2.00	1.25
300	2.49	2.00	2.28	1.47	2.01	1.27	1.77	1.03	1.50	0.83
400	2.23	1.50	1.96	1.10	1.66	0.95	1.42	0.78	1.23	0.63
500	1.96	1.20	1.64	0.88	1.36	0.76	1.15	0.62	0.98	0.50
600	1.69	1.00	1.40	0.73	1.15	0.63	0.97	0.52	0.82	0.42
700	1.47	0.86	1.19	0.63	0.99	0.54	0.83	0.44	0.70	0.36
	v_f = 0.72 cm s^{-1}									
50	3.53	0.20	3.17	7.60	3.01	6.20	2.80	4.48	2.58	3.80
60	3.06	8.50	2.93	6.33	2.75	5.17	2.54	4.00	2.55	3.17
80	2.87	6.38	2.67	4.75	2.51	3.88	2.45	3.00	2.42	2.38
100	2.83	5.10	2.60	3.80	2.39	3.10	2.24	2.40	2.12	1.90
150	2.59	3.40	2.31	2.53	2.12	2.07	1.96	1.60	1.83	1.27
200	2.38	2.50	2.13	1.90	1.91	1.55	1.75	1.20	1.57	0.95
300	2.15	1.70	1.83	1.27	1.59	1.03	1.40	0.80	1.30	0.63
400	1.84	1.28	1.53	0.95	1.37	0.78	1.13	0.60	0.98	0.48
500	1.57	1.02	1.30	0.76	1.08	0.62	0.91	0.48	0.78	0.38
600	1.35	0.85	1.11	0.63	0.92	0.52	0.77	0.40	0.65	0.32
700	1.16	0.73	0.95	0.54	0.79	0.44	0.66	0.34	0.56	0.27
	v_f = 1.08 cm s^{-1}									
50	2.84	9.00	2.73	6.80	2.59	5.60	2.52	4.00	2.79	3.20
60	2.99	7.50	2.83	5.67	2.61	4.67	2.75	3.33	2.81	2.67
80	2.66	5.63	2.46	4.25	2.35	3.50	2.50	2.50	2.41	2.00
100	2.60	4.50	2.37	3.40	2.24	2.80	2.28	2.00	2.23	1.60
150	2.37	3.00	2.25	2.27	2.03	1.87	1.93	1.33	1.78	1.07
200	2.35	2.25	2.07	1.70	1.84	1.40	1.68	1.00	1.50	0.80
300	2.05	1.50	1.76	1.50	1.49	0.93	1.29	0.67	1.11	0.53
400	1.70	1.13	1.42	0.85	1.12	0.70	1.00	0.50	0.85	0.40
500	1.42	0.90	1.16	0.68	0.94	0.56	0.81	0.40	0.68	0.32
600	1.19	0.75	0.97	0.57	0.80	0.47	0.67	0.33	0.57	0.27
700	1.02	0.64	0.83	0.49	0.69	0.40	0.58	0.29	0.49	0.23
	v_f = 1.50 cm s^{-1}									
50	2.82	8.40	2.80	6.00	2.70	5.00	2.26	3.60	2.50	2.80
60	2.91	7.00	2.82	5.00	2.93	4.17	2.46	3.00	2.52	2.33
80	2.70	5.25	2.68	3.75	2.67	3.13	2.23	2.25	2.16	1.75
100	2.65	4.20	2.48	3.00	2.38	2.50	2.04	1.80	1.99	1.40
150	2.29	2.80	2.11	2.00	1.93	1.67	1.73	1.20	1.59	0.93
200	2.14	2.10	1.87	1.50	1.69	1.25	1.51	0.90	1.34	0.70
300	1.83	1.40	1.54	1.00	1.31	0.83	1.15	0.60	1.00	0.47
400	1.52	1.05	1.26	0.75	1.06	0.62	0.89	0.45	0.76	0.35
500	1.28	0.84	1.04	0.60	0.86	0.50	0.73	0.36	0.61	0.28
600	1.07	0.70	0.87	0.50	0.72	0.42	0.60	0.30	0.51	0.23
700	0.91	0.60	0.74	0.43	0.62	0.36	0.51	0.26	0.44	0.20

(d) At the high substrate concentrations, increasing the temperature decreases the extent of diffusion control. This fact may be illustrated by considering a point which lies between $\eta = 0.90$ and $\eta = 0.80$ in Figure 19A. The point is for 10 °C and 1.50 cm s^{-1} flow rate. When the temperature is increased from 10 to 50 °C, keeping the flow rate constant at 1.50 cm s^{-1}, this point shifts to a new region below the line of $\eta = 0.95$. The new region characterizes experiments which are affected by negligibly small diffusional effects.

3.3.2 The Effect of pH

(i) Results

The results of the pH experiments, summarized in Figure 20, show the following:

(a) That the effective rates of the nylon-LDH tubular reactor, measured in the range $7 < pH \leq 10$ decrease with increasing pH. The decrease is more gradual at lower substrate concentrations. This is indicated by the fact that the slopes of the profiles are higher at 0.20 mM than at 0.04 or 0.08 mM.

(b) That the pH optimum is well defined at substrate concentrations of 0.20 mM. When pyruvate is the variable substrate, the optimum is at pH 7. An optimum which ranges from pH 6 to pH 8 is obtained when the varied substrate is NADH.

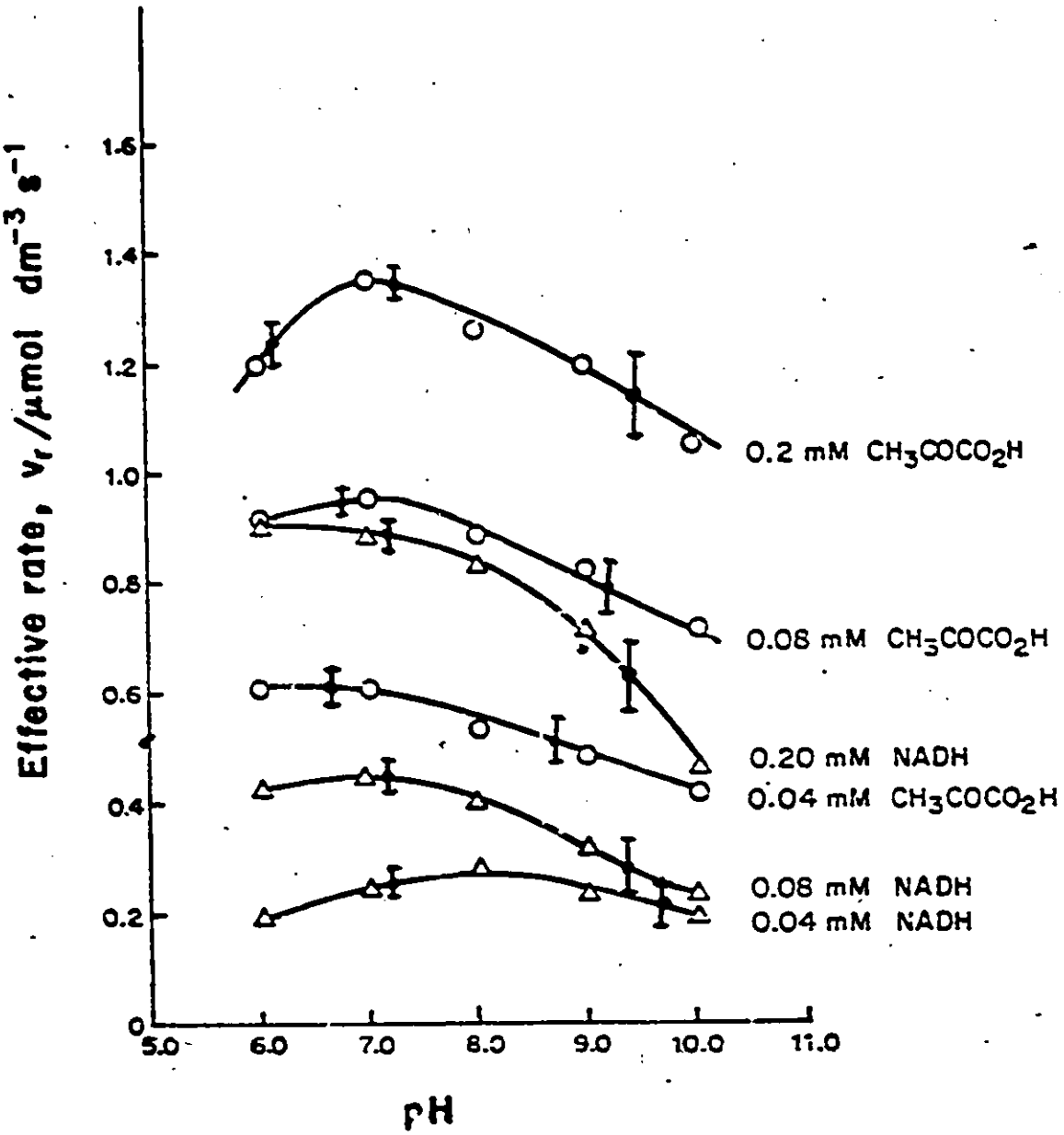

Figure 20. Plots of reaction rates against pH; **A**-variable NADH; fixed pyruvate; **O**-variable pyruvate, fixed NADH; temperature = 35 C; v_f = 1.0 cm s^{-1}.

(c) That the effective rates measured with fixed NADH concentrations (i.e. with variable pyruvate) are higher than those determined with fixed pyruvate or variable NADH.

(ii) Discussion

Trommer et al[200] have recently investigated the inhibition effects of pyruvate on rabbit muscle lactate dehydrogenase and they have found that the enzyme is not inhibited unless extremely high concentrations (> 10 mM) of pyruvate are used. This finding is in good agreement with the results of Holbrook et al[80], Fromm[86] and Stambaugh and Post[87]. We therefore attribute the reduced effective rates observed with variable NADH concentrations as stated in (c) above not to inhibition by pyruvate but to steric hindrances between the enzyme support and the NADH. This is a reasonable suggestion in view of the fact that NADH is a larger molecule than pyruvate and larger molecules suffer steric hindrances more than smaller ones do[20].

In the present investigation, temperature and the flow rate of the substrate solutions were fixed. Therefore, the thickness of the diffusion layer were the same for all substrates at all pH values. Thus, if there is no difference in the degree of diffusion at both higher and lower substrate concentrations, the slopes of the pH-activity profiles should be the same in the two concentration extremes. However, a difference in the slopes was observed as stated in Section 3.3.2(i)a. Thus, higher degrees of diffusion effects at lower substrate concentrations are the chief cause of the more gradual decrease of the effective rates for either NADH or pyruvate at, for example, 0.04 mM.

With variable NADH, the width of the pH optimum of our immobilized LDH is found to be broader than that obtained with variable pyruvate. See (b) in Section 3.3.2(i) above. A combination of effects from diffusion and from steric hindrances on the interaction of NADH with the enzyme seems to be responsible for the wider pH optimum found in the former case. It is not surprising therefore to find that pyruvate which seems to be free of the steric hindrances gives a more definite pH optimum of the present reaction system.

The effect of pH on the kinetics of immobilized enzymes has been investigated by a number of workers, both from the theoretical[1,71] and experimental[103,66,126] points of view. It has been found that shifts in the position of the pH optimum can explain the nature of the charge present on the enzyme's support. For example, Goldstein and Katchalski[126] have carried out pH experiments with chymotrypsin in three different situations. In one case, the enzyme was not bound and in the other two cases, it was immobilized to a positively charged polymer and to a negatively charged polymer, respectively. They found that the optimum pH of the positively charged system appeared at a lower pH value than that obtained with the free enzyme: The results of the experiments done with a negatively charged support gave a pH optimum which was shifted towards more alkaline conditions. Thus, the optimum pH of an enzyme immobilized within a charged environment or carrier would be displaced toward more alkaline or toward more acidic pH values for a negatively or positively charged carrier, respectively. The pH optimum of our work was found to

be at pH = 7.0. Such a value is therefore consistent with the fact that a nylon-LDH surface, produced following the immobilization technique outlined in Chapter II, should have a zero charge.

While shifts in the pH optimum or in the pH-activity profiles may explain the nature of charges surrounding the enzyme, changes in the shapes of the profiles can be used to explain diffusional effects on the immobilized enzyme. For example, Ngo and Laidler[105] have found that the pH dependence of the rates of hydrolysis of acetylcholine by electric eel acetylcholinesterase entrapped in polyacrylamide gel deviates significantly from that observed with the corresponding free enzyme. While the free enzyme showed an optimum at about pH 8.0, the bound enzyme exhibited a continuous increase in the reaction rates with pH up to pH 9.6. This anomaly was explained on the basis of increased diffusional effects when the enzyme is enclosed in a polymer gel.

The variation of the reaction rates with pH shown in Figure 20 is much smaller than that found by Schwert et al[120] and Stinson and Holbrook[83] who used free LDH. This is because our system was controlled by diffusion.

3.4 Summary

In the present work, various lines of evidence pointed to the following general conclusions:

(a) The degree of diffusion control increases as the temperature is lowered. This was revealed by the plots of log $[P]_e$ against log v_f (Figure 18) and by the dimensionless parameters (Figure 19 and Table 13). Increasing temperature

led to increased reaction rates, which implied a reduction in the diffusion resistances.

(b) The degree of diffusion control increases as the flow rate of the substrate solutions decreases. This was shown, for example, by the variation of K_m(app) with $v_f^{-1/3}$ (Figure 16). This fact was also shown very clearly by the plots of the dimensionless parameters (Figures 19A and 19B).

(c) The degree of diffusion control increases with decreasing substrate concentration. This was shown by the dependence of product concentration on the flow rate (Figures 18A and 18B), the pH-activity profile (Figure 20) and by the dimensionless parameters (Figure 19 and Table 13).

(d) The activation energy for the diffusion process is approximately 5.0 kcal mol^{-1}. This was obtained by extrapolating the activation energies calculated from the Arrhenius plots (Figure 17 and Table 11) to infinitely small or zero substrate concentrations, at which maximum diffusion effects should appear. The value of 5.0 kcal mol^{-1} led to self-consistent results of the dimensionless parameter ϕ at different temperatures (Figure 19 and Table 13). It also led to a reasonable interpretation of the temperature-dependence of some product concentrations at the tube exit (Table 12).

(e) The enzyme's behaviour towards NADH is substantially altered when LDH is bound to a solid surface. This is mainly due to steric hindrances that come into play. This was indicated

by the pH-activity experiments (Figure 20). Further evidence was obtained by comparing the diffusion-free Michaelis constants, K'_m calculated around 25 °C (Table 10) with that found in Chapter II for the free enzyme.

(f) The pH-optimum of the immobilized LDH was taken to be at pH 7.0. It was measured with pyruvate as a variable substrate since pyruvate seems not to be affected by steric hindrances because of its relatively small size. The value of the pH optimum suggested that the surface on which the LDH was immobilized had a neutral charge. This conclusion agrees with the predictions of our immobilization technique.

(g) In the present tubular reactor, the chemical process at the surface is fast when substrate concentrations are high. The limiting value of the activation energy is found to be very small, lying between 0 and 1 kcal mol^{-1}. Diffusion resistances are at a minimum when substrate concentrations are high.

3.5 Conclusions

The application of the K-L theory to the kinetic data obtained in the temperature range 10 to 50 °C, with our nylon-LDH tube, suggests that a better reactor efficiency can be achieved by running experiments

at high substrate concentrations, high flow rates and at high temperatures (preferably between 30 °C and 50 °C). The results for the pH experiments also suggest that if the above conditions were obtained with the use of a reaction medium of pH 7.0, the efficiency of the LDH tubular reactor would be even better.

Before this Chapter is finally concluded, it should be pointed out that the effect of the ionic strength on the reaction rates of the present reactor was not investigated in detail. However, kinetic runs made in four different concentrations of the sodium phosphate buffer, namely 0.05, 0.10, 0.50 and 1.0 M at pH 7.5 showed that low ionic strengths lead to high reaction rates of the bound LDH (see Figure 21). In these experiments, the specifications of the nylon-LDH tube were the same as those employed for the temperature and the pH work already discussed. In obtaining the results shown in Figure 21, flow rate, temperature, NADH and pyruvate concentrations were respectively fixed at 1.0 cm s^{-1}, 35 °C, 0.20 mM and 3.0 mM.

So far, we have reported a study of the flow kinetics of immobilized LDH, done in a tube. The next two chapters discuss the same type of kinetics of the same enzyme but now a different reactor configuration, a disc, is considered both from a theoretical and an experimental point of view.

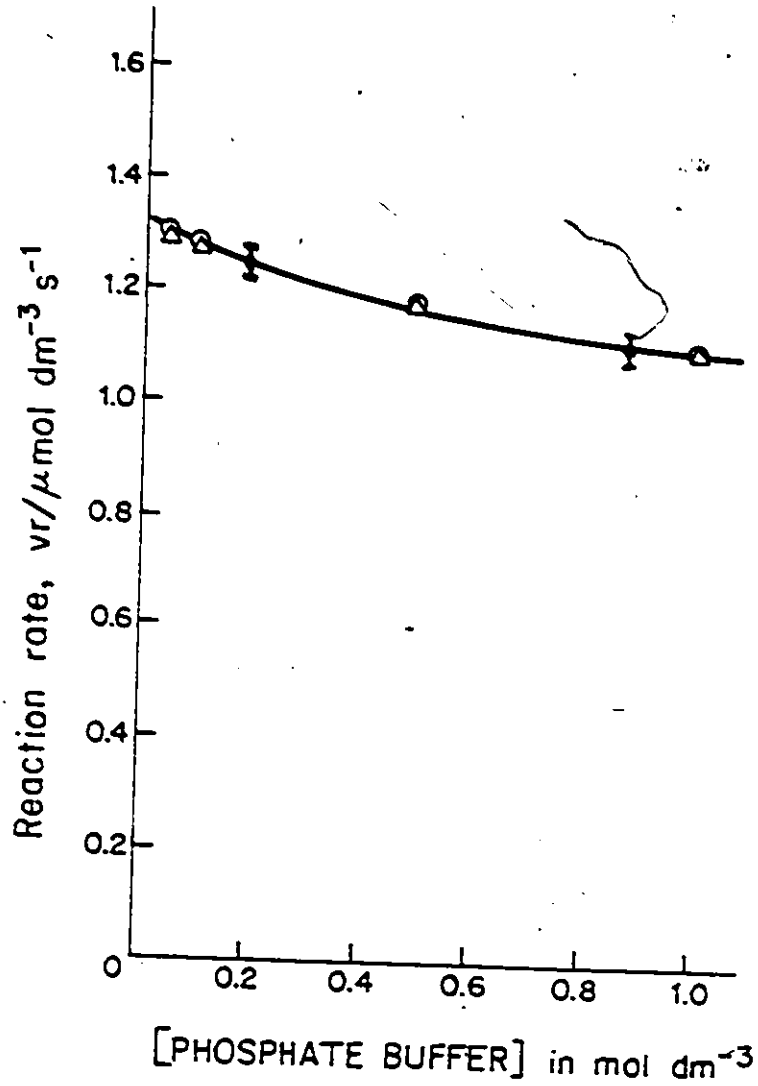

Figure 21. Plots of reaction rates against phosphate buffer concentration at pH = 7.5, T = 25 °C for 0.20 mM pyruvate and 2.0 mM NADH.

CHAPTER IV

KINETICS WITH AN ENZYME AT A SOLID ROTATING DISC

4.1 Introduction

Enzymes have been immobilized in a variety of ways[29,128]. They have been trapped in gels[101,103,129,156], chemically bound to surfaces[99-103,130,131,141,142] and encapsulated[19,129,144-149]. A number of different types of reactors have been used to study the kinetics of these bound species in both static and flow systems[99-103,130,131,141,142]. However, no kinetic investigations have hitherto been carried out with the enzyme present at a rotating disc.

Electrochemists have made considerable use of disc electrodes to study kinetic reactions at electrode surfaces and have found that this configuration offers important advantages. For example, it has been found to be a faster technique than the dropping mercury electrode in the determination of diffusion coefficients of dissolved species[132]. The reasons for employing a rotating disc in the field of immobilized enzymes may include:

(a) It will help to study diffusion effects on the behaviour of bound enzymes.

(b) It can be used to analyze specific substrates in fluids such as blood, urine, milk and syrups, which may be of clinical or industrial importance.

This Chapter reports a preliminary study of the kinetics of LDH covalently bound to an impervious surface of a nylon disc. The immobilization method involving the use of thionyl chloride and 3,3-diaminobenzidine is described. Reaction rates are measured with fixed pyruvate and variable NADH concentration and a theory of a disc carrying an active enzyme is developed and tested.

4.2 Theoretical

The principal characteristic feature of a rotating disc is that when it rotates in a liquid it acts as a pump, sucking the liquid toward itself, spinning it around and throwing it out to the sides. At the same time, a rotating disc creates a diffusion layer on its surface, the thickness of which can be varied and can be calculated at different speeds of rotation. Within this diffusion layer, the concentration of the solute changes linearly from the value in the bulk solution to that at the surface. The system is shown schematically in Figure 22A, and Figure 22B shows the concentration of a substrate as a function of distance along the axis. The technique therefore provides a very valuable means of determining the effect of diffusion on the kinetics at the surface and of eliminating diffusion effects altogether by extrapolation to high speeds of rotation.

The basic theory for a rotating electrode disc has been worked out by von Karman[133] and by Levich[134,135]. We will now extend their treatment so as to make it applicable to an enzyme system obeying Michaelis-Menten kinetics. We assume that the disc is carrying enough

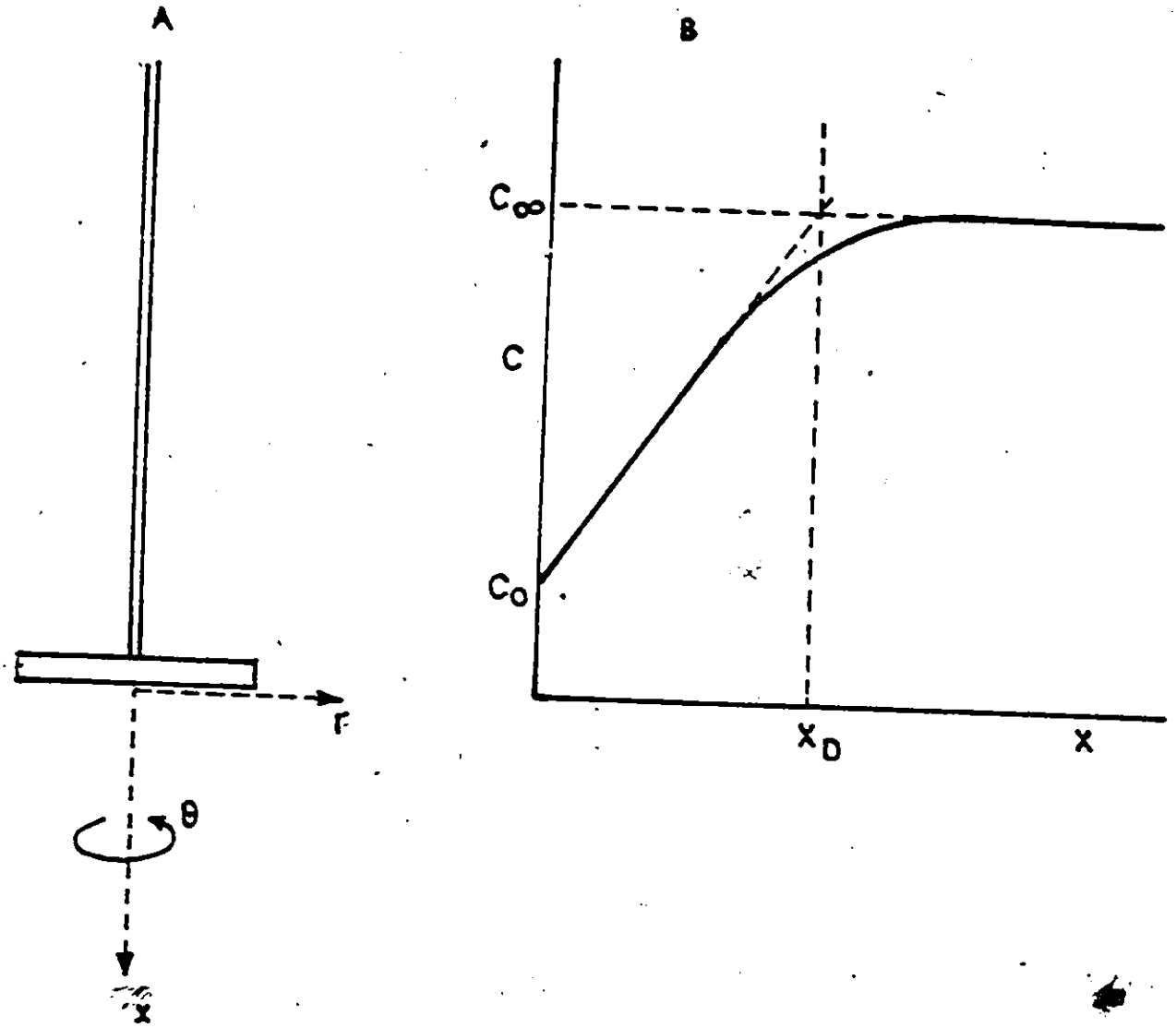

Figure 22. Schematic diagram of a rotating disc, showing the cylindrical polar coordinates X, r and θ.

The variation of concentration with distance x from a spinning disc at which chemical reaction is occurring The variation is approximately linear in the diffusion layer of thickness X_D.

active enzyme and that the reaction on its surface is sufficiently fast that the reaction rate will be controlled by diffusion and by the spinning motion of the disc. The equation relating to concentration (c), time (t) and distance travelled by the reactant can therefore be set up as follows:

$$\frac{\partial c}{\partial t} = D \frac{\partial^2 c}{\partial x^2} - V_x \frac{\partial c}{\partial x} \qquad (30)$$

where v_x is the hydrodynamic component of velocity in the x direction.

The first term on the right-hand side relates to transport by diffusion (Fick's second law) and the second term to the transport brought about by the pumping action created by the spinning motion of the disc.

From the hydrodynamics of the spinning disc, one gets

$$V_x = - (\omega\nu)^{\frac{1}{2}} X(x/x_{hy}) \qquad (31)$$

where ω is the speed of rotation (radian s^{-1}), ν is the kinematic viscosity of the solution (i.e. the ratio of the viscosity η to the density ρ), and X is a function of the ratio of x to x_{hy}. The thickness of the hydrodynamic layer x_{hy} is not the same as the thickness of the diffusion layer, x_D[132]. Since V_x is directed towards the surface of the disc, it is given a negative sign as shown in Eqns. (30) and (31) above.

In the steady state, $\partial c/\partial t$ will be zero and the material will then be transported to the disc's surface where it is reacting at a constant rate and Eqn. (30) then becomes

$$D \frac{\partial^2[S]}{\partial x^2} = V_x \frac{\partial[S]}{\partial x} \tag{32}$$

Levich[134,135] gave a solution of this equation, and we apply it to an enzyme system in which the bulk substrate concentration is $[S]_b$ and the substrate concentration at the surface is $[S]_s$. In other words, at $x=\infty$, $S \rightarrow [S]_b$ and at $x=0$, the substrate concentration is $[S]_s$. The solution is

$$\left(\frac{\partial[S]}{\partial x}\right)_{x=0} = \frac{[S]_b - [S]_s}{X_D} \tag{33}$$

where X_D is the thickness of the diffusion layer, given by

$$x_D = 1.61\ D^{1/3} \omega^{-1/2} \nu^{1/6} \tag{34}$$

It is well known that the diffusive flux J to an area A_s of a surface is given by Fick's first law,

$$J_{x=0} = D\ A_s \left(\frac{\partial[S]}{\partial x}\right)_{x=0} \tag{35}$$

In view of Eqns. (33) and (34), the flux to the disc's surface will therefore be expressed as

$$J_{x=0} = \frac{D\ A_s([S]_b - [S]_s)}{X_D} = \frac{D\ A_s([S]_b - [S]_s)}{1.61\ D^{1/3} \omega^{-1/2} \nu^{1/6}} \tag{36}$$

It is convenient to define a mass transfer coefficient k_L so that we can simplify Eqn. (36) to the following expression

$$J_{x=0} = k_L\ A_s([S]_b - [S]_s) \tag{37}$$

Thus, by Eqns. (36) and (37), the mass transfer coefficient for the disc system is given by

$$k_L = 0.62\, D^{2/3}\omega^{1/2}\nu^{-1/6} \qquad (38)$$

In the present system, the substrate passes through a diffusion layer of thickness x_D before it reaches the disc's surface where it is consumed in the fast enzyme reaction. Previous studies on LDH[130,131], in systems involving diffusion and then enzyme reaction, have indicated Michaelis-Menten kinetics when one or other of the substrates is held in excess, and we can therefore write the following rate expression for the amount of product formed in a unit time at a given surface area A_s:

$$v = \frac{V_{ms}A_s[S]_s}{K_{ms}+[S]_s} \qquad (39)$$

where $[S]_s$ is the surface concentration (amount/area) of the substrate that is not in excess. The kinetic parameters V_{ms} and K_{ms} are the effective Michaelis parameters for the reaction catalyzed by the enzyme at the surface of the disc, and relate to unit surface area. A steady state will be established at which the rate of this chemical removal of $[S]_s$ equals the diffusive flux, given by either Eqn. (36) or (37). Thus,

$$\frac{V_{ms}A_s[S]_s}{K_{ms}+[S]_s} = \frac{A_s D([S]_b-[S]_s)}{x_D} \qquad (40)$$

When $[S]_s$ obtained from Eqn. (40) as a function of V_{ms}, K_{ms}, $[S]_b$, D

and x_D is inserted into Eqn. (39), an expression for the reaction rate as a function of the bulk concentration $[S]_b$ is obtained. Since this new expression is a quadratic equation and may be more difficult to solve, it is more convenient to obtain solutions from Eqn. (40) for the limiting cases and to insert them into the overall Michaelis-Menten equation (39).

(i) $[S]_s >> K_{ms}$. At sufficiently high substrate concentrations, when $[S]_s >> K_{ms}$, Eqn. (40) reduces to

$$V_{ms} = \frac{D([S]_b - [S]_s)}{x_D} \tag{41}$$

and therefore

$$[S]_s = \frac{D[S]_b - V_{ms}x_D}{D} \tag{42}$$

(ii) $[S]_s << K_{ms}$. At low substrate concentrations where $[S]_s << K_{ms}$, Eqn. (40) yields

$$\frac{V_{ms}[S]_s}{K_{ms}} = \frac{D([S]_b - [S]_s)}{x_D} \tag{43}$$

which leads to

$$[S]_s = \frac{K_{ms}D[S]_b}{K_{ms}D + V_{ms}x_D} \tag{44}$$

The amount of product formed per unit time, under these conditions of low substrate concentration, is given by

$$V_o = \frac{V_{ms}A_s[S]_s}{K_{ms}} = \frac{V_{ms}A_sD[S]_b}{K_{ms}D+V_{ms}x_D} \tag{45}$$

The rate of formation of product in a volume V_b of solution can also be expressed as

$$V = \frac{V'_mV_b[S]_b}{K_m(app)+[S]_b} \tag{46}$$

where V'_m and $K_m(app)$ are the conventional Michaelis parameters, in contrast to V_{ms} and K_{ms} which relate to unit surface area. In the limit of low substrate concentrations, this reduces to

$$V_o = \frac{V'_mV_b[S]_b}{K_m(app)} \tag{47}$$

We also have

$$V'_mV_b = V_{ms}A_s \tag{48}$$

Equating the rates given by Eqns. (45) and (47), and using (48), leads to

$$K_m(app) = K_{ms} + \frac{V_{ms}x_D}{D} \tag{49}$$

$$= K_{ms} + \frac{V'_mx_D}{D} \cdot \frac{V_b}{A_s} \tag{50}$$

It is of interest that these equations are of a similar form to those obtained by Hornby et al[136] and by Kobayashi and Laidler[73] for tubular enzyme reactors. With Eqn. (34), Eqn. (50) becomes

$$K_m(app) = K_{ms} + \frac{1.61\ V'_m \nu^{1/6}}{D^{2/3}\omega^{1/2}} \cdot \frac{V_b}{A_s} \qquad (51)$$

This relationship is used later to test the dependence of $K_m(app)$ on the speed of rotation ω and to obtain an extrapolated value of K_{ms}. In the equations above, V_b and A_s respectively denote the volume of the reaction mixture and the surface area of the disc.

Paul et al[137] recently reported some results with a spinning enzyme reactor, but their configuration was not a disc.
To the best of our knowledge, no theoretical or experimental work has so far been done with a rotating disc carrying an enzyme. -

4.3 Experimental Section

4.3.1 Materials

Chemicals used were: rabbit muscle lactate dehydrogenase (EC 1.1.1.27); NADH; pyruvic acid; hydrochloric acid; 3,3-diaminobenzidine; glutaraldehyde; dioxane; dicyclohexylcarbodiimide; thionylchloride; β-mercaptoethanol; sodium chloride and sodium phosphate salts.

A nylon rod from which discs were cut was purchased from the Canus Plastics Company in Ottawa.

The Ostwald viscometer (size 50, A92) used for viscosity measurements was bought from Kimax Kimble Company, U.S.A.

4.3.2 Attachment Procedure

The immobilization method presented in Chapter II of this thesis was used in our initial attempts to covalently attach LDH to a surface

of a nylon disc. Although this technique was very effective in tubular reactors used in Chapters II and III, it produced a disc-LDH system of very low activity. With the tubular reactors, the small bore of the tubes allowed only a small amount of substrate solution to flow through the pipes. Thus, the ratio between the area covered by the enzyme and the volume of the substrate solution was large. In most disc experiments on the other hand, the area to volume ratio is so small that for a satisfactory enzymic activity, it is necessary to have a better method that will attach more enzyme to the surface of the disc. Alternatively, one may use a disc of very large surface area. A combination of a large surface area with a good immobilization method will be even more attractive. The new method described below produced a very effective disc and allowed an experimentally wide range of rotation speeds to be used. The five chemical steps involved in this new immobilization procedure are summarized in Table 14. This preparation, which led to high activity and improved range of rotation speeds, involved the use of thionyl-chloride and 3,3-diaminobenzidine and was carried out as follows.

A nylon disc (5 mm thick and 3.2 cm diameter) joined to a steel rod (Figure 23) was suspended in a beaker containing 4.5 M HCl to bring about partial hydrolysis of the peptide bonds on one of its surfaces. After 45 minutes, the disc was transferred to another beaker of thionyl-chloride to convert carboxyl groups to acid chlorides. The reaction was allowed to proceed for three hours in a fumeboard. Later, the disc was placed in a solution of dioxane containing 1 % w/v, 3,3-diamino-benzidine and 1 % w/v, dicyclohexylcarbodiimide and was left there for

Table 14. Summary of the five steps used to covalently attach LDH to a nylon disc surface (NDS).

Step	Reaction
1.	NDS $\xrightarrow[25\ ^{\circ}C]{4.5M\ HCl}$ NDS(COOH)(NH_2) P Q
2.	Q. $\xrightarrow[25\ ^{\circ}C]{SOCl_2}$ NDS(C(=O)-Cl)(NH_2) R
3.	R $\xrightarrow[Dioxane,\ 25\ ^{\circ}C]{3,3'Diaminobenzidine}$ NDS(C(=O)-NH-biphenyl(NH_2)(NH_2)(NH_2))(NH_2) S
4.	S $\xrightarrow[0.1\ M\ Phosphate\ Buffer,\ pH\ 10,\ 4\ ^{\circ}C]{Glutaraldehyde}$ NDS-C(=O)-NH-biphenyl(NG*)(NG*)(NG*)(NG*) T
5.	T $\xrightarrow[0.1\ M\ Phosphate\ Buffer,\ pH\ 7.5,\ 4\ ^{\circ}C]{Enzyme,\ LDH}$ NDS(NG-LDH)(NG-LDH)(NG-LDH)(NG-LDH) U

* -NG is $-N=CH-CH_2-CH_2-CH_2-CHO$

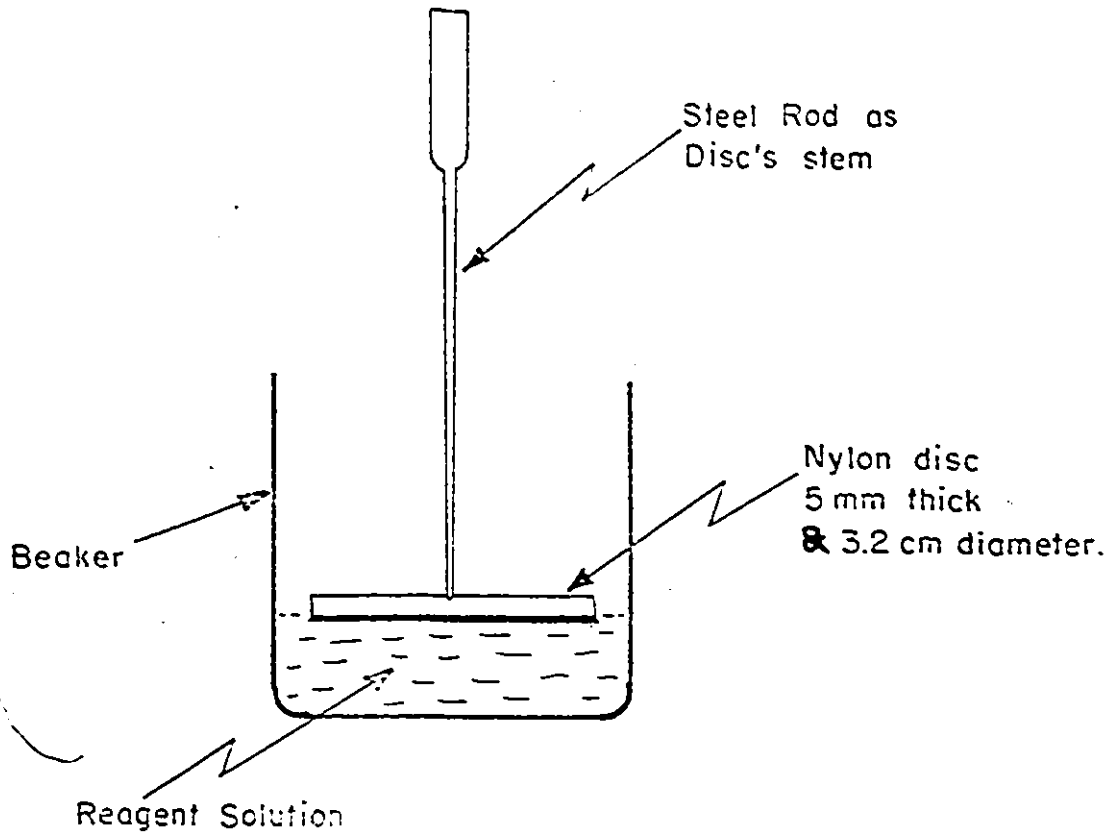

Figure 23. Diagram showing the arrangement of the apparatus for chemical attachment of LDH to an impervious nylon surface of a disc.

12 hours to ensure successful production of the amino groups on the surface. All the above steps were done at 25 °C. At the end of the 12 hours, the disc was washed in 0.1 M sodium phosphate buffer at pH 10, and was then left to stand at 4 °C for 6 hours in a solution of the same buffer containing 50 % w/v glutaraldehyde. The unreacted glutaraldehyde was removed by washing the disc in another buffer solution (0.1 M sodium phosphate, pH 7.5 at 4 °C). Immediately afterwards, the preparation was placed in 10 mL of 0.1 M sodium phosphate buffer at pH 7.5 containing 26 mg of rabbit muscle lactate dehydrogenase and 0.1 mM β-mercaptoethanol (an enzyme activator). The quantity of the enzyme given above was equivalent to 221 units per mL of solution. One unit of LDH will reduce 1.0 μmole of pyruvate to lactate per minute at pH 7.5 at 30 °C. To allow complete reaction between aldehydic groups on the disc and amino groups on the enzyme, the system was left standing in the enzyme solution at 4 °C for 24 hours in a refrigerator. The unbound protein, after 24 hours, was removed by washing the disc with 0.1 M sodium phosphate buffer at pH 7.0 at room temperature. When not in use the disc was left in a solution of 0.1 M sodium phosphate at pH 7.5 and stored at 4 °C.

The disc system showed only 1 % drop in activity after seven days, during which time we measured our kinetics.

4.3.3 Kinetic Procedure

Experiments were done at 25 °C in 0.01 M sodium phosphate buffer at pH 7.5. The volume of the reaction mixture was 150 mL. The pyruvic acid concentration was fixed at 2.0 mM and five NADH concentrations were

used, namely 0.075, 0.10, 0.15, 0.20 and 0.30 mM. The disc was rotated by the variable-speed-laboratory stirrer (Talboys, Model 134-2) at the following spinning speeds: 0.38, 0.70, 0.97, 1.02 and 2.0 revolutions per second (rev s^{-1}). The progress of the reaction was followed by measuring the change in the NADH absorbance at measured intervals. A sample of 3 mL was taken from the reaction mixture (150 mL) at five-minute intervals of time and the absorbance measured at 340 nm on the SP1800 U.V. spectrophotometer. After recording each absorbance reading, the sample solution was immediately and carefully pipetted back into the bulk mixture.

Typical plots of absorbance against time are shown in Figure 24 for the three indicated NADH concentrations at different speeds of rotation.

4.3.4 Kinematic Viscosity Measurements

Some applications of the theory for rotating enzyme discs require the exact value of the kinematic viscosity of the reaction medium. This quantity has already been defined as the ratio of viscosity and density (i.e. $\nu=\eta/\rho$). In our determination of this parameter for 0.01 M sodium phosphate buffer solution at pH 7.5 and at 25 °C, the Ostwald viscometer shown in Figure 25 was used. In the calculations, we used the viscosity of pure water, 0.8904 centipoise, as a reference standard[138]. The cgs unit of g cm^{-1} s^{-1} is called the poise. Most viscosity data are reported in this unit or in centipoise (1 cp = 0.01 poise). The following relationship was used to calculate the kinematic viscosity[139,140].

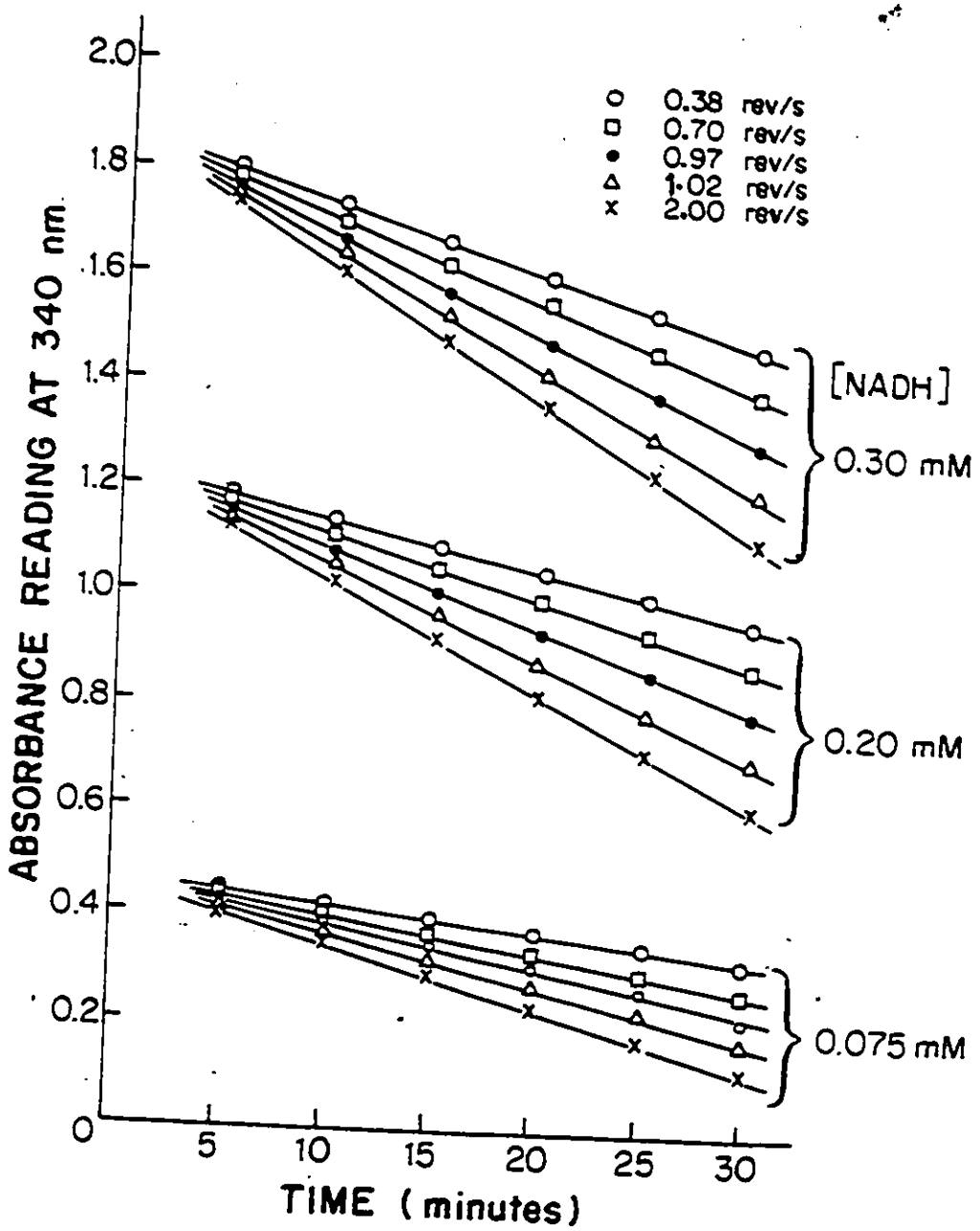

Figure 24. Typical plots of the variation of the absorbance with reaction time for some NADH concentrations at indicated rotation speeds of the disc. [Pyruvate] = 2.0 mM and temperature = 25 °C, pH = 7.5.

$$\frac{\eta_1}{\eta_2} = \frac{t_1\rho_1}{t_2\rho_2} \qquad (52)$$

where the subscripts 1 and 2 refer to the buffer solution and water, respectively.

Measurements were made with a constant volume of the test solution. An amount of 5 mL was carefully pipetted into space F of the Ostwald viscometer (see Figure 25). It was then sucked up limb S until the upper level of the liquid was above point A. The suction was released to allow the liquid to flow back into the volumetric space F under atmospheric pressure. The time t taken by the meniscus of each test liquid to travel from point A to point B was recorded. The experiment was repeated ten times for both the buffer solution and the water. The density of the water ρ_2 was taken to be 1.00 g/cm^3. Since t_1 and t_2 were known, Eqn. (52) led to the value of 9.04×10^{-7} m^2 s^{-1} or 9.04×10^{-3} cm^2 s^{-1} $\pm$ 0.07% for the kinematic viscosity.

4.3.5 Results

Reaction rates for the five NADH concentrations at various rotation speeds of the disc were calculated from the initial slopes of the absorbance-time plots. The relationship was linear within the first forty minutes of the reaction as shown in Figure 24. The results are all shown in Table 15.

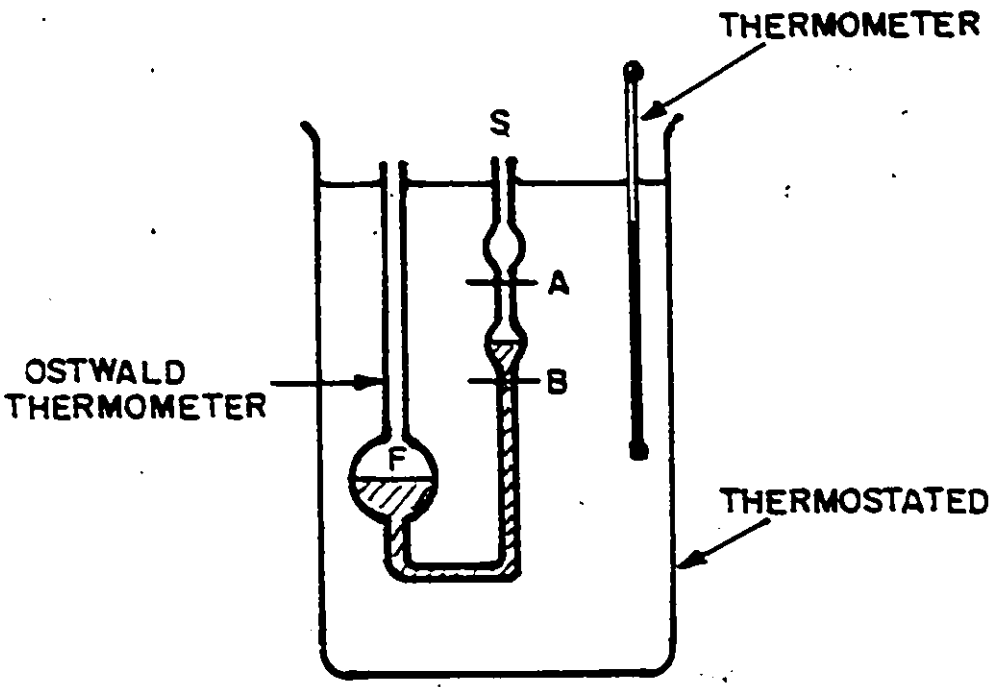

Figure 25. The apparatus used to determine the kinematic viscosity ν, of reaction media.

Table 15. Experimentally determined reaction rates v at indicated rotation speeds f, and at various NADH concentration. [Pyruvate] = 2.0 mM; temperature = 25 °C; diameter of the nylon disc = 3.2 cm. Average percentage error = 0.5%.

	$v.10^9/M\ s^{-1}$ at the following NADH concentrations				
$f/rev\ s^{-1}$	0.075 mM	0.10 mM	0.15 mM	0.20 mM	0.30 mM
0.38	12.50	15.60	21.10	25.64	34.48
0.70	16.69	20.40	27.03	32.15	43.48
0.97	20.41	25.58	33.33	39.84	50.00
1.02	25.00	30.77	40.00	47.62	59.17
2.00	30.77	37.04	50.00	57.14	66.23

4.4 Analysis and Discussion

4.4.1 Lineweaver-Burk Plots

The results of Table 15 were used to make Lineweaver-Burk plots. These initial plots (Figure 26) were used later to calculate apparent Michaelis constants for the substrate whose concentration was varied during the runs. The values of the K_m(app) are shown in Table 16. Paul et al[137], using a rotating membrane reactor of sorbitol dehydrogenase, have also found that Michaelis-Menten kinetics with bound enzymes is obeyed despite the fact that the systems may be affected by diffusional, environmental or partitional effects. The linear Lineweaver-Burk plots such as those shown in Figure 26 are a clear evidence of this fact. The curves show that the reaction rates for our system increased with increasing rotation speed of the disc. This behaviour is correctly predicted by either Eqn. (43) or Eqn. (45) since the thickness of the diffusion layer X_D is inversely proportional to $f^{\frac{1}{2}}$, where f is the rotation speed in revolutions per second.

4.4.2 Determination of K_{ms}

Equation (51) predicts that a plot of diffusion-controlled K_m(app) against $f^{-\frac{1}{2}}$ will be linear and the value of the diffusion-free Michaelis constant K_{ms} can be found at $f^{-\frac{1}{2}} = 0$. This prediction was tested and was found to be true as shown in Figure 27. The value of K_{ms} obtained from this work was 0.084 mM. Thus, the value with an asterisk in Table 16 was calculated by extrapolating the known values of K_m(app) to infinite speeds of rotation. This result, that K_m(app)

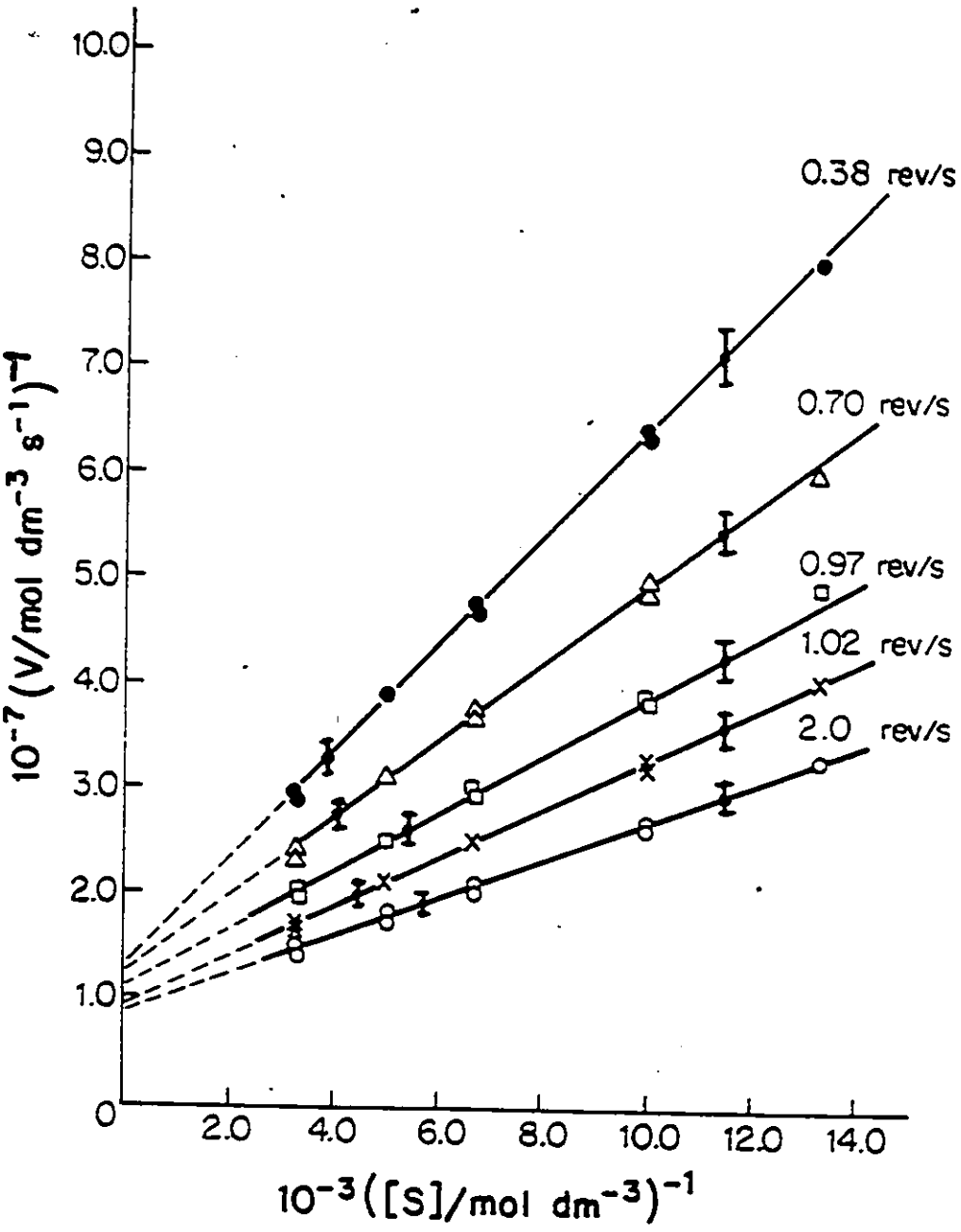

Figure 26. Lineweaver-Burk plots obtained from the use of apparent reaction rates at various NADH concentrations and at indicated rotation speeds of the LDH-nylon disc. [Pyruvate] = 2.0 mM. Temperature = 25 °C, pH = 7.5.

Table 16. The apparent Michaelis constants of NADH at various rotation speeds of the disc: Temperature = 25 °C; [Pyruvate] = 2.0 mM; diameter of the nylon disc = 3.2 cm. Average percentage error = ±2%.

f/rev s^{-1}	K_m(app).10^4/M
0.38	3.86
0.70	3.01
0.97	2.72
1.02	2.45
2.00	2.00
∞	0.84*

* Diffusion-free Michaelis constant

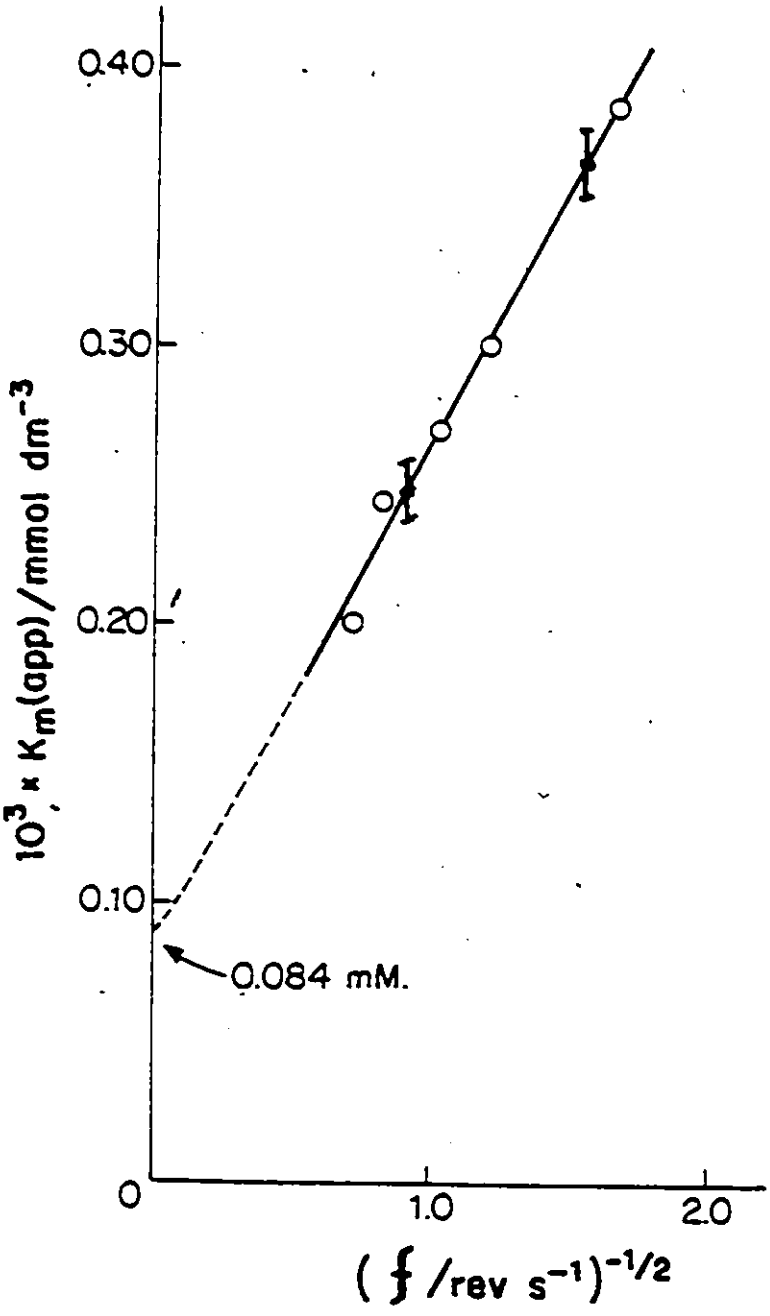

Figure 27. Plots of apparent diffusion-controlled Michaelis constants against $f^{-\frac{1}{2}}$, where f is the speed of rotation of the active nylon disc of LDH. [Pyruvate] = 2.0 mM; Temperature = 25 °C; pH = 7.5.

decreases with increasing flow rates of the substrate, has been obtained in a number of investigations[29,99-103,141,142]. This is because high rotation speeds or high flow rates reduce the thickness of the diffusion layer X_D and allow reactants to reach the catalytic surface more readily, and therefore they improve the efficiency of the system. In the case of immobilized enzymes, this improved efficiency is indicated by the reduction in the Michaelis constant.

4.4.3 Use of the Reaction Rates Found at $f^{-\frac{1}{2}} = 0$

Since, according to Eqn. (34), X_D approaches zero as ω or f approaches infinity (∞), diffusion-free reaction rates at any substrate concentration can be obtained by plotting experimental rates against $f^{-\frac{1}{2}}$ and extrapolating to $f^{-\frac{1}{2}} = 0$. These extrapolated values will therefore correspond to the rates that would be produced by the enzyme if it was left to move freely throughout the reaction mixture.

Figure 28 shows plots of the rates given in Table 15 against $f^{-\frac{1}{2}}$. Extrapolation of the linear portions of the curves to $f^{-\frac{1}{2}} = 0$ produced the theoretical diffusion-free rates which are reported in the form of the Lineweaver-Burk plot of Figure 29. The slope and the intercept calculated by linear regression led to a diffusion-free Michaelis constant equal to 0.089 mM and a V'_m(app) value equal to 1.30×10^{-7} M/s ± 3.2%. The agreement between the K'_m value from Figure 29 and that estimated as an intercept of the K_m(app) – $f^{-\frac{1}{2}}$ plot shown in Figure 27 is excellent.

The diffusion-free values of K_{ms} or K'_m found in the present disc experiments are for the substrate NADH and they are similar to

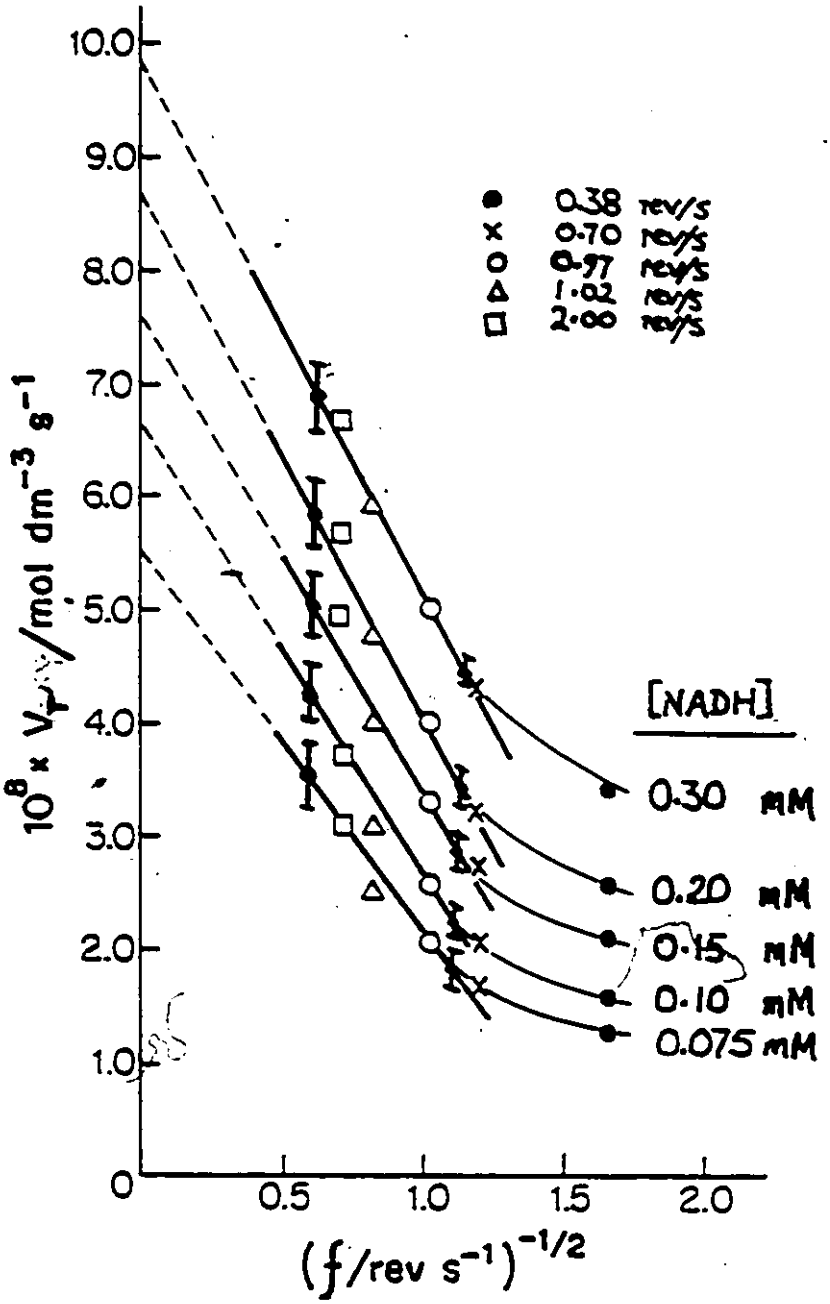

Figure 28. Plots of apparent reaction rates versus $f^{-\frac{1}{2}}$, where f is the rotation speed of the LDH-nylon disc. [Pyruvate] = 2.0 mM; temperature = 25 °C; pH = 7.5.

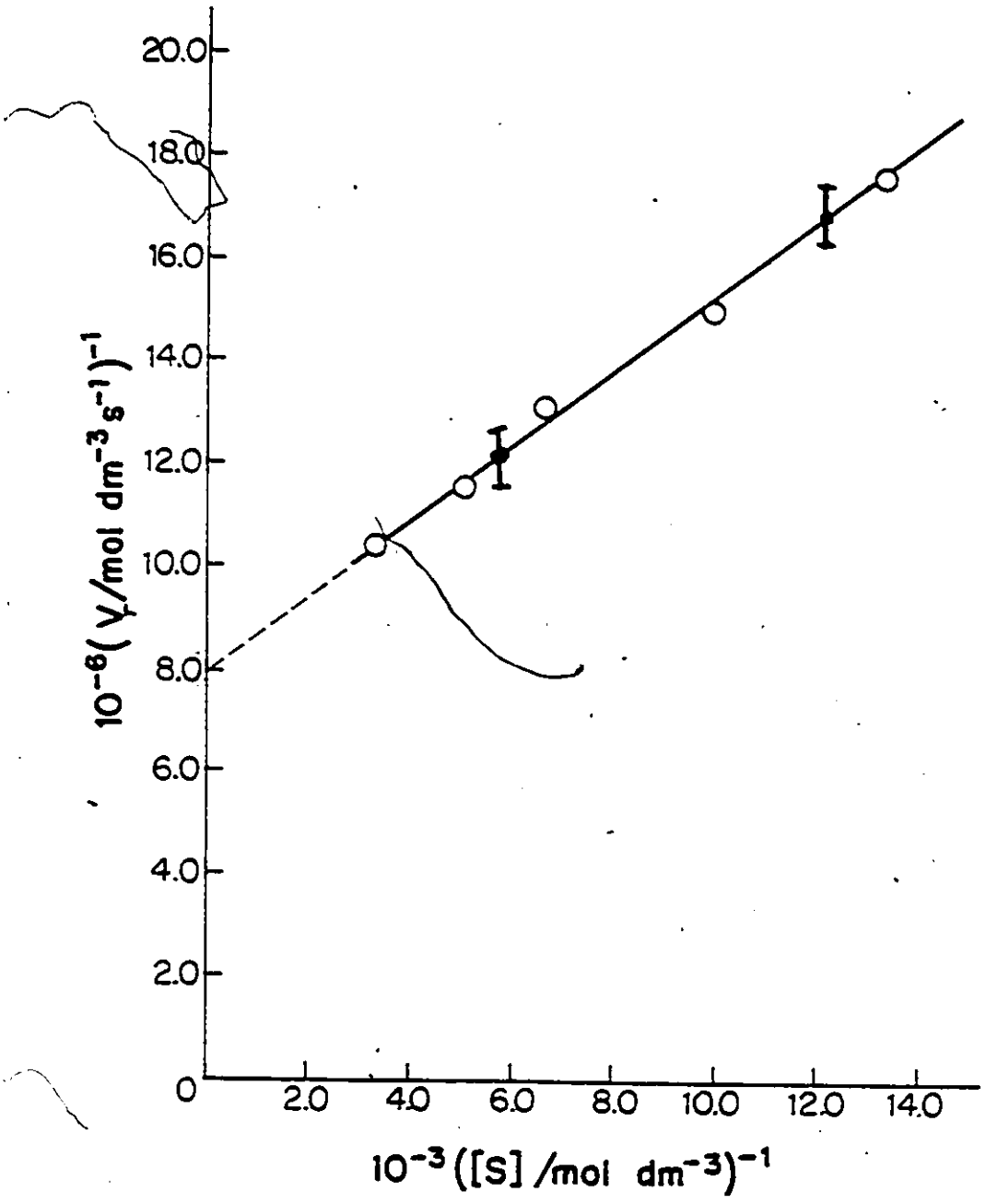

Figure 29. Lineweaver-Burk plots made from the use of diffusion-free reaction rates found at $f^{-\frac{1}{2}} = 0$. Temperature = 25 °C, pH = 7.5.

the corresponding constants found with the tube-LDH systems of Chapters II and III. This similarity suggests that the behaviour of LDH on a nylon surface is the same despite the fact that one surface was found in a tubular configuration and the other on a disc. It also means that the immobilization method of Chapter II is similar to the one just described in the present work. There are evidences in the literature which show that different immobilization techniques can give rise to changes in the kinetic behaviour of an enzyme. For example, Dixon and Stolzenbach[143] have reported a K_m value for lactate of 5.9 mM when LDH was immobilized by the "Diazo Binding" method, but when the binding method of the same enzyme was changed to the "cross-linking" technique, a value of 8.0 mM was found for the substrate.

4.4.4 Use of the Slope from the $K_m(app) - f^{-\frac{1}{2}}$ Plot

According to Eqn. (51), since ω is equal to $2\pi f$, this slope can be expressed as follows:

$$\text{slope} = \frac{1.61\ V'_m\ \nu^{1/6} V_b}{D^{2/3}(2\pi)^{1/2} A_s} \qquad (53)$$

In the present investigation, the only unknown parameter in Eqn. (53) is the diffusion-free maximum velocity V'_m. The values of A_s, V_b, ν, D, π and the slope itself are respectively equal to 8.04 cm^2, 150 cm^3, 9.04×10^{-3} $cm^2\ s^{-1}$, 4.0×10^{-6} $cm^2\ s^{-1}$, 3.14 and 0.19 mM $s^{\frac{1}{2}}$ $rev^{\frac{1}{2}}$. Substitution of these values into Eqn. (53) gives 8.6×10^{-9} M/s for V'_m. The value found from experiments done with the LDH in free

solution, and reported in Chapter II, is 6.8×10^{-9} M/s ± 3%. There is satisfactory agreement between the V'_m and the V^f_m values of NADH from the two experiments. It will be noted that the value of V'_m produced from the use of Eqn. (53) is different from that taken as an inverse of the intercept of the Lineweaver-Burk plot shown in Figure 29. This difference should be expected since the approximations that we make to reduce the complicated expression for a two-substrate-enzyme system (see Eqn. (18) of Chapter II) to pseudo one-substrate-enzyme kinetics (e.g. Eqn. (25) of Chapter II) modify the maximum velocity V'_m(app) very strongly. Thus, the value of V'_m(app) from Figure 29 is an apparent parameter whereas the true value of the maximum velocity V'_m is calculable from the use of Eqns. (51) and (53) as shown above.

CHAPTER V

KINETICS WITH THE ENZYME CONTAINED BEHIND A POROUS DISC

5.1 Introduction

In nature, LDH is found in the cytoplasm as an intracellular enzyme[1]. Due to its large molar mass (140,000 g mol^{-1}), the cell wall prevents it from escaping, but its substrates readily pass through the barrier since the molecules are relatively smaller; the molar mass of NADH is 709.4 g mol^{-1} and that of pyruvate is 110 g mol^{-1}. The enzyme has been extracted from cells and is commercially available in the cell-free form. Kinetic studies have been made with the free enzyme. However, one of the chief concerns of the field of immobilized enzymes is to understand the catalytic behaviour of these biological species when they are in their natural environment. To this end, these species are being immobilized artificially in various ways as shown in Figure 1 of Chapter I. Microencapsulation, which is the incorporation of enzymes within semipermeable membranes, is one of these immobilization techniques. It is a procedure which was started by Chang[144-149] in 1957 and since then several enzymes have been entrapped and applied in medicine, industry and research.

In medicine, examples include the use of entrapped urease in the preparation of artificial kidneys for treatment of patients with chronic renal failure[147,148]. Asparaginase in the form of microcapsules has also bee administered to patients with leukemia[149].

Entrapped glucoamylase[150], glucose isomerase[151], invertase[152] and β-galactosidase[153] are used industrially while encapsulated penicillin acylase[31,154], aminoacylase[31] and tryptophan synthetase[155] find important applications in pharmacy.

In view of the above important applications, studies of the kinetics of entrapped and encapsulated enzymes have been carried out in a number of laboratories. Examples include the works of Laidler and Bunting[129,99], O'Driscoll[156], Chambers et al[157], Goldstein[158] and Thomas and Brown[159].

A rotating disc is one of the best systems for studying the effects of diffusion on reaction kinetics[160,161,132,134]. The present Chapter reports an investigation on the effects of external diffusion on encapsulated LDH, use being made of a rotating porous disc. The reaction between NADH and pyruvate was followed electrochemically by the use of $Fe(CN)_6^{4-}/Fe(CN)_6^{3-}$ couple with a platinum electrode and with the silver-silver chloride electrode as a reference standard[162,163].

Electrochemical detectors have been used already by several workers to monitor enzyme reactions[162-169] and have shown a number of advantages over spectrophotometric and fluorometric methods. For example, the latter require solutions to be optically clear and the concentration range is limited. The electrochemical method, on the other hand, can be applied to opaque solutions, and wide concentration ranges can be covered by merely switching to the appropriate scale[162].

5.2 Theoretical Considerations

If an enzyme is attached to a solid surface, only external diffusion may be considered in the analysis of its kinetics. This has been the case in all the experiments reported in Chapters II to IV with immobilized LDH. On the other hand, when this enzyme is embedded in a porous medium, two types of diffusion come into play, external and internal.

External diffusion affects the transport of a substrate from the bulk solution to the catalyst's surface, while internal diffusion pertains to the movement of a substrate inside the pores of the porous medium before it reaches the enzyme. The rate of a chemical reaction with an encapsulated enzyme therefore increases with increasing porocity of the membrane, increasing speeds of substrate flow, and increasing substrate concentration. This fact has already been confirmed by experiments such as those which have used polyacrylamide films[129,170] collagen-enzyme membranes[171], sephadex[172], agarose[173] and porous glass[174]. For example, Goldman and coworkers[66,175], employing papain-collodion membranes of different thicknesses (470, 156 and 49 μm), found that the reaction rates were highest with the system having the smallest membrane thickness. This is due to the fact that at a small membrane thickness the internal diffusion is at a minimum and this leads to improved penetration of the substrate through the pores. The effect of external diffusion on entrapped enzymes can therefore be studied with thin membranes exhibiting maximum porosity.

Several reviews and original papers have given detailed theoretical treatments of the combined effect of external and internal diffusion on enzyme kinetics[71,176] but the rotating enzyme disc has not as yet been considered. In the present work, since we are interested in studying only the effect of external diffusion on membrane-bound LDH by using the highly porous rotating enzyme disc, we shall use the theory presented in Chapter IV, which applies to cases which do not involve internal diffusion. In the present experiments, it is therefore assumed that internal diffusion and the enzyme's activity are not rate limiting.

5.3 Experimental

5.3.1 Materials

The type and source of the enzyme and its substrates used here were the same as those reported in the previous chapters. Potassium ferrocyanide employed to follow the progress of the reaction electrochemically was bought from J.T. Baker Chemical Company, U.S.A. The buffer solution for kinetic runs was 0.01 M sodium phosphate, pH 7.5.

The pH-meter (Model10) and the Ag-AgCl electrode came from the Fisher Scientific Company, while the linear chart recorder (Model 585) and the variable speed laboratory stirrer (Talboys, Model 134-2) were bought from Canlab, Ottawa. The thermostat (HETO, Type 623) was a product of the Birkerod Company, Denmark.

5.3.2 The Porous Disc Reactor

Our design of the rotating disc is shown schematically in Figure 30. The enzyme solution was entrapped in the hollow space, E

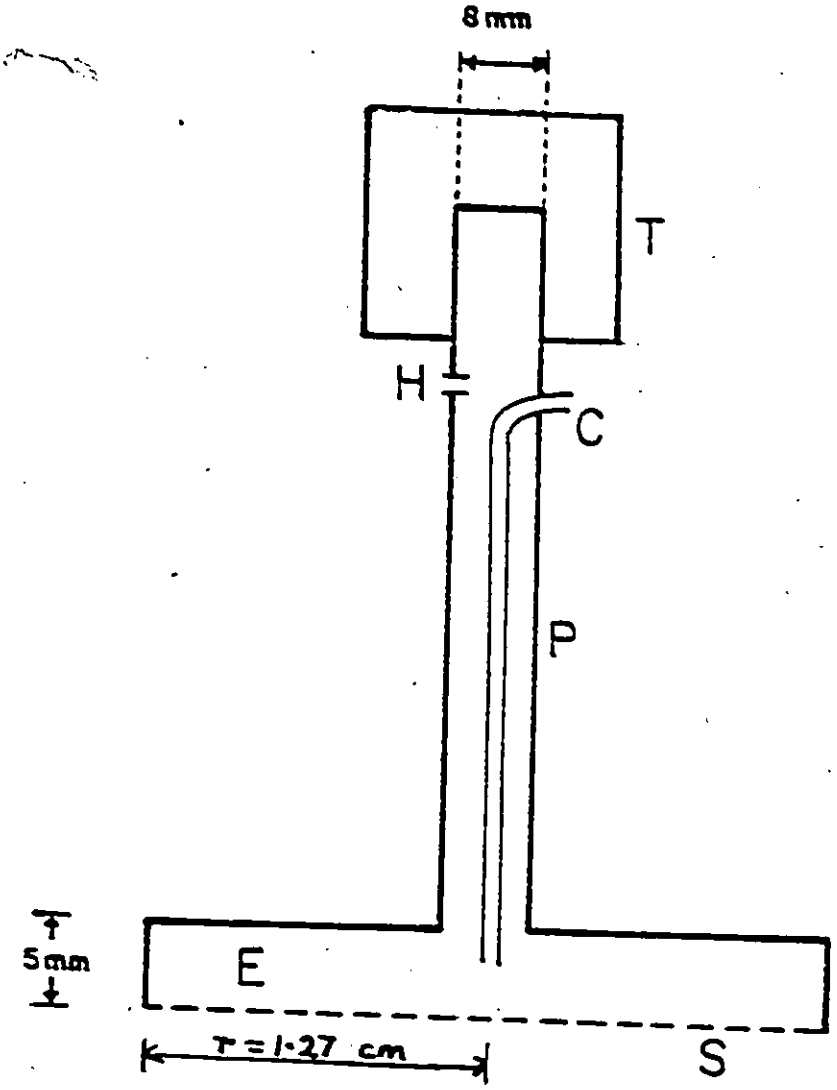

Figure 30. Diagram showing a design of a diffusion cell for entrapped enzymes at a semipermeable rotating disc. In the figure, T = variable speed stirrer; C = capillary nylon tubing; H = hole; P = disc's stem; E = entrapped enzyme space; S = semipermeable membrane.

of the glass cell by the semipermeable membrane of benzoylated cellulose, S. The cut-off molecular weight of membrane S was 2000. It therefore prevented the lactate dehydrogenase from passing into the bulk solution. Smaller species like NADH, pyruvate, NAD^+ and lactate can easily dialyse through it.

The stem P, carrying tube C, connected the disc to the variable speed stirrer, T. Tube C was used to feed the enzyme solution into the cell, by the use of a syringe. The same tube was used to remove the enzyme from the diffusion cell if it was not wanted. This tube and the hole marked H in Figure 31 helped to equalize the pressures on the opposite sides of the membrane.

5.3.3 Kinetic Procedure

The arrangement of the instruments used to study the kinetics of the enzyme reaction is shown schematically in Figure 31. Experiments were done at 25 °C in 250 mL of sodium phosphate buffer (pH 7.5 and 0.01 M ionic strength) containing 0.02 M potassium ferrocyanide. The pyruvic acid concentration was fixed at 2.0 mM. The diffusion cell contained 10 mg of the enzyme protein. There were 815 enzyme units per mg of the protein. The NADH concentration was varied from 0.10 to 0.60 mM. The progress of the reaction was monitored electrochemically[162], the reaction sequence being represented as follows:

(a) $NADH + CH_3COCOOH + H^+ \xrightarrow{LDH} NAD^+ + CH_3CHOHCOOH$

(b) $NAD^+ + Fe(CN)_6^{4-} \xrightarrow{Pt} NADH + Fe(CN)_6^{3-}$.

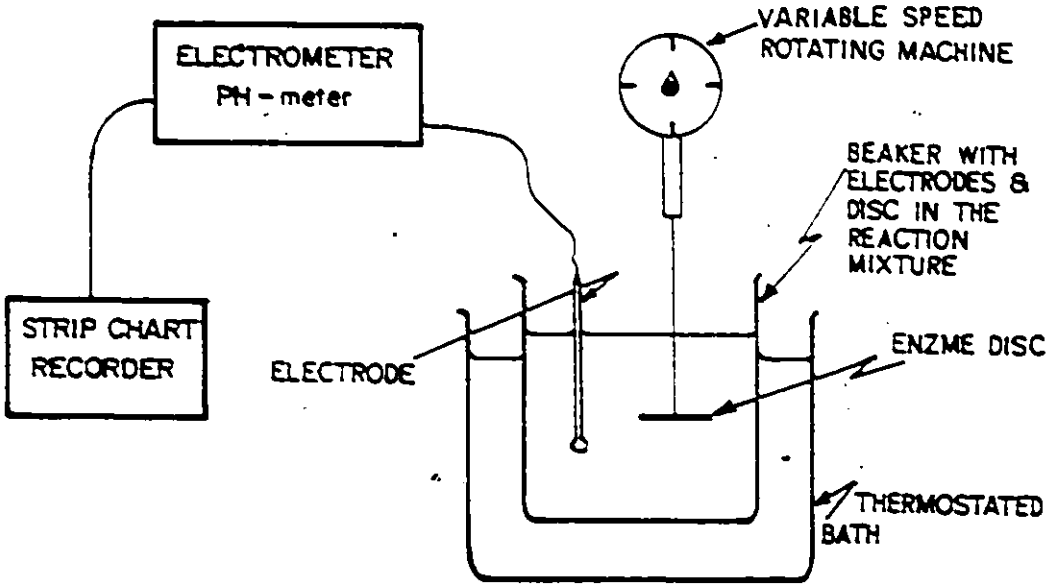

Figure 31. Schematic arrangement of the apparatus used to monitor the progress of the disc immobilized LDH by electrochemical means; use being made of the $Fe(CN)_6^{4-}/Fe(CN)_6^{3-}$ couple.

The change in concentration of NADH produced by the enzyme reaction at a particular rotation speed of the disc, and at a chosen starting substrate concentration, was automatically recorded as a function of time on a calibrated strip chart recorder. The recorder was connected to the reaction system via an electrometer which was a pH-meter switched to the millivolt (mV) scale (see Figure 31).

Since electrochemical responses of these systems are sensitive to the ionic strength of the reaction medium[163], a nomogram of Boyd[177] was used to prepare phosphate buffers of specific ionic strength. It is known that high ionic strengths decrease the sensitivity of the technique[163].

All solutions for kinetic runs were made up on the day of the experiment and when not in use the enzyme disc was stored at 4 °C in 0.1 M phosphate buffer at pH 7.5.

5.4 Results and Analysis

5.4.1 Calculation of K_m(app) and X_D

Reaction rates from the initial slopes of the mV versus time traces of the linear chart recorder are shown in the form of the Lineweaver-Burk plots (Figure 32) for various NADH concentrations at different speeds of rotation. The apparent Michaelis constants K_m(app) calculated from these L-B plots are given in Table 17. Also given in the same table are the values of the thicknesses of the diffusion layer, X_D. These thicknesses were calculated on the basis of Eqn. (34). In the calculations, a diffusion coefficient value of 4.0×10^{6} cm^2 s^{-1}

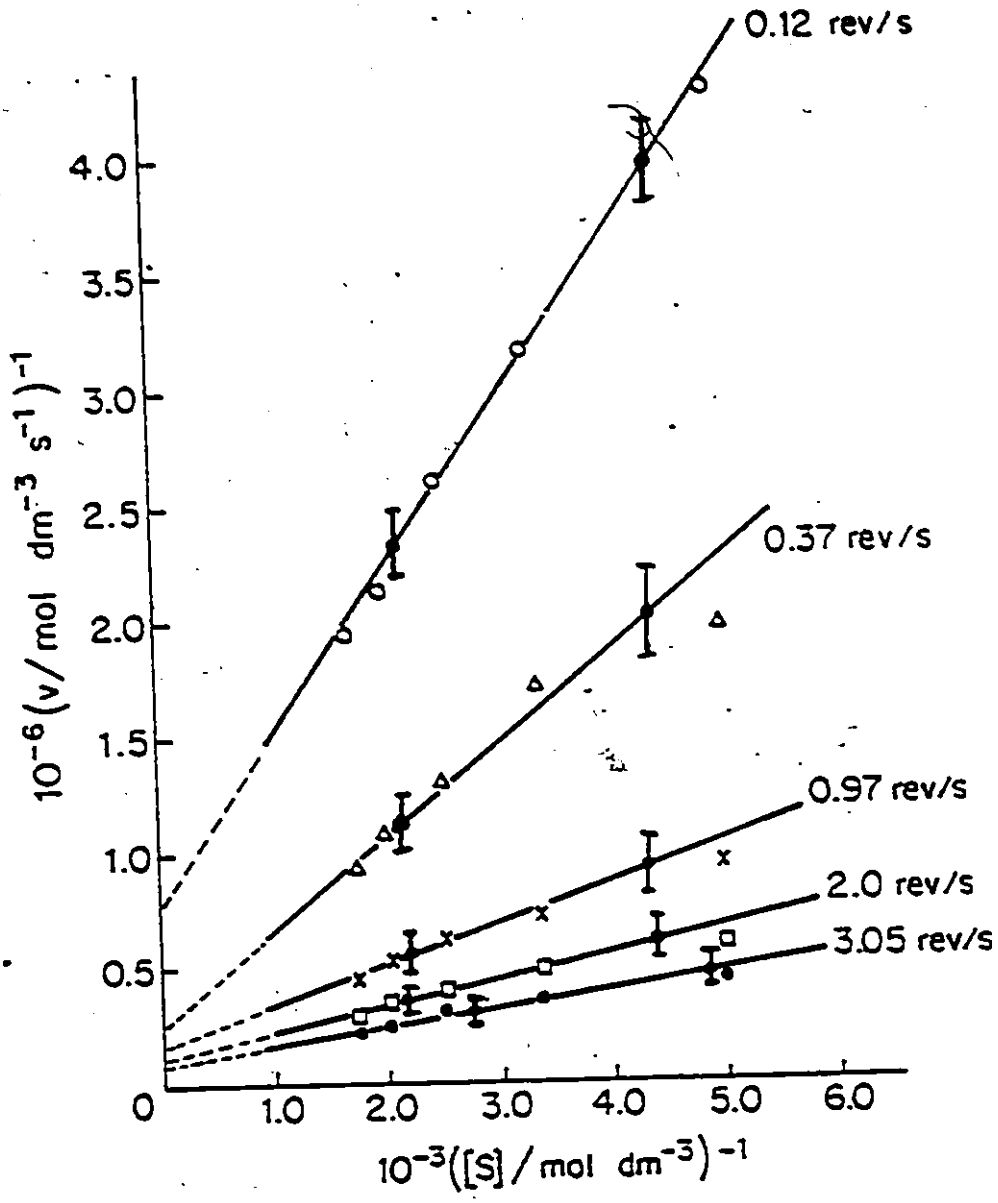

Figure 32. Lineweaver-Burk plots of the apparent rates of a disc of membrane-entrapped LDH at various NADH concentrations and various rotation speeds. Pyruvate concentration = 2.0 mM; temperature = 25 °C; pH = 7.5.

Table 17. Values of K_m(app) and x_D at various speeds of rotation of the membrane enzyme disc; variable NADH; fixed pyruvate (2.0 mM); temperature = 25 °C. Average percentage error = ±6.1%.

Speed of Rotation revolutions/s	K_m(app)/mM	Thickness, x_D/μm
0.12	1.21	290
0.37	1.07	165
0.97	0.82	102
2.00	0.66	71
3.05	0.58	57

and the kinematic viscosity of 9.04×10^{-3} .cm^2 s^{-1} experimentally measured in this work were used.

5.4.2 The Diffusion-Free Michaelis Constant

(i) From the Plot of K_m(app) Against $f^{-\frac{1}{2}}$

This type of plot is predicted by Eqn. (51) as discussed in the previous Chapter. When the apparent Michaelis constants of Table 17 were plotted against $f^{-\frac{1}{2}}$, a diffusion-free value of 0.28 mM was obtained at $f^{-\frac{1}{2}}=0$ as shown in Figure 33. This diagram shows that there was deviation from linearity at low speeds of rotation and such behaviour is probably suggestive of the change in the strength of the pumping action brought about by the disc's rotation. However, the lower portion of the curve was linear and led to the K_{ms} value of 0.28 mM ± 6.1%.

(ii) From the Use of the Extrapolated Reaction Rates

The variation of the diffusion layer with the speed of the disc's rotation was shown in Chapter IV to be given by Eqn. (34), as follows

$$X_D = 1.61\ D^{1/3}\ \nu^{1/6}\ \omega^{-1/2}$$

or

$$X_D = 1.61\ D^{1/3}\nu^{1/6}(2\pi f)^{-1/2}$$

At infinite speeds of rotation, X_D will be zero and the rates will be diffusion-free. A plot similar to Figure 28 of Chapter IV gave diffusion-free reaction rates at $f^{-\frac{1}{2}} = 0$ which were used to make

Figure 34 from which a diffusion-free Michaelis constant K'_m of 0.20 mM was calculated.

5.4.3 The Diffusion-Free Maximum Velocity, V'_m

The apparent maximum velocity V'_m(app) of the present system, calculated from Figure 34, was 7.9 μM s^{-1} ± 7%. A better approximation of the true maximum velocity is obtained from the use of the slope of Figure 33 and from the knowledge of the surface area of the disc. The slope from Figure 33 was 0.51 mM $s^{\frac{1}{2}}$ $rev^{-\frac{1}{2}}$ and the disc's surface area was 5.07 cm^2. Taking the values of the diffusion coefficient and the kinetic viscosity already given in the text led to a calculated value of 1.76 nM/s for V'_m, since the reaction volume V_b was 250 mL.

5.5 Discussion

It should be noted that both the K_{ms} and the K'_m parameters are the Michaelis-Menten constants for the diffusion-free situation of the same enzyme and therefore should be equal. In view of the extrapolations involved in the methods for their determination, a K'_m value of 0.28mM ±7% from Figure 34 is in satisfactory agreement with the K_{ms} value of 0.28mM ± 6.1% from Figure 33. Comparison of these kinetic parameters with those obtained with the solid nylon disc of the previous chapter shows that the present values are about three times higher, and yet, they all represent the diffusion-free behaviour of the same enzyme. These disagreements are an indication that a number of different factors can come into play to influence the kinetics of an enzyme if one changes,

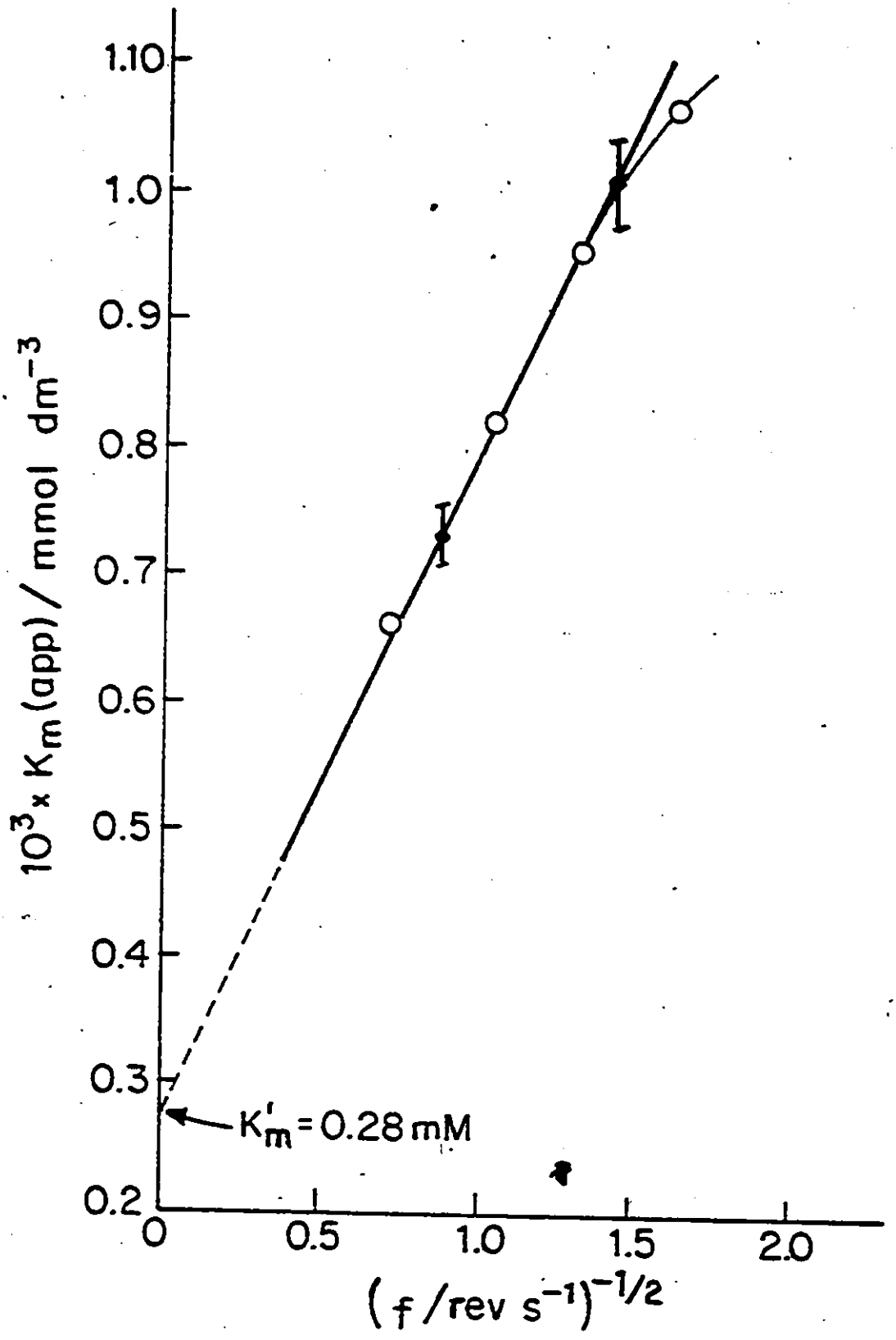

Figure 33. Plots of the apparent Michaelis constants against the inverse of the square root of the speeds of rotation of the porous disc. Temperature = 25 °C; variable NADH; fixed pyruvate (2.0 mM); pH = 7.5.

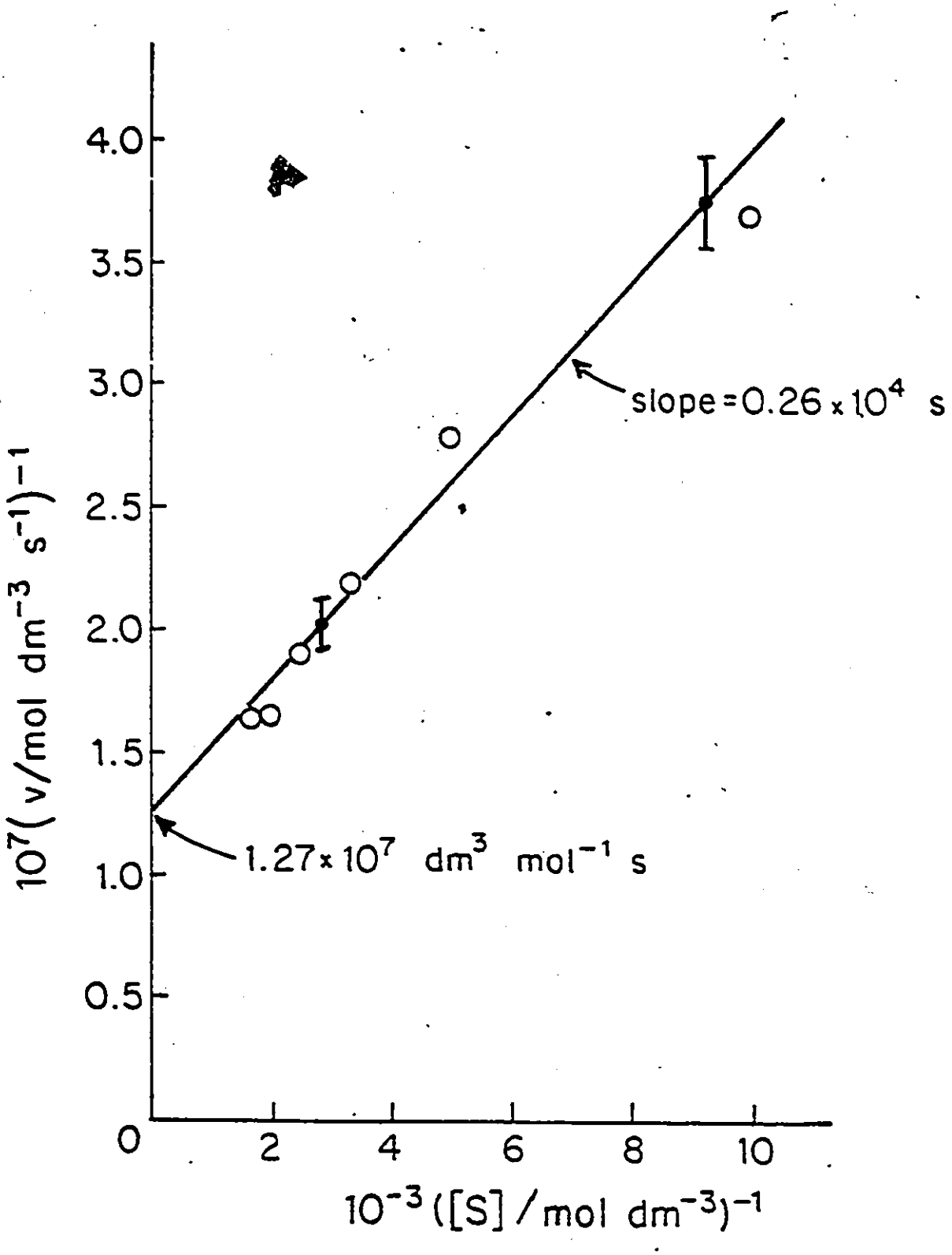

Figure 34. Lineweaver-Burk plots derived from the use of diffusion-free reaction rates found at $f^{-\frac{1}{2}} = 0$ for variable NADH concentrations and [Pyruvate] = 2.0 mM; temperature = 25 °C; pH = 7.5.

for example, (1) the structure of the support for the enzyme, (2) the method of immobilization and (3) the composition of the solution used as a reaction medium. All these factors were different in the two experiments. However, the most significant effect seems to be due to the presence of the membrane.

Since the cut-off molar mass of the membrane that we employed was 2000 g mol^{-1}, the permeability constant[45] P was assumed to be 100 % for the smaller molecules such as NADH. However, it is possible that the passage of the NADH molecules through the pores might have been not as simple as we had anticipated. This passage could have been affected by the population of the pores per unit surface area of the membrane and also by the type of interaction that would be exhibited between the chemical groups surrounding the pores and those of the NADH. Since the membrane was made of benzoylated cellulose, this interaction could well have been hydrophobic in nature. The work of Cresswell and Sanderson[178] and Chibata[20] has shown for enzymes enclosed in semipermeable polymers that their interaction with high molecular weight substrates is intrinsically difficult, mainly because of the steric hindrances. Thus, the high value of the Michaelis constant found in the experiments of the present Chapter are due to the presence of the porous membrane since the ferrocyanide does not affect the enzyme's activity[162].

In Chapter IV, the value of the true maximum velocity was 8.6 x 10^{-9} M/s and in the experiment with the porous membrane we found 1.76 x 10^{-9} M/s. In fact, it can be shown from the use of Eqn. (53) that the V'_m increases as A_s is increased for a fixed value of the slope.

The fact that taking 5.07 cm^2 (a value predicted by πr^2) as A_s for the porous membrane disc leads to a smaller value of the V'_m (i.e. 1.76 x 10^{-9} M/s) compared to 8.6 x 10^{-9} M/s for the impervious disc, is an indication that the experimentally effective area of the porous disc was larger than the πr^2. This is consistent with the fact that the surface is porous.

5.6 Conclusion

This Chapter has been concerned with the effect of external diffusion on the kinetics of entrapped LDH. To simplify the analysis, it was assumed that the influence of internal diffusion was negligible. This is to say that the enzyme activity on the outer surface of the membrane was sufficiently high. However, with a reactor design such as that shown in Figure 30, the effect of internal diffusion on entrapped enzymes can be investigated by employing membranes of various porosities and thicknesses. This work has not yet been done with a rotating disc, and will have to wait until a complete theoretical treatment for rotating porous membranes has been developed.

The work discussed in this Chapter was done with the object of providing some fundamental background to future experimental and theoretical studies.

Once a theory which couples both internal and external diffusion has been developed, it may be possible to determine diffusion coefficients of substrates in membranes and in free solution. For example, the theory given in Chapter IV already suggests that one can obtain diffusion coefficients of substrates in free solution through Eqn. (53) provided that V'_m from free-enzyme experiments is known.

The porous membrane disc also provides an immobilization technique which is very different from the covalent methods discussed in Chapters II to IV. It therefore affords an opportunity for understanding the kinetics of intracellular enzymes such as LDH.

CHAPTER VI

GENERAL DISCUSSION AND CONCLUSION

6.1 Introduction

The general discussion and conclusion to this thesis are presented in this final chapter under three main sections; namely kinetics, immobilization and tests of theories. Based on the results of the experiments reported in Chapters II to V, the extent to which the four factors given in Figure 2 influence the kinetics of immobilized LDH is examined under the kinetic factors section. A summary of the advantages of immobilization, and some important factors which should be known about the enzyme and the support prior to adopting an immobilization technique, are presented in the second section. The boundary conditions under which both the Kobayashi-Laidler theory and the theoretical treatment of the rotating enzyme disc were derived are compared in the last section entitled "Tests of Theories".

6.2 Kinetic Factors

When enzymes are immobilized, the main factors that come into play to influence their kinetics have been discussed in Chapter I and summarized in Figure 2. These factors are diffusional, conformational (i.e. arising from variations in the enzyme's 3-dimensional structure), partitional and environmental.

6.2.1 Diffusion

Two types of diffusional effects have been distinguished in the field of immobilized enzymes; namely internal and external diffusion. When enzymes are entrapped in gels or any other porous medium, the transport of their substrates through the pores and inside the medium may be affected by internal diffusion. External diffusion pertains to situations where enzymes are fixed on impervious surfaces, so that the liquid boundary layer of thickness X_D, between the bulk solution and the enzyme, has to be crossed by the substrate molecules. The former type of diffusion is more pronounced in cases where the gel slices or membrane thicknesses are relatively large. The latter type is particularly common in fast enzymic reactions. The concern of this thesis has been with the latter type of diffusion. Although experiments reported in Chapter V were done with the enzyme enclosed in a porous membrane, the effect of internal diffusion was assumed to be less than that of external diffusion since the membrane had a high cut-off molecular weight.

The kinetic analysis of immobilized LDH given in this thesis leads to the general conclusion that diffusional factors strongly affect the kinetics of the bound LDH. Evidence for this conclusion comes from the Kobayashi-Laidler treatment discussed in Chapters II and III and from the rotating enzyme disc theory as explained in Chapters IV and V. Results of all the experiments have shown that the apparent Michaelis constants (K_m(app)) increase with increasing thicknesses of the Nernst[194] or diffusion layer (e.g. Table 17, Chapter V).

A number of workers have investigated the effect of diffusion on the apparent Michaelis constants and it has been confirmed that both internal and external diffusion lead to an increase in the magnitude of $K_m(app)$[129,196,197].

Sometimes it is possible to infer diffusion from the curvature of the Lineweaver-Burk plots. This curvature is an indication of a reaction transition from one region of kinetic factors to the other and can be due to changes in the degree of diffusion. The results of the experiments reported in Chapters II and III showed curvatures in the Lineweaver-Burk plots (Figures 7 and 15). But various tests of the Kobayashi-Laidler theory confirmed that the extent of diffusion varies with flow rate, temperature and substrate concentration. It was therefore reasonable to attribute the observed curvatures in the above-mentioned figures to changing degrees of diffusion. On the other hand, the Lineweaver-Burk plots from experiments done with rotating disc systems (Chapters IV and V), did not show any break in the curves because the reaction occurred in only the region of diffusion control.

Diffusional effects in experiments done with immobilized enzymes were best revealed by the use of dimensionless parameters such as those described by Kobayashi and Laidler for the tubular enzyme reactor (see Figures 10 and 19). Similar parameters for rotating enzyme discs are yet to be developed. However, reactions that obey disc behaviour especially at low rotation speeds are diffusion controlled, and the results of our disc experiments showed a consistent behaviour.

Since diffusion factors are more pronounced in systems which are intrinsically fast and since the general conclusion reached in our investigation is that diffusional effects strongly affect the kinetics of bound LDH especially at low flow rates and low substrate concentration then immobilization methods described in this thesis leave a high enzyme concentration on the supports.

According to Kobayashi and Laidler[75], the diffusion layer thicknesses in tubular enzyme reactors are defined by Eqn. (8) of Chapter II as follows

$$X_D = 0.75 \left(\frac{DrL}{v_f}\right)^{1/3} \qquad (8)$$

In rotating disc systems, the thickness of the diffusion layer is given by Levich[134] (see Eqn. (34), Chapter IV) as

$$X_D = 1.61\ D^{1/3}\nu^{1/6}\omega^{-1/2} \qquad (34)$$

At infinitely high flow rates (i.e. $v_f \to \infty$) or rotation speeds (i.e. $\omega \to \infty$), the effect of diffusion on the kinetics of an immobilized enzyme will therefore be insignificant. Flow-kinetics experiments keep v_f and ω under control and they afford a good chance of extrapolating to infinite speeds of substrate flow to remove diffusional effects. This is what makes flow kinetics better than those done at invariant flow speeds.

In the absence of diffusional effects, the kinetic behaviour observed with an immobilized enzyme may still be different from that of its free counterpart because:

(a) The bound enzyme may have a conformation which is different from what it has in free solution.

(b) The extent to which substrates distribute themselves between the enzyme at the support and the rest of the bulk solution may be different from that found when the enzyme is free.

(c) The environment of the fixed enzyme is different from that of a free enzyme.

6.2.2 Conformational Changes

The catalytic action of an enzyme depends on the three-dimensional structure of its active sites. Changes in the arrangement of molecules in the whole enzyme structure may affect the three-dimensional structure of the active sites and this will in turn affect the kinetics. Thus, kinetic studies made with enzymes in the absence of diffusional, partitional, and environmental effects can be used to understand conformation changes resulting from immobilization.

One approach to understanding conformations of immobilized enzymes has been concerned with the use of breaks in the Arrhenius plots of diffusion-free catalytic rate constants[173,191,192]. Another approach compares the Michaelis constants found with the free enzymes against those obtained with their immobilized counterparts.

The Michaelis constants for free and bound enzymes, obtained under non-flow conditions, have been compared by a number of people[20,143,183,188-190] in the hope of trying to understand how conformation changes lead to altered kinetic behaviour of enzymes. The

results have not been very successful because the apparent Michaelis constants for immobilized enzymes under such non-flow conditions are diffusion controlled.

Laidler and coworkers[29] have done experiments, the results of which have been analyzed in such a way that the determination of the diffusion-free Michaelis constants for bound enzymes has been possible. This has been achieved by extrapolating the K_m(app) values to infinitely high substrate flow. The diffusion-free Michaelis constants for the bound enzyme (K'_m) have then been compared with those obtained with the free enzyme (K^f_m). Agreement between K'_m and K^f_m values has been taken to suggest that the conformation of a given enzyme in both fixed and free state is the same.

The results of our work reported in Chapter II showed that the K^f_m and the K'_m values for pyruvate were similar (see Table 6). This similarity was therefore evidence that the conformation of LDH before and after immobilization was the same. Thus, the use of the Kobayashi-Laidler theory and the treatment presented in Chapter IV for enzymes on rotating disc may lead to a better understanding of enzyme conformations. However, so far, great success in understanding conformational changes of immobilized proteins has been achieved through the use of non-kinetic, physical methods. These techniques include fluorescence, spectrophotometry and hydrogen exchange. Fluorescence methods seem to be most readily adaptable to protein conformations[193,201-203]. Pye and Chance[193] have reviewed these physical methods.

6.2.3 Partitional or Substrate Distribution Effects

In the absence of diffusion, conformational changes and environmental effects, the kinetic behaviour of an immobilized enzyme may be different from that observed with its free counterpart because the extent to which substrates distribute themselves between the enzyme at the support and the rest of the bulk solution in the two enzyme states may not be the same. The extent of substrate distribution depends on several factors:

(a) the ionic strength of the reaction medium[158,182]

(b) presence of either hydrophilic or hydrophobic effects in the reaction system[180,181]

(c) steric hindrance factors[6,20]

(d) the relative charges of the support and the substrate[1,158,179]

These factors will be discussed below in relation to the results of our investigations.

6.2.3 (i) Ionic Strength of the Reaction Medium

In all our major experiments, the ionic strengths of the reaction media were fixed. Thus, the extent to which ionic strength would influence the distribution of substrates between the enzyme support and the rest of the bulk solution was not known in detail although the results given in Figure 21 in Chapter III show that a medium of low ionic strength favours the enzyme reaction. This result is in good agreement with the work of Goldstein[158] and that of Whatton et al[182].

6.2.3 (ii) Steric Hindrances and the Effects of Hydrophilicity and Hydrophobicity

The results of the experiments reported in Chapter II showed that the Michaelis constant of pyruvate obtained with the free LDH was similar to that found with immobilized LDH. On the other hand, the corresponding values for NADH were different (see Table 6 given in Chapter II). In these experiments, the enzyme support and the ionic strength of the medium were the same for both substrates. To explain this different K_m' value for NADH when LDH was immobilized, attention was focussed on the effects that may arise from either steric hindrances or from the hydrophobicity of the tube system.

The immobilization technique described in Chapter II introduces some hydrophobicity on the nylon surface (see Figure 13). Of the two substrates of LDH, NADH is more hydrophobic than pyruvate. In this regard, NADH was supposed to react faster than pyruvate and to have a K_m' value which would be lower than that of pyruvate. However, the K_m' value for NADH (see Table 6) was higher than that of pyruvate and also higher than its own K_m^f value. The notion that hydrophobic supports will give rise to a rate increase with an enzyme whose substrates are hydrophobic has been investigated and found to be true. For example, Johansson and Mosbach[180] prepared cross-linked copolymers of varying degrees of hydrophobicity and hydrophilicity by changing the ratios of hydrophilic acrylamide and hydrophobic methylacrylate. To these surfaces horse liver alcohol dehydrogenase was attached and kinetic runs made. Ethanol and n-butanol were used as substrates. It was found that for

n-butanol (a more hydrophobic substrate), the apparent Michaelis constants obtained with more hydrophobic enzyme preparations were smaller than those from copolymer-enzyme derivatives which had higher hydrophilicity. It was concluded that hydrophobic supports favour hydrophobic substrates and that hydrophilic supports favour the reaction of hydrophilic substrates. Thus, in our experiments, the interaction of NADH with the enzyme at the nylon surface (Chapters II, III and IV) was expected to be more favourable than that between pyruvate and the immobilized LDH. The fact that this was not the case suggested that a force stronger than those arising from the hydrophobicity of the system was responsible for the observed anomaly. Since the surface of the support was electrically neutral as a result of our immobilization technique, and since the temperature, ionic strength, pH and the reaction medium were experimentally the same for both substrates, we attribute the difference between K'_m and K^f_m for NADH to steric hindrance. NADH, being a larger molecule than pyruvate, is hindered from interacting with the bound enzyme as efficiently as it does when the enzyme is free.

Steric hindrances were also used to explain the difference in the reaction rates exhibited by NADH and pyruvate in the pH experiments of Chapter II. In these measurements, the diffusion layer was fixed since the flow rate was constant. However, the reaction rates produced by NADH at 0.20 mM for example were smaller than those of pyruvate at the same concentration.

6.2.3 (iii) Charge Effect on Partitional Factors

Partitional effects, which depend on the presence of charges on the substrate and on the enzyme support, have been investigated by a number of workers[1,6,158,179]. Goldstein et al[6] and Laidler and Bunting[1] have given an equation with which the prediction of the nature of the charges existing between the substrate and the enzyme support can be made provided the Michaelis constants from the free enzyme and from its immobilized form are known. This equation is

$$\Delta p\ K_m = p\ K_m^f - p\ K_m(app) = 0.43 Ze\psi/kT \qquad (54)$$

where $p\ K_m^f$ and $p\ K_m(app)$ are, respectively, the negative logarithms of the Michaelis constants for the free and fixed enzyme. Also, in the same equation, Ze, ψ, k and T are the substrate's charge, the electrostatic potential, the Boltzmann constant and the absolute temperature respectively.

Equation (54) is used to predict whether the substrate and the enzyme support have the same or opposite charges, or whether one of them has a zero charge. For example, in the case of similar charges, $K_m(app)$ is greater than K_m^f because then Ze and ψ have the same sign[1,6]. Conversely, for dissimilar charges, Ze and ψ have opposite signs and give $K_m(app)$ values which are less than the K_m^f values. Equation (54) has been used by several workers to explain the results of their experiments[6,20,172,183-186]. For example, the apparent Michaelis constant for a polyanionic derivative of trypsin acting on the positively charged substrate, benzoyl-L-arginine amide was found by Goldstein et al[6]

to be lower than that obtained with the free trypsin (i.e. K_m^f = 6.90 mM; K_m(app) = 0.20 mM).

In flow-kinetic studies of immobilized enzymes, Eqn. (54) can be used only after diffusional and conformational effects have been removed from the apparent Michaelis constant, and if also the possibility of all factors except those arising from the presence of charges, have been ruled out. In this case, Eqn. (54) should be modified to suit flow-kinetic problems of immobilized enzymes. Thus it is best to use

$$\Delta p\, K_m = p\, K_m^f - p\, K_m' = 0.43\, Ze\psi/kT \qquad (55)$$

where K_m' is free from the influence of all factors except those due to charges.

In our investigations, pyruvate was found to be free from steric hindrances. Its diffusion-free Michaelis constant obtained from the use of Eqn. (14) given in Chapter II was similar to that found in free-enzyme experiments (see Table 6, Chapter II). When the K_m' and the K_m^f values for pyruvate are substituted into Eqn. (55), a value of zero for $\Delta p\, K_m$ is obtained. This result is consistent with the fact that the nylon support, after LDH immobilization, was electrically neutral. Thus the use of diffusion-free Michaelis constants in Eqn. (54) would lead to better predictions of the nature of the charges present on either the substrate or the support. Diffusion-free Michaelis constants for immobilized enzymes can be obtained by carrying out flow-kinetic investigations which allow the use of extrapolating K_m(app) to infinite speeds of substrate flow.

Several workers have used pH measurements to study partitional effects on enzymes embedded in charged supports[1,6,20,158,172,179,183-186]. Quantitative treatments have been made[1,6]. It has been found that the position of the optimum pH and the pH-activity profile of an enzyme, once it is immobilized within a charged carrier, can be shifted towards higher or lower pH values. When the support is positively charged, the shift is towards lower pH values, and when the support is negatively charged, the shift is towards higher pH values[1,6]. In our pH measurements, the optimum rate obtained with pyruvate at 0.20 mM was at pH 7.0. This is reasonable since the nylon surface, after LDH immobilization, was electrically neutral. However, results of our pH experiments (see Figure 20, Chapter III) showed that diffusion effects, if they are more significant than the charges effect, can broaden the pH optimum. It will be noted in Figure 20 that the pH optima for lower substrate concentrations (e.g. 0.04 mM pyruvate) are not as sharp as those found with higher substrate concentrations (e.g. 0.20 mM pyruvate). This seems to suggest that the sharpness of the pH optimum can sometimes be used to explain the extent of diffusion. The sharper the pH optimum at high substrate concentration the lower the degree of diffusion. However, the interpretation of charge effects on the behaviour of a bound enzyme, based on pH-activity profiles, can be more reliable if measurements are made in the absence of diffusion. In flow kinetics, this can be achieved by running experiments at high temperature, high substrate concentrations and at high flow speeds of the substrates. The experiments of Ngo and Laidler[103] have also shown that significant diffusional effects can give rise to a pH-activity

profile which is extremely different from that obtained in the absence of diffusion.

Dixon and Webb[187] and Bunting and Laidler[1] have given procedures for obtaining ionization constants for acidic and basic groups on the enzyme from pH-activity profiles, in the absence of significant diffusion. They have proposed that comparison of the ionization constants for a free enzyme K_f and of its bound counterpart K_b through the use of the equation

$$\Delta p\ K_i = p\ K_f - p\ K_b = 0.43\ Ze\psi/kT \qquad (56)$$

can give information as to the nature of the charges present on the enzyme support. Thus, an excess of negatively charged groups will give a negative $\Delta p\ K_i$ value since ψ is then less than zero. Conversely, a positively charged surface will be manifested by $\Delta p\ K_i$ being positive[1,187]. In our investigation, the surface of the enzyme supports was known to have a zero charge. Therefore, it can be inferred that the ionization constants for LDH were not affected by immobilization.

The above discussion shows that partitional effects, which come into play as a result of charges on the substrate and on the support, can be explored from measurements of Michaelis constants, pH-activity profiles and ionization constants provided the experiments are not significantly affected by diffusion.

6.2.4 Environmental Effects

These effects have been discussed by Laidler and Bunting[1]. The term "environment" refers to the surrounding in the immediate vicinity of the immobilized enzyme, as opposed to the bulk medium. Thus, "environment" is synonymous to "microenvironment", a terminology generally used by many enzyme technologists. The bulk solution is called the "macroenvironment".

In the absence of diffusional and conformational effects, it may be difficult to separate environmental effects from partitional factors in a given set of kinetic data, because the two influences are interdependent; however, the distinction is qualitatively clear. Whereas partitional effects are concerned with the migration of the species to and from the catalytic surface, environmental effects are a static phenomenon.

The environment of an enzyme changes immediately after immobilization. Also, immobilized derivatives of the same enzyme can be made to have different environments by changing either the immobilization techniques or the chemistry of the support materials. Thus, the environment of our free LDH was different from that of the nylon-LDH derivatives discussed in Chapters II to IV and from the benzoylated cellulose system of Chapter V. This partly explains why the diffusion-free Michaelis constants for NADH changed as LDH was changed from the free state to the nylon surface and finally to the membrane, as shown below.

(a) Free LDH:

K_m^f(NADH) = 9.3 μM ± 2.1% ..Chapter II

(b) Nylon bound LDH:

K'_m(NADH) = 87.3 μM ± 5% ... Chapter II

K'_m(NADH) = 89.0 μM ± 2% and 84.0μM ± 3.2% .... Chapter IV

(c) Membrane bound LDH:

K'_m(NADH) = 200 μM ± 7% and 280μM ± 6.1% ... Chapter V

Unfortunately, partitional effects do change with changing properties of the enzyme's environment and it is usually very difficult to tell which factor brings about the greater change in the enzyme's kinetic behaviour.

Goldstein[158], for example, has also observed differences in the kinetic behaviour of chymotrypsin immobilized on polyornithyl polymer compared to that bound to ethylene-maleic acid support. Using acetyl-L-tyrosine ethyl ester as substrate, he obtained a Michaelis constant with the former system of 7.10 mM, and with the latter system of 2.50 mM. Both partitional and environmental effects were responsible for the difference in the kinetics of chymotrypsin.

In summary, the discussion given above shows that immobilized enzymes are affected by so many factors that great care in treating their kinetic data should be exercised in order to reach satisfactory conclusions. Unreliable conclusions can be avoided through the use of good theories. The Kobayashi and Laidler[73] theory, and the treatment presented in Chapter IV of this thesis for kinetics of rotating enzyme discs, are along the right path. Their application to the flow kinetics

of immobilized LDH have led us to conclude that:

(a) Diffusion factors are generally important.

(b) The immobilization techniques given in Chapters II and IV do not give rise to significant changes in the conformation of LDH.

(c) NADH suffers more steric hindrances than the smaller pyruvate.

(d) Flow kinetic studies made with multi-substrate enzymes are more advantageous than non-flow or single-flow investigations employing one-substrate enzymes, in as far as the elucidation of different kinetic influences on bound biocatalysts is concerned. For example, with experiments reported in Chapter II, the conclusion that NADH must have suffered from steric hindrances, and that no significant conformational changes in LDH molecule took place as a result of immobilization, was possible because two substrates (NADH and pyruvate) and several flow rates were used. Similarities in the K_m^f and K_m' values for pyruvate suggested that the conformation of LDH was little changed by immobilization. Such a conclusion would be almost impossible to arrive at if experiments were done under non-flow conditions and with one-substrate enzymes.

6.3 Immobilization

The types of techniques employed to immobilize any enzyme can be classified as binding or entrapment methods, as illustrated in Figure 1. Binding methods are those which involve adsorption or covalent forces,

while entrapped enzymes can either be matrix-entrapped or microencapsulated. Chibata[20] has recently reviewed these methods in much greater detail. In the kinetic investigations reported in this thesis, two types of immobilization techniques were employed. One was the covalent cross-linking method, and the other was microencapsulation.

6.3.1 Cross-Linking

A covalent cross-linking method involves the use of one or more multifunctional reagents to act as spacers or cross-links between a support and an enzyme. Almost all workers using this technique have employed only one cross-linking agent to make their heterogeneous enzyme reactors. The multifunctional compounds that have been used include[197] glutaraldehyde; dimethyl adipimidate; diphenyl-4,4-diisothiocyanate 2,2-disulfonic acid; 4,4-difluoro-3,3-dinitrodiphenylsulfone; ethyl chloroformate 1,5-difluoro-2,4-dinitrobenzene; trichloro-S-triazine; toluene 2,4-diisocyanate; diethylmalonimidate; benzidine and bis-diazobenzidine-2,2-disulfonic acid. In our work, we have found that preparations of artificial nylon-LDH reactors, which involve a combination of glutaraldehyde with either benzidine or 3,3-diaminobenzidine as cross-linking agents, to be more stable and more active than those in which only one type of a cross-linking agent has been used.

6.3.2 Microencapsulation

Microencapsulation, discussed in Chapter V, did not involve any chemical bond formation between the enzyme and the support. Thus,

chemical alteration of the enzyme was not possible. Some advantages of this mode of physical immobilization include short preparation time and lower labour costs. Confining LDH inside semipermeable membranes affords a better means of understanding its true behaviour in vivo, since in natural systems this particular enzyme is intracellular.

In trying to achieve a successful immobilization, it is helpful to know such factors as the amino acid composition of the enzyme, its active site and also the physical and chemical characteristics of the support material. For example, in the present investigation, the amino acid composition of rabbit muscle LDH was known[55,198]. This is given in Table B1 of Appendix B. A representation of the substrates binding in the active site of LDH is known to be as shown in Figure B1 of Appendix B[50]. The chemical structure of nylon, a product of adipic acid and hexamethylene diamene condensation is shown in Figure B3 of Appendix B. The full structure of NADH is shown in Figure B1 of Appendix B[1]. Given in the same appendix is the chemical structure of benzoylated cellulose (Figure B4). Advantages of using these supports for enzyme immobilization include the following:

(a) They are resistant to microbial attack.

(b) They are mechanically strong.

(c) They are relatively inexpensive, and

(d) they can be found in many forms (e.g. tubes, discs and membranes).

Thus, the basic important information on the enzyme, its substrates and the properties of the supports were well known for our research.

Advantages of immobilizing enzymes have been discussed in Chapter I and they include:

(a) recovery and reuse of the same enzyme

(b) reduction in operation costs

(c) continuous operation

(d) increased stability

(e) easy extraction of clean chemical products

(f) provision of new tools for medical and industrial uses, and

(g) provision of model systems for understanding the catalytic behaviour of enzymes in living organisms.

6.4 Tests of Theories

Experiments reported in this thesis were done to test the validity of the predictions of the Kobayashi-Laidler theory and of the rotating enzyme disc treatment. In planning these experiments, attention was paid to the conditions under which the two theories were developed. Although these two treatments are for reactors of totally different configurations, the conditions which should be experimentally satisfied to maximize their predictions are the same. Both theories require that:

(a) The flow be laminar. To achieve this in our experiments, low flow rates and low rotation speeds were used.

(b) The enzyme reaction at the surface should be very fast. The use of two cross-linking agents (glutaraldehyde with either benzidine or 3,3'-diaminobenzidine) helped in putting enough enzyme on the nylon surfaces to satisfy this condition.

Also, the membrane disc system contained enough enzyme and its high porosity assisted in fulfilling this condition.

(c) The surface on which the enzyme is fixed should be free of charges. The immobilization techniques discussed in this thesis all lead to an electrically neutral surface.

(d) The simple Michaelis-Menten kinetics should be satisfied. The experiments were done in two extremes; with one substrate in excess, the other was varied to reduce the kinetics of LDH to simple Michaelis-Menten behaviour.

Thus, the results of our investigation obeyed the predictions of the Kobayashi-Laidler theory and of the theoretical treatment presented in Chapter IV, because the above conditions were experimentally fulfilled.

SUPPLEMENTARY SECTION

Some Limitation Aspects of the K-L Theory

The K-L theory only applies to steady-state kinetics and to non-turbulent flow. It will also not apply if the calculated thickness of X_D of the diffusion layer is greater than the tube radius. We would now show that our experimental conditions were suitable for application of the theory.

The K-L theory assumes steady-state conditions throughout the tube (see Eqn. (1)) and is not applicable to transient-phase kinetics. Because of the usually great catalytic efficiency of enzymes transient-phase kinetics dies in times much less than one second[204], typically in the millisecond range[205].

The residence time of a substrate solution in tubular reactors is the ratio between the length of the tube and the linear flow velocity of the solution. With this relation, the residence time for the 100 cm tube employed in our initial experiments (see Chapter II) was 16.2 seconds at the highest flow rate (i.e. at v_f = 6.16 cm s^{-1}). Similarly, a 50 cm tube gave a residence time of 33:3 seconds at its highest flow rate (1.50 cm s^{-1}). These times are much larger than the transient-phase time scale. Therefore, steady-state conditions apply practically throughout the tube.

One of the most important conditions necessary for the validity of the K-L theory is laminar flow. This requires that the value of the Reynolds numbers[206] be less than 2100. The Reynolds numbers are

given by $2rv_f\nu^{-1}$, where ν is the kinematic viscosity. Taking 9.04×10^{-3} cm^2 s^{-1} for ν as reported in Chapter IV of this thesis leads to a calculated Reynolds number of 103.6 at v_f = 6.16 cm s^{-1}. Since at the highest flow rate employed in our work, the Reynolds numbers did not exceed 2100, then laminar conditions were established at all times. Note also that the expression for calculating Reynolds numbers suggests that tubes with very small radii give better laminar conditions. It is therefore advantageous to limit the K-L theory to thin tubes and small flow rates.

Apart from the steady-state and laminar conditions, the K-L theory also requires that the X_D be less than the tube radius; this requirement is clear from Figure 3D (in Chapter II). According to Eqn. (8), the X_D values increase with increasing length L of the tube. For the K-L theory to apply, the length of the tube must be chosen in such a way that X_D/r is less than 1.0. The diffusion-layer thicknesses calculated from Eqn. (8) for a 100 cm tube (Chapter II) at flow rates 0.726, 1.32, 2.50, 3.63, 4.84, and 6.16 cm s^{-1} were respectively equal to 0.027, 0.022, 0.018, 0.016, 0.014 and 0.013 cm. These calculations were made with $D = 4 \times 10^{-6}$ cm^2 s^{-1} (see Chapter II) and r = 0.076 cm. The experiments reported in Chapter III were done with tubes 50 cm long. The calculated X_D for the latter reactor systems were 0.027, 0.021, 0.019 and 0.017 cm at flow rates 0.36, 0.72, 1.08 and 1.50 cm respectively. In all our experiments of Chapters II and III, the radius of the tubes was 0.076 cm and all X_D/r ratios were therefore less than 1.0.

One weakness of the theory is its requirement that we extrapolate to $v_f^{-1/3} = 0$ to get diffusion-free behaviour (see Figures 11 and 16). This extrapolation tends to be too long and its results may not be reliable. However, the method has led to reasonable conclusions[99-103,130,131,141,142]

CLAIMS TO ORIGINAL RESEARCH

1. Previous applications of the Kobayashi-Laidler theory for tubular reactors have been confined to one-substrate-enzyme systems. The present work is a first application of the theory to two-substrate enzymes. In particular, the flow kinetics of LDH attached to the inner surface of a nylon tube has been investigated for the first time.

2. The attachment of enzymes to nylon materials has been achieved in various ways by several workers, but so far, no method has involved the coupling of glutaraldehyde with either benzidine or 3,3-diaminobenzidine to act as simultaneous crosslinks between the enzyme and the nylon support. The idea and the accomplishment of this coupling as discussed in Chapters II and IV are original. With this kind of immobilization, LDH shows high activity and stability.

3. The immobilization to nylon, involving thionyl chloride and 3,3-diaminobenzidine as explained in Chapter IV, is also original.

4. Temperature and pH measurements on LDH attached to the inner surface of a nylon tube have been made for the first time.

5. The use of the dimensionless parameters of the Kobayashi-Laidler theory in predicting how temperature would affect diffusional resistances in the kinetics of a tubular reactor has been explained and our experiments of Chapter III show the first application of

the technique. A combination of high temperature, high substrate concentration and high flow rate leads to low diffusional resistances (see Figures 19A and 19B).

6. The prediction of the Kobayashi and Laidler theory that double logarithmic plots of reaction rates against flow rates can indicate the extent of diffusional effects in a tubular reactor has been experimentally verified for the first time (see Figure 9).

7. So far, no kinetic measurements have been made with enzymes present at rotating discs. The theory of rotating disc electrodes has been extended to apply to rotating enzyme discs. This has been done in Chapter IV and the experiments carried out with LDH discs to test our new theory are original.

8. A new type of cell, which can be used to study both internal and external diffusional effects on entrapped enzymes, has been described (see Figure 30).

9. It was found that NADH suffers from steric hindrances once the enzyme is immobilized at a solid support. This conclusion has been possible because of the use of an enzyme which catalyzes the reaction of two substrates. A one-substrate-enzyme system would not reveal clearly whether or not a change in the kinetic behaviour was due to steric, diffusional or conformational effects. Thus, one of the results of our research is a first realization that better information on the extent of the influence of each of the factors shown in Figure 2 on the kinetics of an immobilized enzyme can be obtained by studying the flow kinetics of multi-substrate enzymes.

10. A procedure used by Goldstein, Levin and Katchalski to predict the nature of the charges on a substrate and on a support, through the equation $K_m(app) = K_m^f \exp Ze\psi/kT$, has been discussed in Chapter VI. It has been pointed out for the first time that such an expression can lead to wrong conclusions if diffusional effects are not removed from the kinetic data.

APPENDIX A

Kobayashi and Laidler[73] have given a procedure for preparing theoretical ϕ-ρ diagrams for enzymes attached to the interior surfaces of tubes. The procedure described below is simpler and leads to improved application of the diagrams as shown in Chapter III of this thesis.

Explanation

Kobayashi and Laidler have shown that the dimensionless parameter is defined as

$$\phi = \frac{[P]_e}{[S]} \left(\frac{v_f r^2}{DL}\right)^{2/3} = \frac{3\sqrt{12}}{\Gamma(\frac{1}{3})} \eta \Lambda \qquad (A1)$$

where η is the utilization factor and Λ the Damkohler number. All the other symbols in the equation are as already explained in Chapters II and III. Since $\Gamma(\frac{1}{3})$ is equal to 2.67, the above equation simplifies to

$$\phi = 2.57\ \eta\ \Lambda \qquad (A2)$$

Using Eqn. (A2), one then calculates Λ values with chosen ϕ and η values.

Once Λ values are known, one proceeds to calculate ρ from

$$\eta = \frac{\eta_o + \gamma\eta_1}{1+\gamma} \qquad (A3)$$

where

$$\eta_o = \begin{cases} 1 , & (\Lambda \leq 0.8061) \\ \frac{1}{\Lambda} - \frac{0.1260}{\Lambda^3} , & (\Lambda > 0.8061) \end{cases} \tag{A4}$$

$$\gamma = \sqrt{\rho(\rho+3)} \tag{A5}$$

and

$$\eta_1 = \frac{1}{\Lambda+1} \tag{A6}$$

Thus, when $\Lambda \leq 0.8061$, Eqn. (A3) becomes

$$\eta = \frac{1 + (\frac{1}{\Lambda+1})\sqrt{\rho(\rho+3)}}{1 + \sqrt{\rho(\rho+3)}} \tag{A7}$$

Upon rearrangement, Eqn. (A7) reduces to

$$\rho^2 + 3\rho - \left(\frac{(\eta-1)(\Lambda+1)}{1-\eta(\Lambda+1)}\right)^2 = 0 \tag{A8}$$

Equation (A8) is therefore a quadratic whose roots ρ_1 and ρ_2 can be calculated from

$$\rho_{1,2} = \frac{-3 \pm \sqrt{9+4C}}{2} \tag{A9}$$

where

$$C = -\left(\frac{(\eta-1)(\Lambda+1)}{1-\eta(\Lambda+1)}\right)^2$$

is a constant whose value is known, since η and Λ are known quantities. On the other hand, when $\Lambda > 0.8061$, Eqn. (A3) above becomes

$$\eta = \frac{\frac{1}{\Lambda} - \frac{0.126}{\Lambda^3} + \left(\frac{1}{\Lambda+1}\right)\sqrt{\rho(\rho+3)}}{1 + \sqrt{\rho(\rho+3)}} \qquad \text{(A10)}$$

Upon rearrangement, Eqn. (A10) gives

$$\rho^2 + 3\rho - \left(\frac{\eta\Lambda^3 - \Lambda^2 + 0.126}{\Lambda^3(1-\eta\Lambda-\eta)}\right)^2 = 0 \qquad \text{(A11)}$$

Equation (A11) is different from Eqn. (A8) only in the constant C. Thus, ρ_1 and ρ_2 can be calculated from Eqn. (A11) very easily. Only positive values of these roots are considered. However, to avoid the labour involved in the analysis of Eqns. (A11) and (A8), the original paper gives the following expression

$$\eta = \frac{2}{\Lambda+1+\sqrt{(\Lambda+1)^2-(4\Lambda/\rho+1)}} \qquad \text{(A12)}$$

which upon rearrangement simplifies to

$$\rho = \frac{\Lambda\eta^2}{(\Lambda\eta+\eta-1)} - 1 \qquad \text{(A13)}$$

Thus, once ϕ and η values have been chosen, Λ is calculated from Eqn. (A2) and its value gives the value of ρ from Eqn. (A13). When Eqn. (A13) fails to give satisfactory positive values of ρ, then one returns to the use of either Eqn. (A8) or Eqn. (A11). The choice as to which equation to use will depend on whether Λ is greater than 0.8061 or less (see Eqn. (A4)).

Some values of ϕ, η, Λ and ρ are given in Table A1, and with these, the construction of theoretical ϕ-ρ diagrams is easy. Figure A1 results directly from Table A1.

The above discussion is based on Eqns. (27), (41), (44) and (45) of the original paper of Kobayashi and Laidler.

Table A1. Theoretical values of ϕ, η, Λ and ρ for construction of ϕ-ρ diagrams.

ϕ	η	Λ	ρ
0.15	0.95	0.061	5.875
1.00	0.95	0.205	0.090
2.00	0.95	0.410	0.015
0.50	0.95	0.123	0.280
0.30	0.95	0.082	0.660
0.20	0.95	0.041	1.640
0.30	0.90	0.130	5.176
0.40	0.90	0.173	1.500
0.50	0.90	0.216	0.862
0.60	0.90	0.259	0.579
0.70	0.90	0.303	0.416
0.80	0.90	0.346	0.327
0.90	0.90	0.389	0.260
1.00	0.90	0.432	0.211
1.50	0.90	0.649	0.087
2.00	0.90	0.865	0.032
0.60	0.80	0.292	10.294
0.70	0.80	0.340	4.222
0.80	0.80	0.389	1.243
0.90	0.80	0.438	0.867
1.00	0.80	0.486	0.646
1.20	0.80	0.584	0.401
1.40	0.80	0.681	0.264
1.60	0.80	0.778	0.175
1.80	0.80	0.875	0.120
2.00	0.80	0.973	0.077
2.20	0.80	1.070	0.040
2.30	0.80	1.119	0.030
0.80	0.70	0.445	17.17
0.90	0.70	0.500	3.90
1.00	0.70	0.556	2.06
1.20	0.70	0.667	0.96
1.50	0.70	0.834	0.44
1.80	0.70	1.000	0.23
2.00	0.70	1.112	0.14
2.50	0.70	1.390	0.02
1.20	0.60	0.778	3.179
1.40	0.60	0.908	1.255
1.60	0.60	1.038	0.677
1.80	0.60	1.167	0.400
2.00	0.60	1.297	0.235
2.20	0.60	1.427	0.127
2.40	0.60	1.556	0.050
2.50	0.60	1.621	0.020
1.60	0.40	1.556	10.320
1.80	0.40	1.751	1.800
1.90	0.40	1.848	1.129
2.00	0.40	1.946	0.750
2.20	0.40	2.140	0.336
2.40	0.40	2.335	0.120
2.50	0.40	2.432	0.040
2.34	0.10	9.105	7.282
2.36	0.10	9.183	4.016
2.38	0.10	9.260	2.562
2.40	0.10	9.339	1.755
2.42	0.10	9.416	1.260
2.46	0.10	9.572	0.673
2.48	0.10	9.650	0.485
2.50	0.10	9.728	0.337
2.54	0.10	9.883	0.119
2.56	0.10	9.961	0.036
2.57	0.10	10.000	0.000
5.0	0.01	194.6	8.7×10^{-6}
5.2	0.01	202.5	8.3×10^{-6}
5.4	0.01	210.1	7.7×10^{-6}
5.6	0.01	217.9	7.1×10^{-6}
5.8	0.01	225.7	6.5×10^{-6}
6.0	0.01	233.5	5.9×10^{-6}

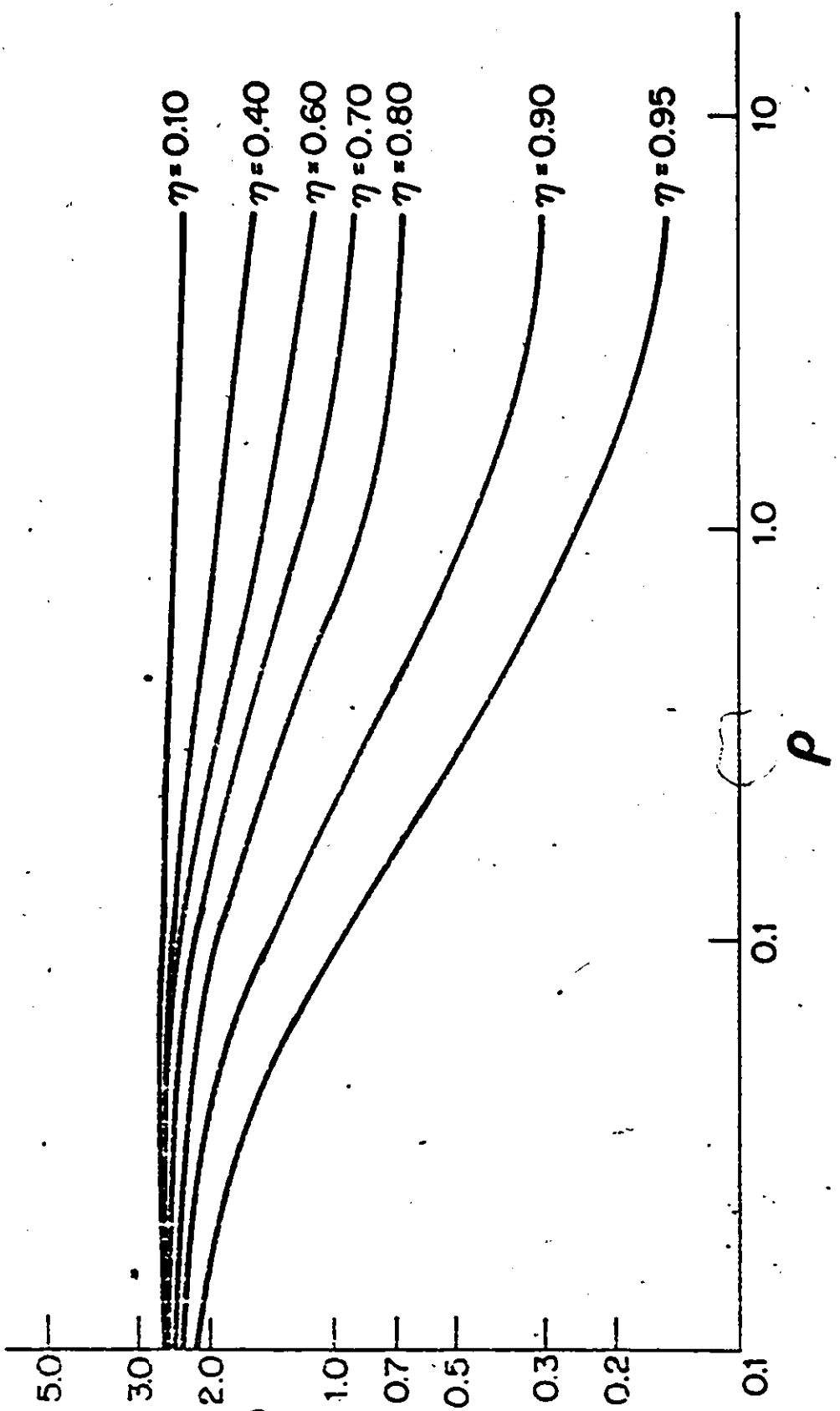

Figure A1. The theoretical ϕ-ρ indicator diagram. The low value of η is associated with high diffusional effects. Conversely, diffusion-free have high η values.

APPENDIX B

Table B1. Approximate amino acid composition of a rabbit muscle LDH subunit[85].

Amino Acid	Abbrev.	Chemical Structure	Molar Mass	Number in Subunit
Lysine	Lys	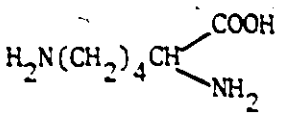	146.2	26
Histidine	His	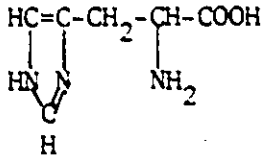	155.2	8
Arginine	Arg	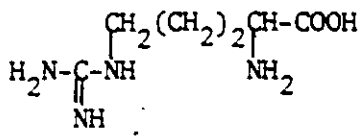	174.2	9
Aspartic Acid	Asp	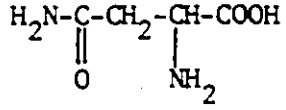	133.1	30
Threomine	Thr	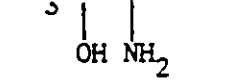	119.1	12
Serine	Ser	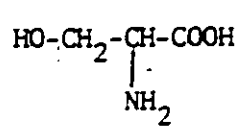	105.1	21
Glutamic Acid	Glu	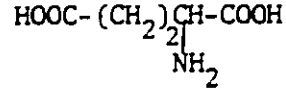	147.1	30

Table B1 (continued)

Amino Acid	Abbrev.	Chemical Structure	Molar Mass	Number in Subunit
Proline	Pro	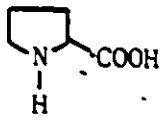	115.1	8
Glycine	Gly	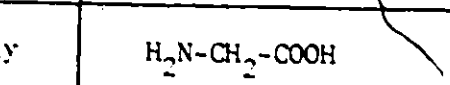	75.1	27
Alanine	Ala	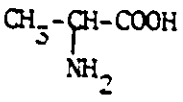	89.1	21
Half-cystine	½ Cys	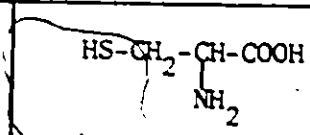	121.2	7
Valine	Val	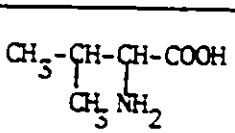	117.1	38
Methionine	Meth	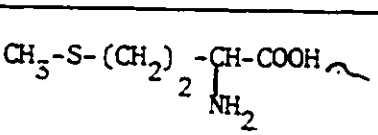	149.2	9
Isoleucine	Ile	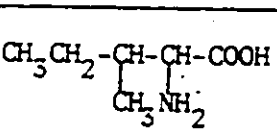	131.2	20
Leucine	Leu	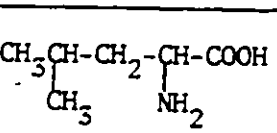	131.2	37
Tyrosine	Tyr	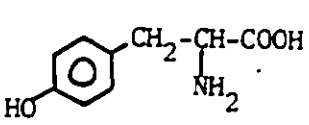	181.2	6
Phenylalamine	Phe	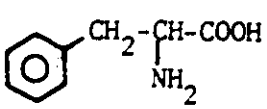	165.2	6
Tryptophan	Trp	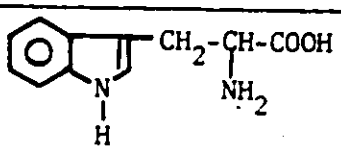	204.2	6

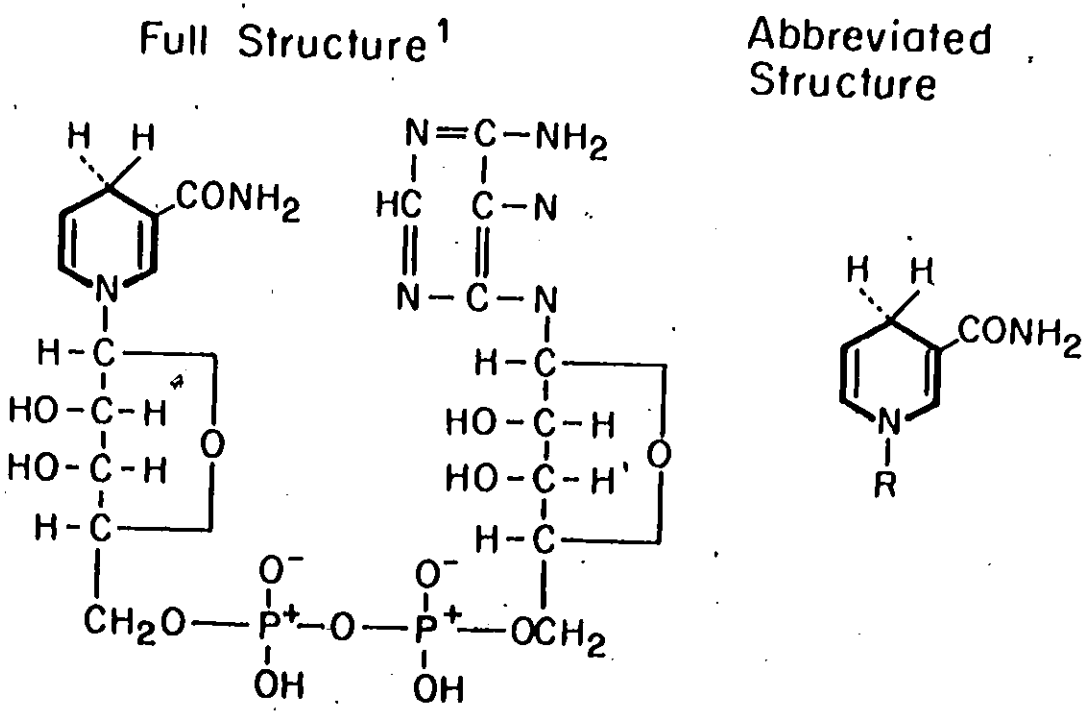

Figure B1. Structure of the reduced form of coenzyme 1; the reduced nicotinamide adenine dinucleotide (NADH).

Figure B2. SUBSTRATE BINDING IN THE ACTIVE SITE OF LDH[80]

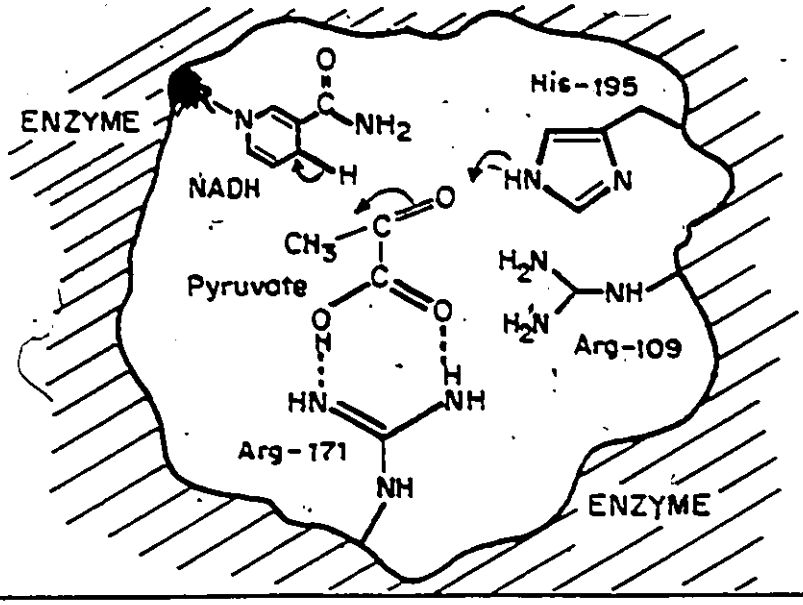

Figure B3. NYLON 66

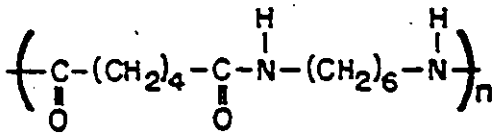

Figure B4. BENZOYLATED CELLULOSE

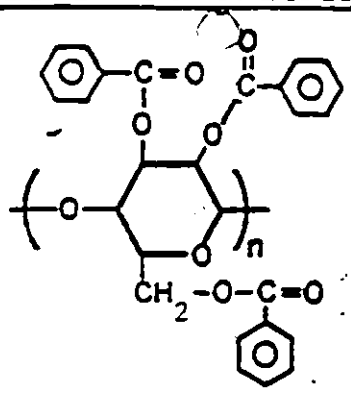

REFERENCES

1. Laidler, K.J. and Bunting, P.S. (1973) The Chemical Kinetics of Enzyme Action, Clarendon Press, Oxford.

2. Sundaram, P.V., Pye, E.K., Chang, T.M.S., Edwards, V.H., Humphrey, A.C., Mosbach, K., Potchornik, A., Porath, J., Weetall, H.H., and Wingard, L.B. (1972) in Enzyme Engineering (Wingard, L.B., ed.) Vol. 1, 15-18, Wiley, Interscience, New York.

3. Grubhofer, N. and Schleith, L. (1953) Naturwissenschaften, 40, 508-509.

4. Grubhofer, N. and Schleith, L. (1954) Hoppe-Seyler's, Z. Physiol. Chem. 297, 108-112.

5. Brandenberger, H. (1956) Rev. Ferment. Ind. Aliment. 11, p. 237.

6. Goldstein, L., Levin, Y., and Katchalski, E. (1964) Biochemistry 3, 1913-1919.

7. Katchalski, E. (1962) Polyamino Acids, Polypeptides, Proteins, Proc. Inter. Symp.

8. Bar-Eli, A. and Katchalski, E. (1963) J. Biol. Chem. 238, 1690-1698.

9. Riesel, E. and Katchalski (1964) ibid 239, 1521-1524.

10. Silman, I.H., Albu-Weissenberg and Katchalski, E. (1966) Biopolymers 4, 441-448.

11. Goldstein, L. (1970) Method. Enzymol. 19, 935-978.

12. Lindsey, A.S. (1970) Rev. Macromolec. Chem. Vol. 4, Marcel Dekker, New York.

13. O'Driscoll, K.F. (1976) Advances in Biochemical Engineering, Vol. 4, Springer Verlag, New York.

14. Mosbach, K. (1976) Techniques of Chemistry, Vol. 10, Part 2, John Wiley and Sons.

15. Goldstein, L. and Manecke, G. (1976) in Applied Biochem. Bioeng. (Wingard, L.B., Katchalski, E. and Goldstein, L., eds.) 1, 23-110, Academic Press, New York.

16. Weetall, H.H. (ed.) Immobilized Enzymes, Anitgens, Antibodies and Peptides (1975) Marcel Dekker.

17. Weetall, H.H. and Suzuki, S. (1975) Immobilized Enzyme Technology, Plenum Press.

18. Wingard, L.B. (Jr.), Katchalski-Katzir, E. and Goldstein, L. (1976), Applied Biochemistry and Bioengineering, Vol. 1, Academic Press.

19. Chang, T.M.S. (1977) Biomedical Application of Immobilized Enzymes and Proteins.

20. Chibata, I. (1978) Immobilized Enzymes, Research and Development, Halsted Press Book and John Wiley and Sons.

21. Wang, D.I.C., Cooney, C.L., Demain, A.L., Dunnilt, P., Humphrey, A.E. and Lilly, M.D. (1979) Fermentation and Enzyme Technology, John Wiley and Sons.

22. Wieland, H. (1972) Enzymes in Food Processing and Products, Noyes Data Corp, New Jersey.

23. Chang, T.M.S. and Poznansky, M.J. (1968) Nature, 218, 243-245.

24. Chang, T.M.S. and Poznansky, M.J. (1969) Proc. Can. Fed. Biol. Soc. 12, p. 54.

25. Chang, T.M.S. (1969) ibid 12, p. 62.

26. Chang, T.M.S. (1971) Nature 229, 117-118.

27. Allison, J.P., Davidson, L., Hartman, A.G. and Kitto, G.B. (1972) Biochem. Biophys. Res. Commun. 47, 66-73.

28. Chang, T.M.S. (1966) Trans. Am. Soc. Artificial Internal Organ, 12, 13-19.

29. Laidler, K.J. and Bunting, P.S. (1980) Method. Enzymol. 64B, 227-248.

30. Chibata, I., Tosa, T., Sato, T., Mori, T. and Matuo, Y. (1972) Proc. 4th Intern. Ferm. Symp., Ferment. Technol. Today, Society of Fermentation Technol., Japan.

31. Chibata, I. and Tosa, T. (1976) in Appl. Biochem. and Bioeng. 1, 329-357 (Wingard, L.B., Katchalski, E., Goldstein, L., eds.) Academic Press.

32. Chibata, I., Tosa, T., Sato, T. and Mori, T. (1976) Method. Enzymol. 44, 746-759.

33. Smiley, K.L. (1971) Biotechnol. Bioeng. 13, 309-317.

34. Weetall, H.H. (1975) Process. Biochem. 10, 3-7.

35. Ory, R.L. and St. Angelo, A.J. (1977), Enzymes in Food and Beverage Processing, ACS Symposium Series 47, 1, 100-131.

36. Messing, R.A. (1974) Biotechnol. Bioeng. 16, 525-529.

37. Strandberg, G.W. and Smiley, K.L. (1972) ibid 14, 509-551.

38. Davis, J.C. (1970) Chem. Eng. Aug. 19, p. 52.

39. Weetall, H.H. (1977) in Biotechnol. Applic. Proteins and Enzymes, 103-127 (Bohak, Z. and Sharon, N., ed.) Academic Press.

40. Volesky, B. and Emond, C. (1979) Biotechnol. Bioeng. 12, 1251-1276.

41. Olson, A.C. and Stanley, W.L. (1973) J. Agr. Food. Chem. 21, 440-445.

42. Green, M.L. and Cru[redacted]ield, G. (1969) Biochem. J. 115, 183-190.

43. Schreiner, H.R. (1966) U.S. Patent 3282702.

44. Shipe, W.F., Senyk, G. and Weetall, H.H. (1972) J. Dairy Sci. 55, 647-648.

45. Hochstrasser, K., Muss, M. and Werle, E. (1967) Hoppe-Seyler's Z. Physiol. Chem. 348, 1337-1340.

46. Fritz, H., Hutzel, M. and Werle, E. (1967) ibid 348, p. 950.

47. Fritz, H. Schult, H., Hutzel, M. and Wiedemann, M. (1967) ibid 348, 308-312.

48. Stewart, K.K. and Doherty, R.F. (1971) FEBS Letters, 16, 226-228.

49. Lindberg, M.U. and Skoog, L. (1970) Eur. J. Biochem. 13, 326-335.

50. Sundberg, L. and Kristians, T. (1972) FEBS Letters, 22, 175-177.

51. Blumenthal, R., Caplan, S.R., and Kedem, O. (1967) Biophys. J., 7, 735-757.

52. Wingard, L.B. (Jr.), Liu, C.C. and Nagda, N.L. (1971) Biotechnol. Bioeng. 13, 629-639.

53. Goldstein, L., Lifshitz, A. and Sokolovsky, M. (1971), Int. J. Biochem. 2, 448-456.

54. Humphrey, A.E. and Pye, E.K. (1972) Chemical Eng. News, Jan. 3, p. 25.

55. Witt, P.R. (Jr.), Sair, R.A., Richardson, T. and Olson, N.F. (1970), Brewers Digest, Oct Issue, p. 70.

56. Yamato, K., Sato, T., Tosa, T. and Chibata, I. (1974) Biotechnol. Bioeng. 16, 1601-1610.

57. Bunting, P.S. (1973) Ph.D. Thesis.

58. Zaborsky, O.R. (1973) Immobilized Enzymes, 127-144 (Chemical Rubber Co., Press).

59. Wang, D.I.C., Cooney, C.L., Demain, A.L., Dunnill, P., Humphrey, A.E. and Lilly, M.D., eds. (1979) Fermentation and Enzyme Technology, John Wiley and Sons.

60. Guilbault, G.G. and Hrabankova, E. (1971) Anal. Chim. Acta 56, 333-338.

61. Aizawa, M., Karube, I. and Suzuki, S. (1974) Anal. Chim. Acta 69, 431-437.

62. Senn, D.R., Carr, P.W. and Klatt, L.N. (1976) Anal. Chem. 48, 954-958.

63. Guilbault, G.G. and Shu, F.R. (1972) ibid 44, 2161-2166.

64. Hicks, G.P. and Updike, S.J. (1966) ibid. 38, 726-730.

65. Hornby, W.E., Inman, D.J. and McDonald, A. (1972) FEBS Letters 23, 114-116.

66. Goldman, R., Silman, H.I., Caplan, S.R., Kedem, O. and Katchalski (1965) Science 150, 758- (b) (1968) Biochem 7, 486-500.

67. Goldman, R., Kedem, O. and Katchalski, E. (1968) ibid 7, 4518-4531.

68. Srere, A.P., Mattiason, B. and Mosbach, K. (1973) Proc. Nat. Acad. Sc. 70, 2534-2538.

69. Mattiason, B. and Mosbach, K. (1971) Biochim. Biophys. Acta 235, 253-257.

70. Fell, D.A. and White, C.J.B. (1975) Biochem. Biophys. Res. Commun. 67, 1013-1018.

71. Engasser, J.M. and Horvath, C. (1976) Appl. Biochem. Bioeng. 1, 127-220 (Wingard, L.B., Katchalski, K.E. and Goldstein, L., eds.) Academic Press.

72. Wang, S.S., King, C.K. (1979) in Advances in Biochemical Engineering (Gose, T.K., Fiechter, A. and Blakebrough, N., eds.) Springer-Verlag.

73. Kobayashi, T. and Laidler, K.J. (1974) Biotechnol. Bioeng. 16, 77-97.

74. Sundaram, P.V., Tweedale, H. and Laidler, K.J. (1970) Can. J. Chem. 48, 1498-1504.

75. Kobayashi, T. and Laidler, K.J. (1973) Biochim. Biophys. Acta 302, 1-12.

76. Kobayashi, T. and Moo-Young, M. (1973) Biotechnol. Bioeng. 15, 27-45, 47-67.

77. Horvath, C. and Engasser, J.M. (1974) Biotechnol. Bioeng. 16, 909-923.

78. Horvath, C., Solomon, B.A., and Engasser, J.M. (1973) Ind. Eng. Chem. Fundam. 12, 431-439.

79. Fersht, A. (ed.) (1977) Enzyme Structure and Mechanism, pp. 288-354.

80. Holbrook, J.J., Liljas, A., Steindel, S.J. and Rossmann, M.G. (1975) in The Enzymes, 11, 191-292.

81. Straub, F.B. (1940) Biochem. J. 34, 483-486.

82. Fine, I.H. and Costello, L.A. (1963) Method. Enzymol. 6, 958-972.

83. Stinson, R.A. and Holbrook, J.J. (1973) Biochem. J. 131, 719-749.

84. Brodelius, P. and Mosbach, K. (1973) FEBS (Fed. Eur. Biochem. Soc.) Letters 35, 223-226.

85. Pesce, A. Fondy, T.P., Stolzenbach, F.E., Castillo, D. and Kaplan, N.D. (1967) J. Biolog. Chem. 242, 2151-2167.

86. Fromm, H.J. (1963) ibid 238, 2938-2944.

87. Stambaugh, R. and Post, D. (1966) ibid 241, 1462-1467.

88. Klibanov, A.M. (1979) Analytical Biochemistry 93, 1-25.

89. Ory, R.L. and St. Angelo, A.J. eds. (1977) Enzymes in Food and Beverage Processing, A.C.S. Symposium Series.

90. Abbott, B.J. (1976) Advanced Applied Microbiology 20, 203-257.

91. Hornby, W.E., Campbell, J., Inman, D.J. and Morris, D.L. (1974) in Enzyme Engineering (K. Pye and Wingard, L. Jr., eds.) Vol. 2, Plenum, New York.

92. N. Itoh, N. Hagi, T. Iida, A. Tanaka and S. Fukui (1979) J. Appl. Biochem. 1, 291-300.

93. Thomas, D., Brown, G. and Selegny, E. (1972) Biochimie 54, 229-244.

94. Michaelis, L. and Menten, M.L. (1913) Biochem. Z, 49, p. 333.

95. Sundaram, P.V. and Hornby, W.E. (1970) FEBS Lett. 10, 325-327.

96. Hornby, W.E. and Filippusson, H. (1970) Biochim. Biophys. Acta 220, 343-345.

97. Allison, J.P., Davidson, A., Gatierrez-Hartman, A. and Kitto, G.B. (1972) Biochim. Biophys. Res. Comm. 47, 66-73.

98. Filippusson, H., Hornby, W.E. and McDonald, A. (1972) FEBS Lett. 20, 291-293.

99. Bunting, P.S. and Laidler, K.J. (1974) Biotech. Bioeng. 16, 119-134.

100. Ngo, T.T. and Laidler, K.J. (1975) Biochim. Biophys. Acta 377, 317-330.

101. Narinesingh, D., Ngo, T.T. and Laidler, K.J. (1975) Can. J. Biochem. 53, 1061-1069.

102. Ngo, T.T., Narinesingh, D. and Laidler, K.J. (1976) Biotech. Bioeng. 18, 119-127.

103. Ngo, T.T. and Laidler, K.J. (1978) Biochim. Biophys. Acta 525, 93-102.

104. Neilands, J.B. (1955) Method. Enzymol. 1, 449-454.

105. Horecker, B.L. and Kornberg, A. (1948) J. Biol. Chem. 175, 385-389.

106. Schellenberg, K.A. (1967) ibid 242, 1815-1820.

107. (1973-1974) The CRC Handbook of Chemistry and Physics, 54th Edition. Table F56.

108. Othmer, D.F. and Thakov, M.S. (1953) Industrial and Engineering Chemistry Vol. 45, Number 3, pp. 589-593.

109. Daniels, F., Williams, J.W., Bender, P., Alberty, R.A., Cornwell, C.D. and Harriman, J.E. (1970) Experimental Physical Chemistry, McGraw-Hill Book Company.

110. Garbarini, G.R., Eaton, R.F., Kwei, T.K. and Tobolsky, A.V. (1971) J. Chem. Ed. 48, 226-230.

111. Kegeles, G. and Gosting, L.J. (1947) J. Am. Chem. Soc. 69, 2516-2523.

112. Longsworth, L.G. (1952) J. Am. Chem. Soc. 74, 4155-4159; (1953) ibid 75, 5705-5709.

113. Coulson, C.A. et al (1948) Proc. Roy. Soc. London Ser. A 192, p. 382.

114. Sherwood, T.K., Pigford, R.L. and Wilke, G.R. (1975) Mass Transfer, McGraw-Hill, New York.

115. Wykes, J.R., Dunmill, P. and Lilly, M.D. (1975) Biotechnol. Bioeng. 17, 51-68.

116. Cho, C. and Swaisgood, H. (1974) Biochim. Biophys. Acta 334, 243-256.

117. Hakala, M.T., Glaid, A.J., Schwert, G.W. (1953) Proc. Fed. Am. Soc. Exp. Biol. 12, p. 213.

118. Meistes, A. (1950) J. Biol. Chem. 184, 117-129.

119. Hakala, M.T., Glaid, A.J. and Schwert, G.W. (1956) ibid 221, 191-209.

120. Schwert, G.W., Miller, D.B.S. and Peanasky, R.J. (1967) ibid 242, 3245-3252.

121. Schwert, G.W. (1969) ibid 244, 1285-1290.

122. Glasstone, S., Laidler, K.J. and Erying, H. (1941) Theory of Reaction Rates, McGraw-Hill, New York.

123. Cohen, E. and Bruins, H.R. (1923) Z. Phys. Chem. (Liepzig) 103, 404-450.

124. Barrer, R.M. (1939) Trans. Faraday Soc. 35, 644-656.

125. Segel, H., ed. (1975) "Enzyme Kinetics , Behaviour and Analysis of Rapid Equilibrium and Steady State Enzyme Systems", John Wiley and Sons, New York.

126. Engasser, J.M. and Horvath, C. (1974) Biochim. Biophys. Acta 358, 178-192.

127. Goldstein, L. and Katchalski, E. (1968) Z. Anal. Chem. 243, 375-396.

128. Mosbach, R., Koch-Schmidt, A.C. and Mosbach, K. (1976) Method. Enzymol. 44, 53-332.

129. Bunting, P.S. and Laidler, K.J. (1972) Biochem. 11, 4477-4483.

130. Daka, N.J. and Laidler, K.J. (1978) Can. J. Biochem. 56, 774-779.

131. Daka, N.J. and Laidler, K.J. (1980) Biochim. Biophys. Acta 612, 305-316.

132. Pleskov, Y.V. and Filinovski (1976) ed. The Rotating Disc Electrode, Consultants Bureau, New York and London.

133. von Karman (1921) Zeitschrift fur angewandte Mathematic u. Mechanic 1, 244-247.

134. Levich, V.G. (1962) Physicochemical Hydrodynamics, Prentice-Hall, Englewood, Cliffs, New York.

135. Levich, V.G. (1942) Acta Phys. Chim., U.R.S.S. 17, 257.

136. Hornby, W.E., Lilly, M.D. and Crook, E.M. (1968) Biochem. J. 107, 669-674.

137. Paul, F., Goulet, P.R., Gautheron, D.C. and Engasser, J.M. (1978) Biotechnol. Bioeng. 20, 1785-1796.

138. Weast, C. (1973-77) The CRC Handbook of Chemistry and Physics 54th Edition, F43-F45.

139. Vlassis, C.G. (1978) A Laboratory Guide for Chemistry (The Williams and Williams Company).

140. Laidler, K.J. (1978) Physical Chemistry with Biological Applications, Chapter 11: The Benjamin/Cummings Publishing Company.

141. Mazid, M.A. and Laidler, K.J. (1980) Biochim. Biophys. Acta 614, 237-241.

142. Mazid, M.A. and Laidler, K.J. (1980) ibid 614, 225-236.

143. Dixon, J.E. and Stolzenbach, F.E. (1974) Israel J. Chem. 12, 529-541.

144. Chang, T.M.S., MacIntosh, F.C. and Mason, S.G. (1963) Proc. Can. Fed. Biol. Sci. 6, p. 16.

145. Chang, T.M.S. (1964) Science 146, 524-525.

146. Chang, T.M.S., MacIntosh, F.C. and Mason, S.G. (1966) Can. J. Physiol. Pharmacol. 44, 115-128.

147. Chang, T.M.S. (1966) Trans. Amer. Soc. Artif. Intern. Organ 12, 13-19.

148. Chang, T.M.S. (1975) Kidney Int. 7, S387-S392.

149. Chong, E.S. and Chang, T.M.S. (1974) Enzyme J. 18, 218-239.

150. Corno, C., Galli, G., Morisi, F., Bettonte, M. and Stopponi, A. (1972) Staerke 24, 420-424.

151. Giovenco, S., Morisi, F. and Pansolli, P. (1973) FEBS Lett. 36, 57-60.

152. Marconi, W., Gulinelli, S. and Morisi, F. (1974) Biotechnol. Bioeng. 16, 501-511.

153. Pastore, M., Morisi, F. and Viglia, A. (1974) J. Dairy Sci. 57, 269-272.

154. Marconi, W., Cecere, F., Morisi, F., Penna, G.D. and Rappuoli, (1973) J. Antibiot 26, 228-232.

155. Dinelli, D., Marconi, W., Morisi, F. (1976) Method. Enzymol. 44, 227-243.

156. O'Driscoll, K.F. (1976) ibid 44, 169-183.

157. Chambers, R.P., Cohen, W. and Baricos, W.H. (1976) ibid 44, 291-317.

158. Goldstein, L. (1976) ibid 44, 397-444.

159. Thomas, D. and Brown, G. (1976) ibid 34, 901-929.

160. Funt, B.L. and Hsu Li-Chien (1979) Polymer 20, 81-83.

161. Albery, W.J. and Hitchman, M.L. (1971) Ring-Disc Electrodes, Oxford University Press, London.

162. Chen, A.K. and Liu, C.C. (1977) Biotechnol. Bioeng. 19, 1785-1792.

163. Shinbo, T. and Sugiura, M. (1979) Anal. Chem. 51, 100-104.

164. Guilbault, G.G. and Lubrano, G.J. (1974) Anal. Chim. Acta 69, 183-188.

165. Mascini, M. and Libert, A. (1974) ibid 69, 189-194.

166. Guilbault, G.G. and Nanjo, M. (1974) Anal. Chem. 46, 1769-1772.

167. Papariello, G.J., Mukherji, A.K. and Shearer, C.M. (1973) Anal. Chem. 45, 790-792.

168. Nanjo, M. and Guilbault, G.G. (1975) Anal. Chim. Acta 75, 169-180.

169. Blaedel, W.J. and Jenkins, R.A. (1976) Anal. Chem. 48, 1240-1247.

170. Duijn, P.V., Pascoe, E. and Ploeg, M.V. (1967) J. Histochem. Cytochem. 15, 631-645.

171. Vieth, W.R. and Venkatasubramanian (1976) Method. Enzymol. 34, 243-263.

172. Axen, R., Myrin, P.A. and Jansson, J.C. (1970) Biopolymers 9, 401-413.

173. Kasche, V. and Bergwall, M. (1974) in Insolubilized Enzymes (Salmona, M., Soronio, C. and Garathini, S., eds.) Raven, New York.

174. Marsh, D.R., Lee, Y.Y. and Tsao, G.T. (1973) Biotechnol. Bioeng. 15, 483-492.

175. Goldman, R., Kedem, O., Silman, I.H., Kaplan, S.R. and Katchalski, E. (1968) Biochemistry 7, 486-500.

176. Engasser, J.M. (1980) in Enzymic and Non-Enzymic Catalysis (Dunmill, P., Wiseman, A. and Blakebrough, N. eds.), Ellis Horwood Ltd., London.

177. Boyd, C.W. (1965) J. Biol. Chem. 240, 4097-4098.

178. Cresswell, P. and Sanderson, A.R. (1970) Biochem. J. 119, 447-452.

179. Engasser, J.M. and Horvath, C. (1975) Biochem. J. 145, 431-435.

180. Johansson, A.C. and Mosbach, K. (1974) Biochim. Biophys. Acta 370, 348-353.

181. Filippusson, H. and Hornby, W.E. (1970) Biochem. J. 120, 215-219.

182. Wharton, C.M., Crook, E.M. and Brocklehurst, K. (1968) Eur. J. Biochem. 6, 572-578.

183. Mori, T., Tosa, T. and Chibata, I. (1974) Cancer Res 34, 3066-3068.

184. Uy, R., Liu, V.S.H. and Royer, G.P. (1976) J. Solid Phase Biochem 1, 51-65.

185. Tosa, T., Sato, T., Mori, T., Matuo, Y. and Chibata, I. (1973) Biotechnol. Bioeng. 15, 69-84.

186. Fogarty, W.M. and Kelly, C.T. (1979) in Topics in Enzyme and Fermentation Biotechnol (Wiseman, A., ed.) 3, 44-102.

187. Dixon, M. and Webb, E.C. (1964) Enzymes 2nd Ed., Longmans, Green, New York.

188. Weetall, H.H. (1971) Res. Develop. 22, No. 12, 18.

189. Hornby, W.E., Lilly, M.D. and Crook, E.M. (1968) Biochem. J. 107, 669-674.

190. Kleine, R., Spangenberg, P. and Flemming, C. (1976) Hoppe-Seyler's Z. Physiol. Chem. 357, 629-639.

191. Knights, R.J. and Light, A. (1974) Arch. Biochem. Biophys. 160, 377-386.

192. Gabel, D. and Kasche, V. (1976) Method. Enzymol. 44, 527-546.

193. Pye, K. and Chance, B. (1976) ibid 44, 357-372.

194. Nernst, W. (1904), Z. Phys. Chem. 47, 52.

195. Lilly, M.D., Hornby, W.E. and Crook, E.M. (1966) Biochem. J. 100, 718-723.

196. Lilly, M.D. and Dunnill, P. (1976) Method. Enzymol. 44, 717-738.

197. Guilbault, G.G. (1975) in Immobilized Enzymes, Antigens, Antibodies and Peptides, Preparation and Characterization (Weetall, H.H., ed.) 293-417.

198. Reeck, G. (1970) CRC Handbook of Biochemistry; Selected Data for Molecular Biology, 2nd Edition, C281-C293.

199. Hornby, W.E. and Morris, D.L. (1975) in Immobilized Enzymes, Antigens, Antibodies, and Peptides (Weetall, H.H., ed.) 141-169.

200. Trommer, W.E., Huth, H. and Wenzel, H.R. (1979) Biochim. Biophys. Acta 567, 49-59.

201. Peterman, B.F. and Laidler, K.J. (1980) Arch. Biochem. Biophys. 199, 158-164.

202. Peterman, B.F. and Laidler, K.J. (1979) Canad. J. Chem. 57, 1471-1474.

203. Peterman, B.F. and Laidler, K.J. (1979) Biochim. Biophys. Acta 577, 314-323.

204. Buckingham, A.D. and Herschbach, D.R. (1976) Chemical Kinetics; the International Review of Science, 79-86.

205. Cornish-Bowden, A. (1976) Principles of Enzyme Kinetics; Butterworths, 21-23.

206. Bird, R.B.; Stewart, W.E. and Lightfoot, E.N. (1960) Transport Phenomena; Chapter 2, 41-47.